

极大平面图的结构与着色理论

(2) 多米诺构形与扩缩运算

许进*

(北京大学高可信软件技术教育部重点实验室 北京 100871)

(北京大学信息科学技术学院 北京 100871)

摘要: 业已证明四色猜想的数学证明可归结为刻画 4-色漏斗型伪唯一 4-色极大平面图的特征。为刻画此类极大平面图的结构特征, 本文提出一种构造极大平面图的方法——扩缩运算。研究发现: 此方法的关键问题是需要清楚一种构形, 称为多米诺构形。文中构造性地给出了多米诺构形的充要条件; 在此基础上提出并建立了一个图的祖先图与子孙图理论与构造方法。特别证明了: 任一最小度 ≥ 4 的 $n(n \geq 9)$ -阶极大平面图必含 $(n-2)$ -阶或 $(n-3)$ -阶祖先图; 给出极大平面图的递推构造法, 并用此方法构造出 6~12-阶所有最小度 ≥ 4 的极大平面图。扩缩运算是本系列文章的基石。

关键词: 极大平面图; 扩缩运算; 多米诺构形; 祖先图; 子孙图; 递推构造法

中图分类号: O157.5

文献标识码: A

文章编号: 1009-5896(2016)06-1271-57

DOI: 10.11999/JEIT160224

Theory on Structure and Coloring of Maximal Planar Graphs

(2) Domino Configurations and Extending-Contracting Operations

XU Jin

(Key Laboratory of High Confidence Software Technologies, Peking University, Beijing 100871, China)

(School of Electronics Engineering and Computer Science, Peking University, Beijing 100871, China)

Abstract: The first paper of this series of articles revealed that Four-Color Conjecture is hopefully proved mathematically by investigating a special class of graphs, called the 4-chromatic-funnel, pseudo uniquely-4-colorable maximal planar graphs. To characterize the properties of such class of graphs, a novel technique, “extending-contracting operation”, is proposed which can be used to construct maximal planar graphs. The essence of this technique is to study a special kind of configurations, domino configurations. In this paper, a necessary and sufficient condition for a planar graph to be a domino configuration is constructively given, on the basis of which it is proposed to construct the ancestor-graphs and descendent-graphs of a graph. Particularly, it is proved that every maximal planar graph with order $n(n \geq 9)$ and minimum degree ≥ 4 has an ancestor-graph of order $(n-2)$ or $(n-3)$. Moreover, an approach is put forward to construct maximal planar graphs recursively, by which all maximal planar graphs with order 6~12 and minimum degree ≥ 4 are constructed. The extending-contracting operation constitutes the foundation in this series of articles.

Key words: Maximal planar graphs; Extending-contracting operations; Domino configurations; Ancestor-graphs; Descendent-graphs; Recursive construction approach

1 引言

众所周知, 在数学领域内有 3 大著名猜想: 费

马尔猜想(费马尔大定理)、哥德巴赫猜想和四色猜想。这 3 个著名猜想具有初中水平的人都能理解, 而目前人类几乎都具有初中文化水平, 也就是说, 这 3 个猜想几乎“家喻户晓”。如费马尔猜想: 当自然数 $n \geq 3$ 时, 基于变量 x, y, z 的方程 $x^n + y^n = z^n$ 无解。理解此猜想仅需初中数学基础即可; 哥德巴赫猜想: 任一 ≥ 6 的偶数 n 可分解为两个素数的和。这个猜想显然具有小学数学基础的人都可理解; 四色猜想: 世界上任意的地图都可以用四种颜色进行着色, 使得有共同边界的国家(或地区)着不同颜色。

收稿日期: 2016-01-24; 改回日期: 2016-04-21; 网络出版: 2016-04-26

*通信作者: 许进 jxu@pku.edu.cn

基金项目: 国家 973 规划项目(2013CB329600), 国家自然科学基金(61372191, 61472012, 61472433, 61572046, 61502012, 61572492, 61572153, 61402437)

Foundation Items: The National 973 Program of China (2013CB329600), The National Natural Science Foundation of China (61372191, 61472012, 61472433, 61572046, 61502012, 61572492, 61572153, 61402437)

没有上过学的人都可理解此猜想。虽然在 1976 年 APPEL 与 HAKEN 宣布用计算机给出了四色猜想的“证明”^[1-3]，但在数学界，该成果仍不是令人满意的。因此，给出四色猜想的数学证明仍是一个尚待解决的困难问题。四色猜想的研究对象可归结于极大平面图，因此，弄清楚极大平面图的结构与构造是极为重要的。

其实，早在1891年，EBERHARD^[4]就对极大平面图的构造问题展开了研究，给出了构造所有极大平面图的运算系统，把这个运算系统记为 $\langle K_4; \Phi = \{\varphi_1, \varphi_2, \varphi_3\} \rangle$ ，其中，4-阶完全图 K_4 称为初始对象， $\Phi = \{\varphi_1, \varphi_2, \varphi_3\}$ 称为运算系统， $\varphi_1, \varphi_2, \varphi_3$ 是它的3个算子，其功能如图1所示。

设 G 是一个极大平面图， C 是 G 中的一个圈。若在 C 内不含顶点，只是 C 上某些不相邻的顶点之间通过连接边使得 C 内每个面都是三角形面，则我们把 C 称为图 G 的一个纯弦圈，并把 C 内每条边称为 C 的弦。为叙述方便，把极大平面图中的一个三角形也视为一个纯弦圈。

EBERHARD 的构造方法实际上是把一个极大平面图中长度分别为 3, 4, 5 的纯弦圈中所有的弦删去，然后在圈内添加一个顶点，并让该顶点与其圈上每个顶点相邻。

1999 年到 2000 年，王绍文^[5,6]给出了类似构造极大平面图方法，该方法实际上是把 EBERHARD 的构造方法从长度分别为 3, 4, 5 的纯弦圈扩展到任意长度的纯弦圈上。其方法与 EBERHARD 的完全一样：首先把纯弦圈内的所有弦删去，然后在其圈

内添加一个新的顶点，并让该顶点与圈上所有顶点相连即可。

EBERHARD之后，时隔83年的1974年，BARNETTE^[7]与BUTLER^[8]分别独立地给出了构造所有5-连通极大平面图的方法。不同于EBERHARD的初始对象 K_4 ，BARNETTE与BUTLER的初始对象是正二十面体，运算算子也有3个，把他们的运算系统记为 $\langle Z_{20}; \Phi = \{\varphi_4, \varphi_5, \varphi_6\} \rangle$ ，其中， Z_{20} 为正二十面体， $\varphi_4, \varphi_5, \varphi_6$ 是它的3个算子，其功能如图2所示，其中省略号表示该顶点所关联的两条边之间可能含有边，也可能不含边，以示每个顶点的度数至少为5。

简言之，BARNETTE与BUTLER的构造方法是：从正二十面体出发，通过不断地使用如图2给出的3种算子 φ_4, φ_5 或 φ_6 可得到所有的5-连通极大平面图。

1983年，BATAGELJ^[9]对BARNETTE与BUTLER的方法进行了改进，更确切地讲，是将运算系统中的1个算子进行了更换，故该方法初始对象仍是正二十面体，算子也有3个，把他们的运算系统记为 $\langle Z_{20}; \Phi = \{\varphi_4, \varphi_5, \varphi_7\} \rangle$ ， φ_7 称为翻转算子，它的功能如图3所示，其中在 φ_7 作用前的图中(图3(a)示)，顶点 x 与 y 不相邻。

其实，翻转算子并不是 BATAGELJ 首次提出的，这个概念早在 1936 年就由 WAGNER^[10]提出了。由于目前对翻转算子的研究较为深入，故在后面专门对其给予较为详细的讨论。

2005 年，BRINKMANN 和 MCKAY^[11]对

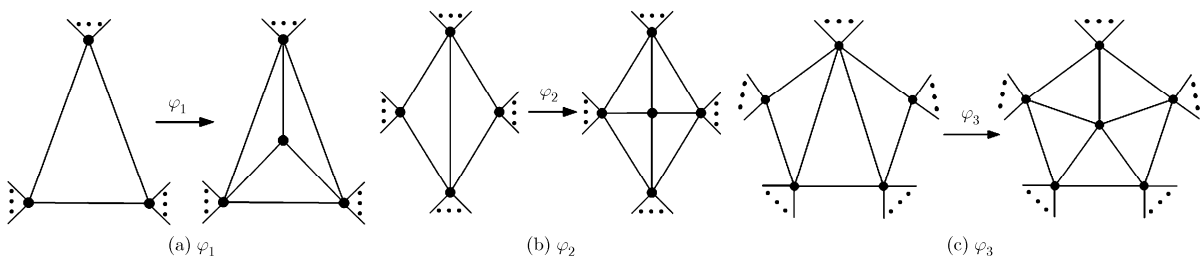


图1 EBERHARD构造极大平面图的3种算子

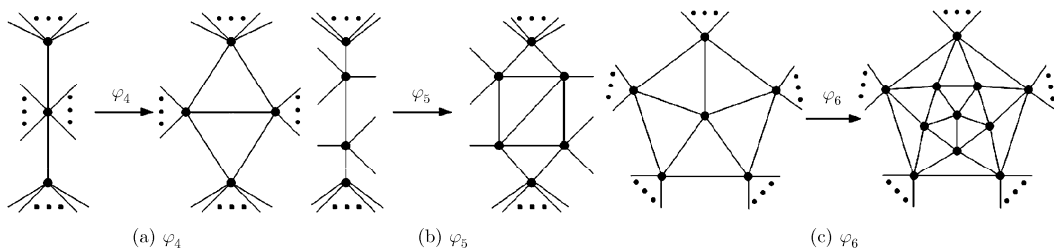


图2 BARNETTE与BUTLER构造极大平面图的3种算子

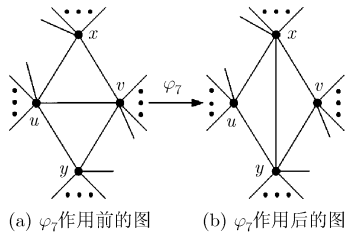


图3 翻转算子

BARNETTE, BUTLERY 以及 BATAGELJ 的工作进行了更为细致的研究, 给出了构造最小度为 5 的极大平面图的一种有效方法, 指出上述 4 种算子 $\varphi_4, \varphi_5, \varphi_6, \varphi_7$ 中在什么情况下可以构造出不含分离 3-圈以及不含 4-圈与分离 5-圈的最小度为 5 的极大平面图。在此基础上, 利用上述 4 种算子, 给出了用于电子计算机构造的算法程序。特别地, 利用构造性的方法, 给出了 12-40 阶的所有最小度为 5 的极大平面图的个数。其中阶数为 40 且最小度为 5 的 3-连通, 4-连通, 5-连通的极大平面图分别有 8469193859271, 7488436558647, 5925181102878 个。这里要说明的是, 在处理同构问题时, 利用的是 MCKAY^[12] 在 1998 年所建立的算法。

关于生成极大平面图的算法, AVIS^[13] 在 1996 年给出了一个时间复杂度为 $O(r \cdot f(n, r))$ 的生成所有 n -阶带根的 3-连通极大平面图的算法, 主要步骤为: 首先构造 n -阶标准极大平面图(恰含两个度数为 $n-1$ 的顶点的极大平面图), 再通过边翻转运算得到所有极大平面图。

2004 年, NAKANO^[14] 给出的算法可在 $O(r \cdot f(n, r))$ 时间内生成所有 n -阶带根的 3-连通极大平面图。2007 年, BRINKMANN 与 MCKAY^[15] 利用标准构型路^[12]的方法引入了 Plantri 运算规则, 并给出了生成极大平面图的算法实现——Plantri 程序^[16]。

设 G 为一个极大平面图, 边 $e = uv$ 所在两个三角形为 Δuvx 与 Δuvy 。若在 G 中删去边 e , 再添加一条新边 $e' = xy$ 后, 所得之图仍是极大平面图, 则称此运算为**边翻转运算**, 或简称为**翻转算子**, 并将边 e 称为**可翻转的**, 如图 3 所示。

显然, 翻转算子将一个极大平面图转化为另一个与其边数相等的极大平面图。自然会提出下面的问题: 一个 n -阶极大平面图能否在有限次翻转运算后转化为另一个给定的 n -阶极大平面图? 1936 年, WAGNER^[10] 首次对此问题给出了肯定的回答。虽然 n -阶极大平面图的个数是 n 的指数级的, 但是 WAGNER 采用将任意极大平面图转化为一类标准极大平面图的方法, 有效地回避了图同构问题, 证

明了一个 n -阶极大平面图在至多 $2n^2$ 次边翻转后可转化为另一个给定的 n -阶极大平面图。其中标准极大平面图是 WAGNER 提出的 n -阶极大平面图记为 Δ_n 。

此后, 有许多学者对这个问题也进行了研究, 并改进了此上界。1993 年, NEGAMI 与 NAKAMOTO^[17] 证明了任意 n -阶极大平面图经过 $O(n^2)$ 次边翻转可转化为 Δ_n 。KOMURO^[18] 证明了两个 n -阶极大平面图可至多通过 $8n - 54$ ($8n - 48$) 次边翻转相互转化, 其中 $n \geq 13$ ($n \geq 7$)。MORI 等人^[19] 证明了任意 n -阶 Hamilton 极大平面图可至多通过 $2n - 10$ 次边翻转转化为 Δ_n , 并保持 Hamilton 性不变; 任意 n -阶极大平面图至多通过 $n - 4$ 次边翻转可转化为 4-连通的; 任意两个 n -阶极大平面图可至多通过 $6n - 30$ 次边翻转相互转化。

2001 年, GAO 等人^[20] 证明了每个 n -阶极大平面图 G 至少包含 $n - 2$ 条可翻转的边, 且存在一类极大平面图使得其可翻转的边数恰好为 $n - 2$ 。进一步, 若 $\delta(G) \geq 4$, 则 G 至少包含 $2n + 3$ 条可翻转的边, 且这个下界也是可达的。

2011 年, BOSE 等人^[21] 证明了任意 n -阶极大平面图至多通过 $\lfloor (3n - 6)/5 \rfloor$ 次边翻转可转化为 4-连通的, 并且任意两个 n -阶极大平面图可至多通过 $5.2n - 32.8$ 次边翻转运算相互转化。

以上概述了极大平面图的几种构造方法与算法, 它们的缺点是: 不易与图的顶点着色结合起来。基于此, 本文提出了一种新的极大平面图的构造方法, 称为**扩缩运算法**, 此方法能够有机地将着色与构造融为一体(见本系列文章(5)), 证明了任意两个极大平面图间均可通过 4 对基本扩缩运算到达对方。弄清楚了扩缩运算本质上与一种称为**多米诺构形**的半极大平面图息息相关。故本文刻画了多米诺构形的特征, 给出了构造多米诺构形的运算系统; 在此基础上, 给出了构造任一最小度 ≥ 4 的非可分极大平面图 G 的所有祖先图与子孙图的方法, 并且证明了任意最小度 ≥ 4 的 n ($n \geq 9$)-阶非可分极大平面图均可由 $(n - 2)$ -阶或 $(n - 3)$ -阶的极大平面图通过多米诺扩轮运算得到。而对**可分极大平面图**的构造, 给出了简洁方法与步骤。

特别要说明的是: 按照本系列文章(1)^[22]中所给出的证明四色猜想的思路, 需用到本文所提出的极大平面图扩缩运算系统。

从着色的角度, 4-色极大平面图中的 3 度顶点删除与添加对结构与着色之间关系的研究几乎没有意义, 故本文一般考虑的是最小度 ≥ 4 的极大平面图。作为扩缩运算系统的应用, 文中构造出了

6~12 阶的所有最小度 ≥ 4 的极大平面图。

本文所言之图皆指有限简单无向图。对于给定图 G ，分别用 $V(G)$ ， $E(G)$ ， $d_G(v)$ 和 $N_G(v)$ 来表示图 G 的顶点集，边集，顶点 v 的度数和顶点 v 的邻域 (即与顶点 v 相邻的所有顶点构成的集合)，可分别简记为 V ， E ， $d(v)$ ， $N(v)$ 。图 G 的阶是 $V(G)$ 中元素的个数 $|V(G)|$ 。若 $V' \subseteq V$ ， $E' \subseteq E$ ，且 E' 中每条边的两个端点均在 V' 中，则称图 $H = (V', E')$ 是图 G 的一个子图。在子图 H 中，如果对于 $\forall u, v \in V(H)$ ， u, v 在 G 中相邻当且仅当它们在图 H 中相邻，则称 H 为 G 的一个由 V' 导出的子图，记为 $G[V']$ 。对于点不交的两个图 G, H ，若将图 G 中的每个顶点与图 H 中的每个顶点相连边，则得到的新图称为图 G 与图 H 的联图，记为 $G \vee H$ 。用 K_n 表示 n -阶完全图。 K_1 与 n 阶圈 C_n 的联图 $C_n \vee K_1$ 称作轮图或 n -轮，记作 W_n (图 4 分别列出了轮图 W_3, W_4, W_5)，其中 C_n 称为 W_n 的轮圈； K_1 的顶点称为该轮的轮心。若 $V(K_1) = \{x\}$ ，则有时也把 W_n 的圈 C_n 用 C^x 来表示。

如果一个图能够画在平面上使得它的边仅在顶点相交，则称这个图为平面图。平面图的这样一种画法称为它的一个平面嵌入，本文所研究的平面图均是指基于它的一个平面嵌入下的平面图。对于一个平面图，如果只要任何两个不相邻的顶点之间再加一条边，其平面性一定被破坏，则称该平面图为极大平面图。若一个平面图的每个面 (包括无穷面) 都由三条边界组成，则称该平面图为三角剖分图。易证，极大平面图和三角剖分图是等价的。若一个最小度 ≥ 4 的极大平面图含有一个顶点导出真子图是极大平面图，则称该极大平面图是可分图。

把满足下列条件的平面图 G^C 称为基于 C 的半极大平面图：只有含 ∞ 面的边界 C 满足 $|C| \geq 4$ ，其余面的边界均为三角形。称 C 为 G^C 的外圈。

文中未定义的记号与定义参见文献[22,23]。

2 极大平面图的基本扩缩运算系统

本节给出极大平面图基本扩缩运算系统，它由

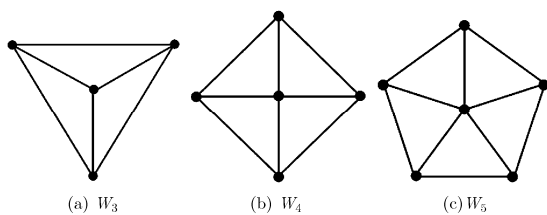


图 4 3 个最小的轮图

运算对象与基本算子两个部分构成，其中运算对象是极大平面图，基本算子有 4 对：扩 i -轮运算及逆运算缩 i -轮运算， $i = 2, 3, 4, 5$ 。该运算系统的基本功能是：以 K_4 作为初始运算对象，通过反复使用 4 种基本扩轮运算，可以生成任意一个给定的极大平面图。

扩 2-轮运算的步骤为：(1)在某条边 uv 的两端点之间再连接一条边，使其产生 2 重边，即产生 2-圈；(2)在该 2-圈内部添加一个新的顶点 x ，并令 x 与 2-圈的两顶点 u 与 v 相连边，产生一个 2-轮；缩 2-轮运算的作用对象子图是一个 2-轮，其步骤是：(1)删除该 2-轮的轮心及相关联的两条边；(2)删除 2 重边中的一条。扩 2-轮与缩 2-轮的运算过程见图 5 所示。扩 2-轮运算在极大平面图中的对象子图是一条边，如图 6(a)所示。

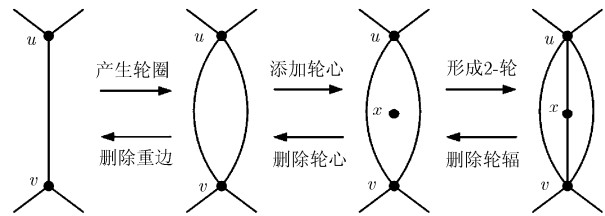


图 5 扩缩 2-轮运算过程示意图

扩 3-轮运算：在极大平面图的某一个面上加入一个顶点 x ，并让 x 与构成该面的 3 个顶点相连边。因此，扩 3-轮运算在极大平面图中的对象子图是一个三角形，如图 6(b)所示。缩 3-轮运算：将某个 3 度顶点以及与该顶点相关联的边删去。

扩 4-轮运算的步骤为：(1)在极大平面图中某条 2-长路 $P_3 = v_1v_2v_3$ 上，从顶点 v_1 出发，沿着 $v_1 \rightarrow v_2 \rightarrow v_3$ 方向，从边-点-边的内部划开，即将边 v_1v_2 ，顶点 v_2 以及边 v_2v_3 从中间划开，使得顶点 v_2 变成两个顶点，分别记作 v_2 与 v'_2 ； v_1v_2 与 v_2v_3 均变成了两条边，分别是 v_1v_2 与 $v_1v'_2$ ， v_2v_3 与 v'_2v_3 ，原来在 P_3 左侧与 v_2 关联的边变成与 v_2 关联，原来在 P_3 右侧与 v_2 关联的边变成与 v'_2 关联，从而保持平面性，该过程如图 7 中第 1 个到第 4 个图所示；(2)在顶点 v_1, v'_2, v_3, v_2 这 4 个顶点形成的 4-圈内增加一个新顶点 x ，并将 x 分别与顶点 v_1, v'_2, v_3, v_2 相连边，如图 7 中的第 5 个图所示。缩 4-轮运算：在极大平面图中，将某 4-度顶点以及与它关联的边均删去，并对该顶点邻域中的某一对不相邻的顶点实施收缩运算，其过程如图 7 中第 5 个到第 1 个图所示。

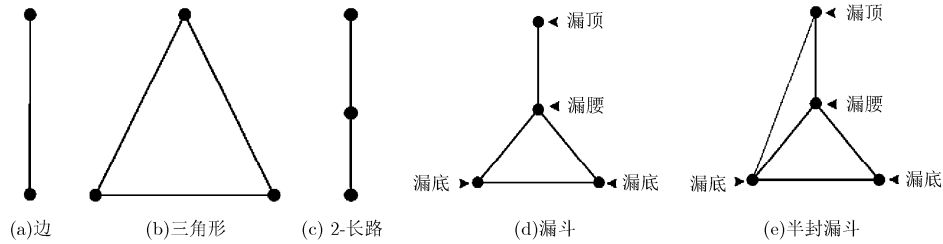


图 6 基本扩轮运算的 4 个对象子图及半封漏斗子图

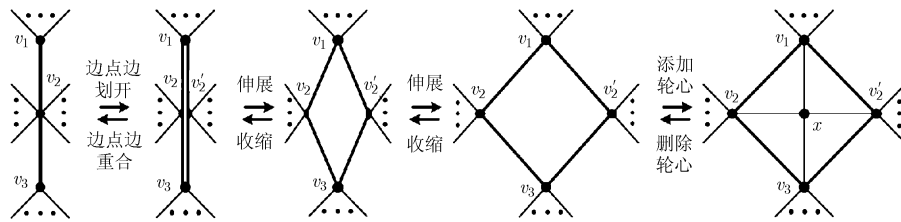


图 7 扩缩 4-轮运算的示意图

把图 6(d)中所示的图称为漏斗，它是极大平面图中施行扩 5-轮运算的对象子图，其中度数为 1 的顶点称为漏顶；度数为 3 的顶点称为漏腰；两个度数为 2 的顶点称为漏底。若一个图的顶点导出子图是漏斗，则该子图称为漏斗子图。在漏斗上给漏顶与一个漏底连边所形成的图称为半封漏斗，如图 6(e) 示。若在一个极大平面图中由 4 个顶点导出的子图是半封漏斗，则称该子图为半封漏斗子图。半封漏斗子图是构造子孙图与祖先图的一个对象子图。

扩 5-轮运算的步骤如图 8 示，其步骤为：(1)对极大平面图中某漏斗子图 $L = v_1 - \Delta v_2 v_3 v_4$ ，从顶点 v_1 出发，沿着 $v_1 \rightarrow v_2$ 方向，从边-点内部划开，即将边 $v_1 v_2$ ，顶点 v_2 从中间划开，使得顶点 v_2 变成两个顶点，分别记作 v_2 与 v_2' ； $v_1 v_2$ 变成了两条边，分别是 $v_1 v_2$ 与 $v_1 v_2'$ ；原来在 L 左侧与 v_2 关联的边变成与 v_2 关联，原来在 L 右侧与 v_2 关联的边变成与 v_2' 关联，从而保持平面性，该过程如图 8 中第 1 个到第 4 个图所示；(2)在顶点 v_1, v_2, v_3, v_4, v_2' 这 5 个顶点形成的 5-圈内增加一个新顶点 x ，并将 x 分别与顶点 v_1, v_2, v_3, v_4, v_2' 相连边，如图 8 中的第 5 个图所示。**缩 5-轮运算**：在极大平面图中，将某 5-度顶点以及与其关联的边均删去，并对该顶点邻域中的某一对不

相邻的顶点实施收缩运算即可，其过程如图 8 中第 5 个到第 1 个图所示。

以上给出了基本扩缩运算系统的 8 种运算(或算子)，用 $\Psi = \{\zeta_2^-, \zeta_2^+, \zeta_3^-, \zeta_3^+, \zeta_4^-, \zeta_4^+, \zeta_5^-, \zeta_5^+\}$ 来表示。我们把其中的 $\zeta_2^-, \zeta_2^+, \zeta_3^-, \zeta_3^+$ 均称为过程运算，把 $\zeta_4^-, \zeta_4^+, \zeta_5^-, \zeta_5^+$ 称为终结运算。用 $\zeta_i^-(G)$ 表示在极大平面图 G 中缩 i -轮运算后得到的图，用 $\zeta_i^+(G)$ 表示在极大平面图 G 中扩 i -轮运算后得到的图。在不考虑缩或扩 i -轮运算中 i 值大小时，分别用 $\zeta^-(G)$ 与 $\zeta^+(G)$ 来代替 $\zeta_i^-(G)$ 与 $\zeta_i^+(G)$ ；用 $\zeta^{2-}(G)$ 表示对 $\zeta^-(G)$ 实施 1 次缩轮运算，或对 G 实施 2 次缩轮运算后所得之图；同理，用 $\zeta^{m+}(G)$ 表示对 G 实施 m 次扩轮运算后所得之图。

显然，对于一个最小度 ≥ 4 且非可分的极大平面图，只经过 1 次扩轮，或缩轮运算，所得之图 $\zeta^+(G)$ ， $\zeta^-(G)$ 虽然均为极大平面图，但 $\zeta^+(G)$ 与 $\zeta^-(G)$ 的最小度可能为 2 度或 3 度，也可能是可分图。无论 $\zeta^+(G)$ 与 $\zeta^-(G)$ 的最小度是多少，下列结论是成立的：

定理 1 设 G 是一个最小度 ≥ 4 的极大平面图，且 G 的阶数为 n 。则

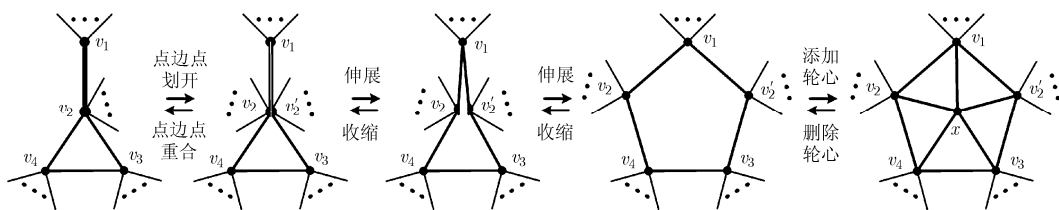


图 8 扩缩 5-轮运算的示意图

$$|\zeta_2^-(G)| = |\zeta_3^-(G)| = |V(G)| - 1 = n - 1 \quad (1)$$

$$|\zeta_4^-(G)| = |\zeta_5^-(G)| = |V(G)| - 2 = n - 2 \quad (2)$$

证明略。

3 多米诺扩缩运算系统

3.1 连续扩缩运算与多米诺扩缩运算

上节给出了 4 对基本扩缩运算。基本扩缩运算系统是一种用于构造极大平面图的操作系统，更确切地讲，是一种能有机地将着色与结构相融合的极大平面图的构造方法。在基本扩缩运算系统中，基于 K_4 可构造出任一极大平面图。因此，一般需要实施多次扩缩运算方能实现，我们把连续多次实施扩缩运算也称为连续扩缩运算。

如前面所述，本文主要考虑最小度 ≥ 4 的极大平面图。因此，当通过 1 次扩或缩运算所得之图 $\zeta^+(G)$ 或 $\zeta^-(G)$ 含有 2 度或 3 度顶点时，需要继续实施扩或缩运算，直到所得之极大平面图的最小度 ≥ 4 ，或为 K_4 。

设 G 是一个最小度 ≥ 4 的极大平面图。 W_4 (或 W_5) 是它的一个 4-轮 (或 5-轮)。对 W_4 (或 W_5) 实施缩 4-轮 (或 5-轮) 运算，若 $\zeta^-(G)$ 的最小度 ≥ 4 ，则本次缩轮运算结束，并把此运算称为一次多米诺缩轮运算；若 $\zeta^-(G)$ 中含有 2-度或 3 度顶点，则实施缩 2-轮或缩 3-轮运算。若所得之图 $\zeta^{2-}(G)$ 的最小度 ≥ 4 ，则本次缩轮运算结束，并把此连续 2 次缩轮运算称为一次多米诺缩轮运算；若 $\zeta^{2-}(G)$ 中含有 2 度或 3 度顶点，则继续实施缩 2-轮或缩 3-轮运算，若缩轮之后仍含 2 度或 3 度顶点，则仍继续进行缩 2-轮或缩 3-轮运算，如此步骤，不断重复 (设总共实施了 m 次缩轮运算)，则可能出现两种情况，(1) m 次缩轮运算之后所得之极大平面图 $\zeta^{m-}(G)$ 的最小度 ≥ 4 ，对此情况，我们把这连续 m 次缩轮运算称为一次多米诺缩轮运算；(2) $\zeta^{m-}(G) \cong K_4$ ，则称 G 为可多米诺极大平面图。如图 9(a) 给出了一个 9-阶可多米诺极大平面图，对粗线所标的 4-轮实施缩 4-轮运算，其中 u, v 为收缩点，所得 $\zeta^-(G)$ 如图 9(b) 所示，由

于 $\zeta^-(G)$ 含 2 个 2 度顶点，因此分别对这两个 2 度顶点实施缩轮运算，所得 $\zeta^{3-}(G)$ 含 3 度顶点，于是继续实施缩 3-轮运算，如此反复，直到所得之图的最小度 ≥ 4 或者为 K_4 ，其过程如图 9(b)~图 9(d) 所示。

设 G 是一个最小度 ≥ 4 的极大平面图， P_3 (或 L) 是它的一条 2-长路 (或漏斗子图)。则对 G 实施基于 P_3 (或 L) 的扩 4-轮 (或扩 5-轮) 运算所得之图 $\zeta^+(G)$ 过程为一次多米诺扩轮运算。若对 G 首先实施扩 2-轮或扩 3-轮运算，则所得之图 $\zeta^+(G)$ 含 2 度或 3 度顶点，需继续对 $\zeta^+(G)$ 实施扩轮运算，若所得之图 $\zeta^{2+}(G)$ 的最小度 ≥ 4 ，则把这 2 次的扩轮运算称为一次多米诺扩轮运算；若 $\zeta^{2+}(G)$ 中含有 2 度或 3 度顶点，则继续实施扩轮运算，若扩轮之后仍含 2 度或 3 度顶点，则仍继续进行扩轮运算，如此步骤，不断重复，若 m 次扩轮运算之后所得之极大平面图 $\zeta^{m+}(G)$ 的最小度 ≥ 4 ，则我们把这连续 m 次的扩轮运算称为一次多米诺扩轮运算。关于多米诺扩轮运算的实例在 3.2 节中给出。

3.2 轮心数 ≤ 3 的多米诺扩缩运算与多米诺构形

对于一个最小度 ≥ 4 的极大平面图 G ，经过 m 次连续扩轮运算构成的一次多米诺扩轮运算后所得之图 $\zeta^{m+}(G)$ ， G 与 $\zeta^{m+}(G)$ 之间结构的变化与一种称为多米诺构形的子图有关，下面，我们根据 $m = 1, 2, 3$ 的情况来详细分析多米诺构形。

若 $m = 1$ ，则 $\zeta^+(G)$ 由扩 4-轮或扩 5-轮运算获得，将扩轮的轮心及它的邻域构成顶点的导出子图，即 4-轮 W_4 与 5-轮 W_5 均称为多米诺构形，这两个构形的外圈分别为 4-圈与 5-圈，其中扩轮前对象子图分别为 2-长路与漏斗子图，如图 10 所示。设 $\zeta^+(G)$ 是一个最小度 ≥ 4 的极大平面图， $W_4 = x - v_1 v_2 v_3 v_4$ 是一个如图 10(a) 所示的 4-轮，它满足： $d_{\zeta^+(G)}(v_1), d_{\zeta^+(G)}(v_3) \geq 6$ 。则对 W_4 实施基于点对 $\{v_2, v_4\}$ 的缩 4-轮运算后的图记作 G ，显然 $\delta(G) \geq 4$ ，故从 $\zeta^+(G)$ 到 G 的缩轮运算是一次多米诺缩轮运算，将 $\zeta^+(G)$ 中的 W_4 称为多米诺构形。

同理，若 $W_5 = x - v_1 v_2 v_3 v_4 v_5$ 是 $\zeta^+(G)$ 的一个 5-轮，且 $d_{\zeta^+(G)}(v_1) \geq 6$ ， $d_{\zeta^+(G)}(v_3), d_{\zeta^+(G)}(v_4) \geq 5$ ，则对

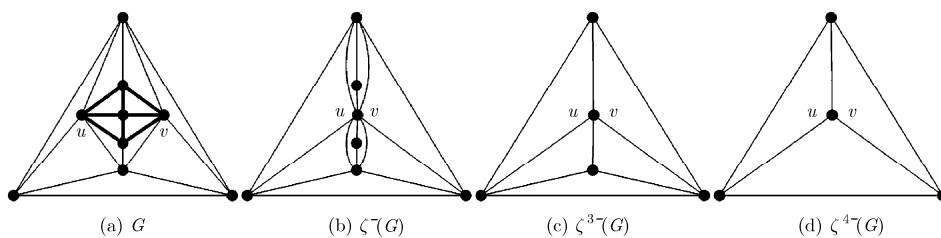


图 9 一个 9-阶可多米诺极大平面图

W_5 实施基于点对 $\{v_2, v_2'\}$ 的一次缩 5-轮运算是一个多米诺缩轮运算，将 $\zeta^+(G)$ 中的 W_5 称为多米诺构形；如图 10(b) 示。

若 $m = 2$ ，则 $\zeta^{2+}(G)$ 可由扩 24-轮(即先实施扩 2-轮，再实施扩 4-轮的运算，其余定义类似)、扩 34-轮、扩 25-轮及扩 35-轮运算(2 种：**I-型扩 35-轮**，即扩 3-轮的轮心是扩 5-轮的漏顶；**II-型扩 35-轮**，即扩 3-轮的轮心是扩 5-轮的漏底)获得，将扩轮过程中的 2 个轮心及它的邻域构成顶点子集的导出子图称为多米诺构形，其中扩轮前的对象子图分别为 2-长路、漏斗子图和哑铃子图(即有一个公共顶点的两个三角形构成的子图)，如图 11 所示。

注：扩 25-轮、扩 34-轮和 II-型扩 35-轮所得之多米诺构形相同。因此，含两个轮心的多米诺构形共有 3 个。

类似于图 10 中关于多米诺缩轮运算的讨论，含有 2 个轮心的扩轮运算的逆运算共有 5 个：缩 24-轮运算、缩 25-轮运算、缩 34-轮运算、I-型缩 35-轮运算与 II-型缩 35-轮运算，如图 11 所示。易推出这 5 种多米诺缩轮运算的必要条件。如缩 24-轮运算的必要条件是构形的外圈上非收缩顶点的度数均 ≥ 6 。

若 $m = 3$ ，则 $\zeta^{3+}(G)$ 可能是由下列扩轮运算获得：扩 224-轮运算；扩 234-轮运算；2 种扩 334-轮(一

种是两个扩 3-轮轮心不相邻的情况，如图 12(c) 所示，称为不相邻型的扩 334-轮、另一种是两个扩 3-轮轮心相邻的情况，如图 12(d) 所示，称为相邻型的扩 334-轮)；2 种扩 235-轮运算(一种是扩 2-轮与扩 3-轮的两个轮心相邻的情况，如图 12(e) 所示，称为相邻型的扩 235-轮、另一种是扩 2-轮与扩 3-轮的两个轮心不相邻的情况，如图 12(f) 所示，称为不相邻型的扩 235-轮)；3 种扩 335-轮运算(一种是不相邻型的扩 335-轮，如图 12(g) 示、一种是非对称相邻型，如图 12(h) 示、另一种是对称相邻型，如图 12(i) 示)。我们把扩轮过程中的 3 个轮心及它们的邻域构成的顶点子集的导出子图，均称为多米诺构形。图 12 所示的 9 个多米诺构形中，扩轮前的对象子图有 3 种类型：2-长路、漏斗子图和哑铃子图。把不相邻型的扩 334-轮运算称为哑铃变换，在后面的纯树着色研究中起关键作用^[24]，这方面更详细研究见本系列文章(3)。

注：图 12 给出了 9 个含 3 个轮心的扩轮运算，但其中的相邻型扩 334-运算与扩 235-运算所得的多米诺构形相同；扩 234-运算与非对称相邻型扩 335-运算所得之多米诺构形相同。因此，含 3 个轮心的多米诺构形共有 7 个。

类似前面含 1~2 个轮心的缩轮运算，含 3 个轮心的缩轮运算共 9 个，分别是：缩 224-轮运算、缩

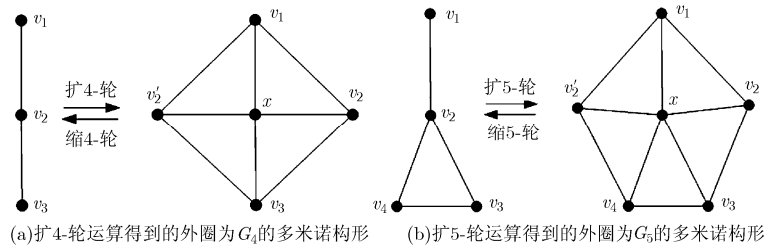


图 10 含 1 个轮心的 2 个多米诺构形

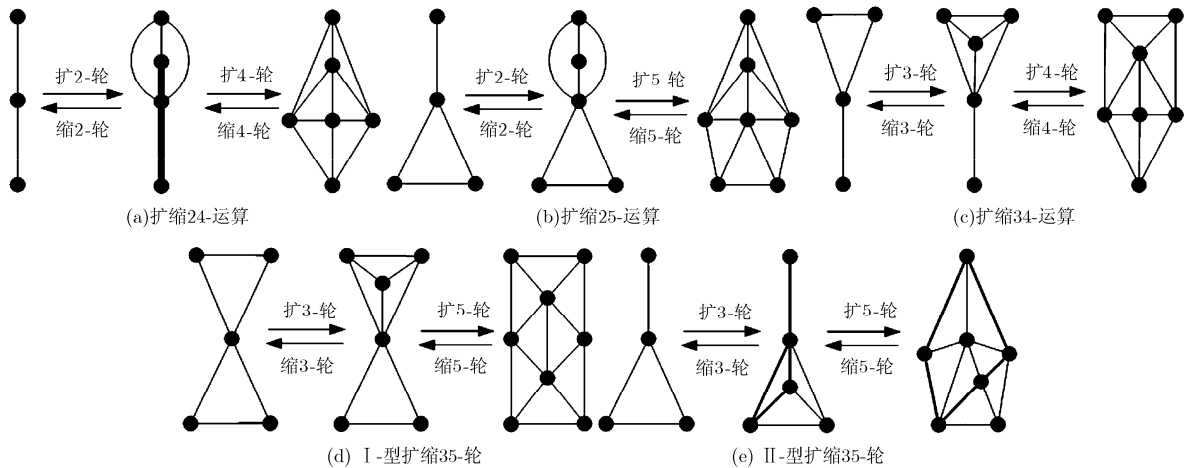


图 11 含 2 个轮心的多米诺构形

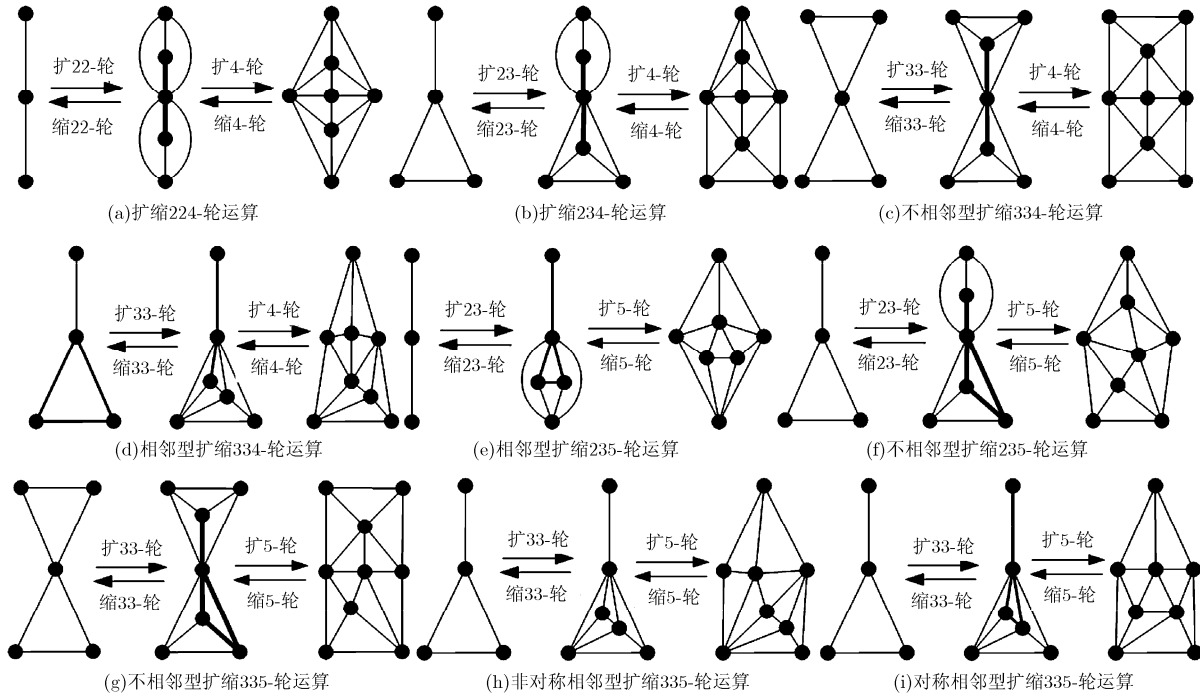


图 12 含 3 个轮心的 7 个多米诺构形

234-轮运算、不相邻型缩 334-轮运算、相邻型缩 334-轮运算、相邻型缩 235-轮运算、不相邻型缩 235-轮运算、不相邻型缩 335-轮运算、非对称相邻型缩 335-轮运算、对称相邻型缩 335-轮运算，如图 12 所示。易推出这 9 种多米诺缩轮运算的必要条件。这里不再赘述。

综上所述，含 1-3 个轮心的多米诺构形共有 12 个，为方便，我们把从图 10~图 12 中的全部 12 个多米诺构形集中于图 17。并将图 17 前两行中所示的 5 个多米诺构形称为基本多米诺构形。今后有时把多米诺构形的轮心又称为多米诺构形的内点。

3.3 扩轮对象集

在 3.2 节所给出的扩 4-轮与扩 5-轮运算中，只有 1 次扩轮运算对象子图分别是 2-长路 $P_3 = v_1v_2v_3$ 和 $L = v_1 - \Delta v_2v_3v_4$ 。若在 $P_3 = v_1v_2v_3$ 中， v_1 与 v_3 相邻，或在 $L = v_1 - \Delta v_2v_3v_4$ 中顶点 v_1 恰与其中一个漏底相邻，则进行一次基本扩 4-轮或 5-轮运算之后所得之图均为可分图。故对只扩 1 次的基本扩轮对象，要求 P_3 的两个端点不相邻、也要求在 L 中漏顶与漏底不相邻。但对于施行 2 次，或者 3 次基本扩轮运算，则情况有所不同，下面逐一说明之：

注 1: 设 G 是最小度 ≥ 4 的极大平面图。 $P_3 = v_1v_2v_3$ 是 G 中一条 2-长路，且 v_1 与 v_3 相邻。当这种情况的 P_3 作为扩轮的初始对象时，则对基于 P_3 的任一 $m \geq 1$ 次扩轮运算所得之图 $\zeta^{m+}(G)$ 是含有以 $\Delta v_1v_2v_3$ 可作为无穷面的可分子图。

注 2: 设 G 是最小度 ≥ 4 的非可分极大平面图。 $L = v_1 - \Delta v_2v_3v_4$ 中顶点 v_1 恰与其中一个漏底相邻，是 G 的一个半封漏斗子图，其中设 v_1 与 v_3 相邻。则对基于 L 的任一 $m \geq 2$ ， $\zeta^{m+}(G)$ 是非可分极大平面图。此结论可由图 13(g)~图 13(j) 给予说明。

注 3: 设 G 是最小度 ≥ 4 的非可分极大平面图。 $Y = \Delta v_1v_2u - \Delta uv_3v_4$ 是 G 的一个哑铃子图，如图 13(c) 所示。无论 v_1 与 v_3 ，或 v_2 与 v_4 相邻与否，则对基于 Y 的任一 $m \geq 2$ ， $\zeta^{m+}(G)$ 是非可分极大平面图，此结论可由图 13(k)~图 13(l) 给予说明。

基于上述 3 个注，推出多米诺扩轮运算中的对象子图共有如图 13(a)~图 13(f) 6 个。

3.4 多米诺构形的定义

3.2 节中给出了所有的含 1~3 内点的多米诺构形。自然，当多米诺构形的内点数 $m \geq 4$ 时，对应的多米诺构形结构如何？为此，先给出多米诺构形的一般性定义。然后在此基础上，刻画了多米诺构形的特征。首先给出内点数 $m \geq 4$ 的 3 个多米诺构形的例子，如图 14 所示。

注意到 3.2 节中含 1~3 个内点的多米诺构形，乃至按照上述方法得到的含更多内点的多米诺构形均至少包含一个满足下列条件的 4-轮 W_4 或 5-轮 W_5 ：(1) 将它们的轮心均记作 x ，在 C^x 上存在不相邻的顶点对 $\{u, v\} \subset V(C)$ ；(2) 以 W_4 或 W_5 为初始缩轮对象子图，以 $\{u, v\}$ 为初始收缩点对实施一次多米诺缩轮运算，所得到的图只能是：2 长路、漏斗或哑铃。

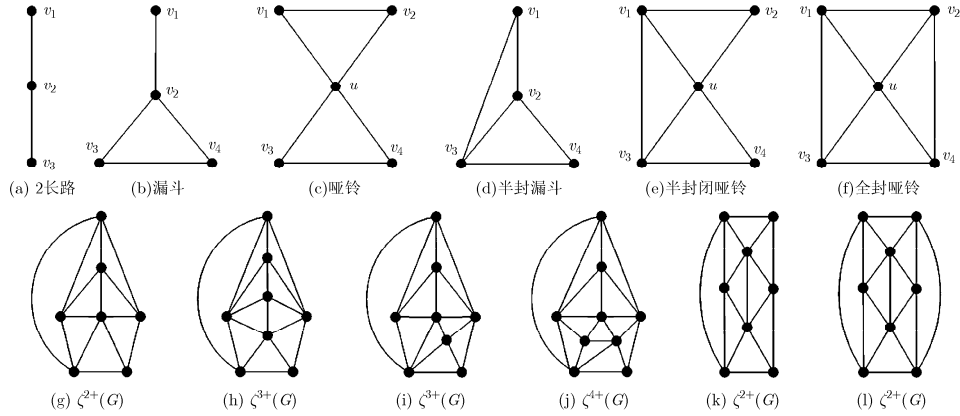


图 13 多米诺运算中扩轮运算的 6 个对象子图及说明

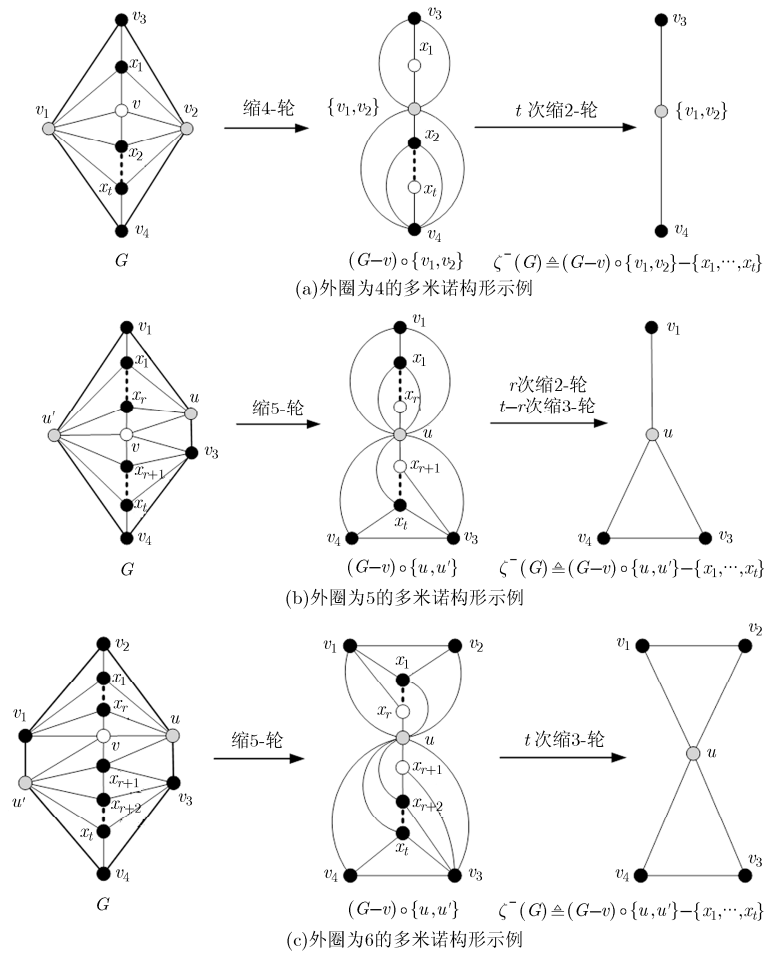


图 14 内点数 ≥ 4 的 3 个多米诺构形

基于上述讨论，下面给出多米诺构形的定义：设 G^C 是一个半极大平面图，若在 G^C 中存在满足下列条件的 4-轮 W_4 或 5-轮 W_5 ，则称 G^C 为一个多米诺构形：(1)用 x 表示 W_4 或 W_5 的轮心，则在 C^x 上存在不相邻的顶点对 $\{u, v\} \subset V(C)$ ；(2)以 W_4 或 W_5 为初始缩轮对象子图，以 $\{u, v\}$ 作为初始收缩点对实施一次多米诺缩轮运算，则所得之图不含内点。并称

$\{u, v\}$ 为 G^C 的缩点对，称 x 为 G^C 的初始收缩轮心。设 G^C 是一个多米诺构形，用 x 表示可缩 4-轮或 5-轮的轮心，即 G^C 的初始收缩轮心。用 $X(x)$ 表示 G^C 的内点集。在不致混淆的情况，将 $X(x)$ 简记为 X 。易证，一个多米诺构形 G^C 收缩之后要么是 2 长路，要么是漏斗，要么是哑铃，并由此推出多米诺构形的外圈长度 $|C| = 4, 5, 6$ ，即有

定理 2 设 G^C 是一个多米诺构形。 $\{u, v\}$ 是 G^C 的缩点对。则

(1) 基于 $\{u, v\}$ 的多米诺收缩运算后所得的之图为 2-长路, 漏斗或哑铃;

(2) $4 \leq |C| \leq 6$ 。

基于定理 2, 我们有

引理 1 设 G^C 是一个多米诺构形, $\{u, v\}$ 是收缩点对。则

(1) 若 $|V(C)| = 4$, 记 $C = uz_1vz_2u$, 则 $d_{G^C}(z_1), d_{G^C}(z_2) \leq 4$;

(2) 若 $|V(C)| = 5$, 记 $C = uz_1vz_2z_3u$, 则 $d_{G^C}(z_1) \leq 4, d_{G^C}(z_2)$ 或 $d_{G^C}(z_3) = 3$;

(3) 若 $|V(C)| = 6$, 记 $C = uz_1z_2vz_3z_4u$, 则 $d_{G^C}(z_1)$ 或 $d_{G^C}(z_2) = 3, d_{G^C}(z_3)$ 或 $d_{G^C}(z_4) = 3$ 。

证明 (1) 若 $d_{G^C}(z_1) \geq 5$, 令 $u, y_1, y_2, \dots, y_l, v$ 是 G^C 内与 z_1 依次相邻的顶点, 其中 $l \geq 3$ 。由于 G^C 是多米诺构形, 设 x 是 G^C 的初始收缩轮心, 则对 G^C 实施基于 x 的多米诺收缩运算, 可使其收缩为 2 长路 P_3 。易知, 在 $G^C[V(C) \cup \{y_1, y_2, \dots, y_l\}]$ 中, 顶点 y_1, y_2, \dots, y_l 的度数均 ≥ 3 。设在多米诺收缩运算过程中, y_1, y_2, \dots, y_l 中第 1 个被收缩的顶点为 y 。记收缩以 y 为轮心的轮之前的图为 $\zeta^-(G^C)$ 。当 $y = y_1$ 或 y_l 时, 在 $\zeta^-(G^C)$ 中 y_2 与 x_v^u 相邻或 y_{l-1} 与 x_v^u 相邻, 其中 x_v^u 是将顶点 u 与 v 收缩后的新顶点。故在 G^C 中 y_2 与 u 相邻或 y_{l-1} 与 v 相邻, 即有 $d_{G^C}(y_2) = 3$ 或 $d_{G^C}(y_{l-1}) = 3$, 与 G^C 是多米诺构形矛盾; 当 $y = y_i, 2 \leq i \leq l-1$ 时, 在 $\zeta^-(G^C)$ 中 y_{i-1} 与 y_{i+1} 相邻, 因此, 在 G^C 中 y_{i-1} 与 y_{i+1} 也相邻, 矛盾。所以, $d_{G^C}(z_1) \leq 4$ 。同理可证, $d_{G^C}(z_2) \leq 4$ 。

(2) 类似情形(1)中证明过程, 可得 $d_{G^C}(z_1) \leq 4$ 。显然, $d_{G^C}(z_2), d_{G^C}(z_3) \geq 3$ 。假设 $d_{G^C}(z_2), d_{G^C}(z_3) \geq 4$ 。令 $u, y_1, y_2, \dots, y_r, \dots, y_l, v$ 是 G^C 内与 z_2, z_3 依次相邻的顶点, 其中 y_r 是 z_2, z_3 的公共邻点, $2 \leq r \leq l-1, l \geq 3$ 。则在 $G^C[V(C) \cup \{y_1, y_2, \dots, y_l\}]$ 中, 顶点 y_r 的度数为 4, $\{y_1, y_2, \dots, y_l\} \setminus \{y_r\}$ 中所有顶点的度数均 ≥ 3 。考虑在多米诺收缩运算过程中 y_1, y_2, \dots, y_l 中第 1 个被收缩的顶点 y 。类似情形(1)中证明过程, 无论 y 是 y_1, y_2, \dots, y_l 中的哪个顶点, 都会导致 G^C 中出

现 3 度顶点, 矛盾。所以, $d_{G^C}(z_2)$ 或 $d_{G^C}(z_3) = 3$ 。

(3) 类似情况(2)的证明, 可得 $d_{G^C}(z_1)$ 或 $d_{G^C}(z_2) = 3, d_{G^C}(z_3)$ 或 $d_{G^C}(z_4) = 3$ 。证毕。

基于引理 1, 易推下述

定理 3 设 G^C 是一个多米诺构形, x 是 G^C 的初始收缩轮点, $\{u, v\}$ 是缩点对。则

(1) 对 C 上的 2-长路 $P_3 = uz_1v$, 其中 z_1 与 x 不相邻, 有 $G^C - z_1$ 是以 x 为初始收缩轮点, $\{u, v\}$ 为缩点对的多米诺构形;

(2) 对 C 上的 3-长路 $P_4 = uz_2z_3v$, 其中 z_2, z_3 与 x 不相邻, 若 $d_{G^C}(z_2) = d_{G^C}(z_3) = 3$, 则 $G^C - \{z_2, z_3\}$ 是以 x 为初始收缩轮点, $\{u, v\}$ 为缩点对的多米诺构形; 若 $d_{G^C}(z_2) = 3, d_{G^C}(z_3) \geq 4$, 则 $G^C - z_2$ 是以 x 为初始收缩轮点, $\{u, v\}$ 为缩点对的多米诺构形。

3.5 多米诺构形的特征

为了刻画多米诺构形的特征, 先给出 4 个运算: $\tau_1, \tau_1', \tau_2, \tau_3$, 称它们为多米诺构形的生成运算, 分别定义如下:

设 G^C 是一个多米诺构形, $\{u, v\}$ 为 G^C 是它的缩点对。 G^C 上的 τ_1 运算是指: 选择 C 上的 2-长路 $P = uvv$ 是, 在 G^C 外添加一个顶点 z , 并令该顶点分别与 u, v, v 相连边, 所得之图记作 $\tau_1(G^C)$, 如图 15(a)所示。

G^C 上的 τ_1' 运算是指: 选择 C 上的 2-长路 $P = xyv$, 且 $x \notin \{u, v\}$ 。在 G^C 外添加一个顶点 z , 并令该顶点分别与 x, y, v 相连边, 所得之图记作 $\tau_1'(G^C)$, 如图 15(b)所示。

G^C 上的 τ_2 运算是指: 选择 C 上的 2-长路 $P = uvv$, 在 G^C 外添加两个相邻顶点 z_1, z_2 , 并令 z_1, z_2 均与 y 相连边, 且 z_1 与 u 相连边, z_2 与 v 相连边, z_1 与 z_2 相连边, 所得之图记作 $\tau_2(G^C)$, 如图 15(c)所示。

G^C 上的 τ_3 运算是指: 选择 C 上的 3-长路 $P = uy_1y_2v$, 在 G^C 外添加一个顶点 z , 并令该顶点分别与 u, y_1, y_2, v 相连边, 所得之图记作 $\tau_3(G^C)$, 如图 15(d)所示。

由上述 4 种运算, 引入多米诺构形生成运算系统, 记作 $\langle \{W_4, W_5\}; \Gamma \rangle$, $\Gamma = \{\tau_1, \tau_1', \tau_2, \tau_3\}$, 该系统

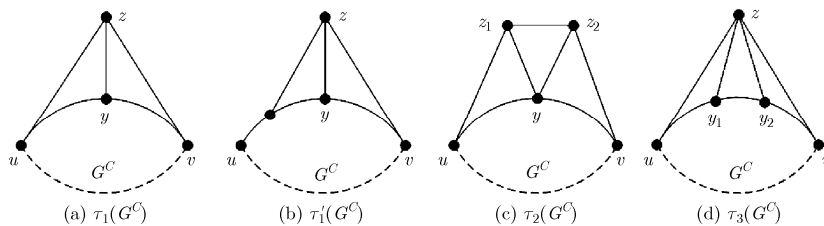


图 15 多米诺构形的 4 个生成算子

意在基于 W_4 与 W_5 ，可生成所有的多米诺构形。如对 W_4 ，相继实施 $\tau_1, \tau_2, \tau_3, \tau_1, \tau_2, \tau_3$ 运算，所得之图 $\tau_3\tau_2\tau_1\tau_3\tau_2\tau_1(W_4)$ 如图 16(a)所示；对 W_5 ，相继实施 $\tau_1, \tau_2, \tau_3, \tau_1, \tau_2, \tau_3$ 运算，所得之图 $\tau_3\tau_2\tau_1\tau_3\tau_2\tau_1(W_5)$ 如图 16(b)所示；对 W_5 ，相继实施 $\tau_1, \tau_2, \tau'_1, \tau'_{11}, \tau'_1, \tau'_1, \tau'_1, \tau'_1$ 运算，所得之图 $\tau'_1\tau'_1\tau'_1\tau'_1\tau'_1\tau'_1\tau'_1\tau'_1(W_5)$ 如图 16(c)所示。

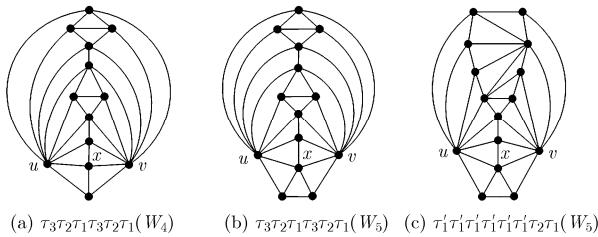


图 16 基于 $\{W_4, W_5\}; \Gamma$ 的 3 个多米诺构形

通过这 3 个例子可以看到，若 G^C 是一个多米诺构形， $\{u, v\}$ 是缩点对。则有下列事实：

事实 1 一次 τ_1 运算等同于一次扩 2-轮运算，故 G^C 是多米诺构形的充要条件是 $\tau_1(G^C)$ 是多米诺构形，且 G^C 与 $\tau_1(G^C)$ 有等长的外圈，即 $|V(\tau_1(C))| = |V(C)|$ ，其中， $\tau_1(C)$ 表示 $\tau_1(G^C)$ 的外圈，下同；

事实 2 一次 τ'_1 运算等同于一次扩 3-轮运算，故 G^C 是多米诺构形的充要条件是 $\tau'_1(G^C)$ 是多米诺构形，且 G^C 与 $\tau'_1(G^C)$ 有等长的外圈，即 $|V(\tau'_1(C))| = |V(C)|$ ；

事实 3 一次 τ_2 运算等同于一次扩 23-轮运算，故 G^C 是多米诺构形的充要条件是 $\tau_2(G^C)$ 是多米诺

构形，但 $|V(\tau_2(C))| = |V(C)| + 1$ ；

事实 4 一次 τ_3 运算等同于一次扩 3-轮运算，故 G^C 是多米诺构形的充要条件是 $\tau_3(G^C)$ 是多米诺构形，但 $|V(\tau_3(C))| = |V(C)| - 1$ 。

定理 4 任一多米诺构形均可通过多米诺运算系统 $\{W_4, W_5\}; \Gamma$ 获得。

证明 对多米诺构形的内点数 n 实施数学归纳法。

当内点数 $n = 2, 3$ 结论成立，其证明如下。

由 3.2 节知含 2 个内点的多米诺构形有 3 个，如图 11，或图 17 中的第 2 行所示。

对 W_4 分别实施 τ_1 与 τ_2 运算，分别得到图 17 中第 2 行的第 1, 2 个含 2 个内点的多米诺构形；对 W_5 实施 τ_1, τ'_1, τ_2 及 τ_3 运算，分别得到图 17 中第 2 行的第 2, 3 个含两个内点的多米诺构形及第 3 行中最后一个含 3 个内点的多米诺构形，其中被收缩顶点对可能不同。

对第 2 行中的第 1 个多米诺构形分别实施 τ_1 与 τ_2 运算，得到第 3 行中第 1 与第 2 个含 3 个内点的多米诺构形；对第 2 行中的第 2 个多米诺构形分别实施 $\tau_1, \tau'_1, \tau'_1, \tau_2$ 与 τ_2 运算，其中被收缩顶点对可能不同，分别得到第 3 行中第 2 个、第 3 个、第 4 个、第 5 个与第 6 个含 3 个内点的多米诺构形；对第 2 行的第 3 个实施 τ'_1 运算，得到第 3 行中的第 6 个含 3 个内点的多米诺构形。

假设内点数 $\leq n (\geq 3)$ 时结论成立。考察多米诺构形 G^C 的内点数为 $n + 1$ 的情况。设 $\{u, v\}$ 是 G^C 的缩点对。基于引理 1，分如下 3 种情况讨论：

情况 1 若 $|V(C)| = 4$ ，且 $C = uz_1vz_2u$ ，则 $d_{G^C}(z_1)$ ，

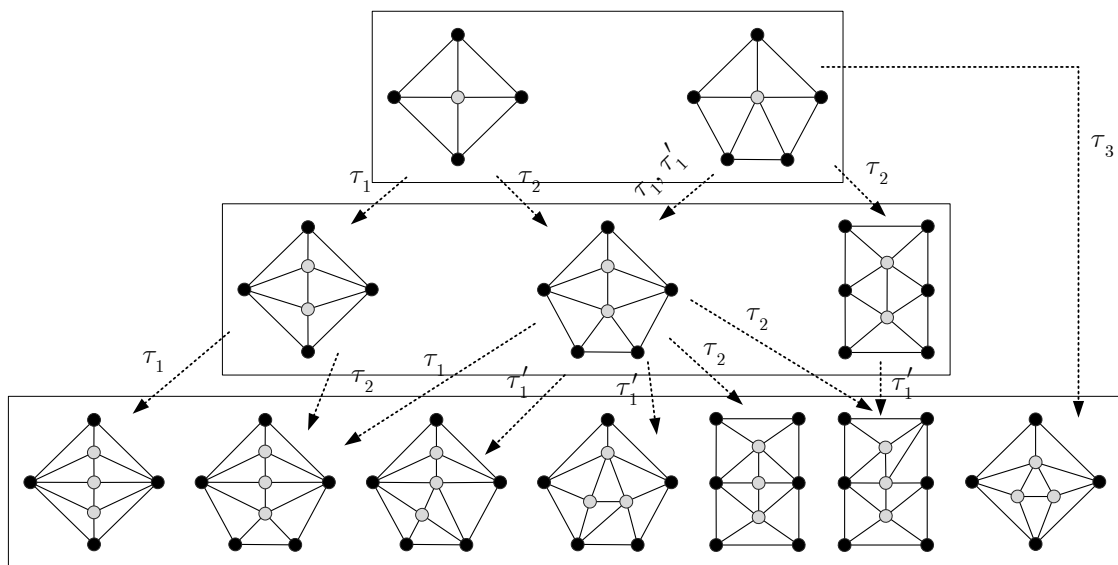


图 17 多米诺生成算子应用实例

$d_{G^C}(z_2) \leq 4$, 且 z_1, z_2 中至少有一个, 设为 z_1 , 与初始轮心点 x 不相邻. 若 $d_{G^C}(z_1)=3$ 时, 则由定理 4 知, $G^C - z_1$ 是多米诺构形, 于是, 由归纳假设知, $G^C - z_1$ 是由 $\langle \{W_4, W_5\}; \Gamma \rangle$ 构造出来的. 注意到 $G^C = \tau_1(G^C - z_1)$, 从而证明了 G^C 可通过 $\langle \{W_4, W_5\}; \Gamma \rangle$ 构造出来的; 若 $d_{G^C}(z_1)=4$ 时, 则由定理 4 知, $G^C - z_1$ 是多米诺构形, 于是, 由归纳假设知, $G^C - z_1$ 是由 $\langle \{W_4, W_5\}; \Gamma \rangle$ 构造出来的. 注意到 $\tau_3(G^C - z_1)=G^C$, 从而证明了 G^C 可通过 $\langle \{W_4, W_5\}; \Gamma \rangle$ 构造出来的. 由此证明了 $|V(C)|=4$ 时, 内点数为 $n+1$ 时情况成立.

情况 2 若 $|V(C)|=5$, 且 $C = uz_1vz_2z_3u$, 则 $d_{G^C}(z_1) \leq 4$, $d_{G^C}(z_2)$ 或 $d_{G^C}(z_3) = 3$. 不失一般性, 设 $d_{G^C}(z_2) = 3$. 则由定理 4 知, $G^C - z_2$ 是多米诺构形, 于是, 由归纳假设知, $G^C - z_2$ 是由 $\langle \{W_4, W_5\}; \Gamma \rangle$ 构造出来的. 注意到 $G^C = \tau'_1(G^C - z_2)$, 从而证明了 G^C 可通过 $\langle \{W_4, W_5\}; \Gamma \rangle$ 构造出来的, 由此证明了 $|V(C)|=5$ 时, 内点数为 $n+1$ 时情况成立.

情况 3 若 $|V(C)|=6$, 且 $C = uz_1z_2vz_3z_4u$ 时 $d_{G^C}(z_1)$ 或 $d_{G^C}(z_2) = 3$, $d_{G^C}(z_3)$ 或 $d_{G^C}(z_4) = 3$. 不失一般性, 设 z_1 与初始轮心点 x 不相邻, 且 $d_{G^C}(z_1)=3$. 基于由定理 3 知, $G^C - z_1$ 是多米诺构形. 由归纳假设知, $G^C - z_1$ 是由 $\langle \{W_4, W_5\}; \Gamma \rangle$ 构造出来的. 注意 $G^C = \tau'_1(G^C - z_1)$, 从而证明了 G^C 可通过 $\langle \{W_4, W_5\}; \Gamma \rangle$ 构造出来的, 由此证明了 $|V(C)|=6$ 时, 内点数为 $n+1$ 时情况成立.

综合上述 3 种情况, 我们证明了内点数为 $n+1$ 时情况成立. 故本定理获证. 证毕

定理 4 给出了多米诺构形的一种构造性方法, 即多米诺构形生成运算系统, 该方法可通过 4-轮与 5-轮构造出任一所需多米诺构形. 而多米诺构形是极大平面图扩缩运算系统的核心.

4 祖先图与子孙图

在极大平面图构造方面, 有两个基本问题: (1) 一个极大平面图从何而来, 更确切地讲, 哪些极大平面图可通过扩轮运算生成该极大平面图; (2) 一个极大平面图能生成多少个不同构的极大平面图. 要解决这两个问题, 定理 5 起关键作用. 为此, 引入祖先图与子孙图概念.

对一个最小度 ≥ 4 的极大平面图 G , 若它可从阶数较低, 且最小度 ≥ 4 的极大平面图 $\zeta^-(G)$ 通过扩轮运算而获得的. 则我们把 $\zeta^-(G)$ 称为 G 的祖先图, 而把 G 称为 $\zeta^-(G)$ 的子孙图. 当然, 对于一个最小度 ≥ 4 的极大平面图 G , 经过扩轮运算后所得到的最小度 ≥ 4 的极大平面图 $\zeta^+(G)$ 而言, G 是 $\zeta^+(G)$

的祖先图, 而 $\zeta^+(G)$ 是 G 的子孙图. 现在, 我们给出精确的定义.

4.1 子孙图

多米诺构形 G^C 的外圈长度可为 4, 5, 6. 我们一般用 $G_{v_2v_2}^{C_4}$, $G_{v_2v_2}^{C_5}$ 和 $G_{v_2v_2}^{C_6}$, 分别表示外圈长度为 4, 5, 6 的多米诺构形; 用 $\mathfrak{S}_{v_2v_2}^{C_4}$, $\mathfrak{S}_{v_2v_2}^{C_5}$, $\mathfrak{S}_{v_2v_2}^{C_6}$, 分别表示外圈长分别为 4, 5 和 6 的所有多米诺构形构成的集合, 其中下标 v_2v_2 表示缩点对 $\{v_2, v_2\}$. 类似于多米诺构形, 我们将一个最小度 ≥ 4 的极大平面图 G 的子孙图相应的分为 3 种类型:

类型 1 路型子孙图: 设 $P_3 = v_1v_2v_3$ 是 G 中的一条 2 长路. 基于 P_3 的扩 4-圈型半极大平面图, 记作 $G_{P_3}^{C_4}$, 是指按下列方法获得的半极大平面图: 在 P_3 上, 从顶点 v_1 出发, 沿着 $v_1 \rightarrow v_2 \rightarrow v_3$ 方向, 从边-点-边的内部划开, 即将边 v_1v_2 , 顶点 v_2 以及边 v_2v_3 从中间划开, 使得顶点 v_2 变成两个顶点, 分别记作 v_2 与 v'_2 ; v_1v_2 与 v_2v_3 均变成了两条边, 分别是 v_1v_2 与 $v_1v'_2$, v_2v_3 与 v'_2v_3 , 原来在 P_3 左侧与 v_2 关联的边变成与 v_2 关联, 原来在 P_3 右侧与 v_2 关联的边变成与 v'_2 关联, 该过程如图 18 所示, 并将顶点对 $\{v_2, v'_2\}$ 称为 $G_{P_3}^{C_4}$ 的扩点对.

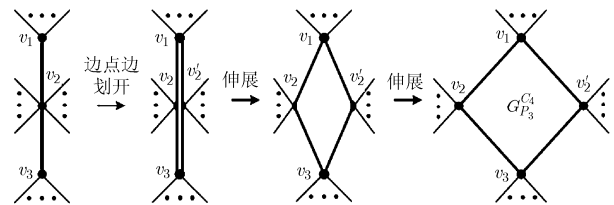


图 18 扩 4-圈型半极大平面图的过程示意图

设 $G_{P_3}^{C_4}$ 是一个扩 4-圈型半极大平面图, 外圈 $C_4 = v_1v'_2v_3v_2$, 且 $\{v_2, v'_2\}$ 是 $G_{P_3}^{C_4}$ 的扩点对, 如图 18 中的最后一个图示. $G_{P_3}^{C_4} \in \mathfrak{S}_{v_2v_2}^{C_4}$, 且外圈 $C_4 = v_1v'_2v_3v_2$, $\{v_2, v'_2\}$ 是 $G_{P_3}^{C_4}$ 的缩点对. 如果 $G_{P_3}^{C_4} \cap G_{v_2v_2}^{C_4} = C_4 = v_1v'_2v_3v_2v_1$, 则称 $H = G_{P_3}^{C_4} \cup G_{v_2v_2}^{C_4}$ 是图 G 的一个路型子孙图. 更详细地, 称为图 G 的一个基于 $\{P_3, G_{v_2v_2}^{C_4}\}$ 的子孙图.

类型 2 漏斗型子孙图: 设 $L = v_1 - \Delta v_2v_3v_4$ 是 G 中的一个漏斗子图. 基于 L 的扩 5-圈型半极大平面图, 记作 $G_L^{C_5}$, 是指按下列方法获得的半极大平面图: 从 L 的顶点 v_1 出发, 沿着 $v_1 \rightarrow v_2$ 方向, 从边-点内部划开, 即将边 v_1v_2 , 顶点 v_2 从中间划开, 使得顶点 v_2 变成两个顶点, 分别记作 v_2 与 v'_2 ; v_1v_2 变

成了两条边，分别是 v_1v_2 与 $v_1v'_2$ ；原来在 L 左侧与 v_2 关联的边变成与 v_2 关联，原来在 L 右侧与 v_2 关联的边变成与 v'_2 关联，该过程如图 19 所示，并将顶点对 $\{v_2, v'_2\}$ 称为 $G_L^{C_5}$ 的扩点对。

设 $G_L^{C_5}$ 是一个扩 5-圈型半极大平面图，其外圈 $C_5 = v_1v'_2v_3v_4v_2$ ，且 $\{v_2, v'_2\}$ 是 $G_L^{C_5}$ 的扩点对，如图

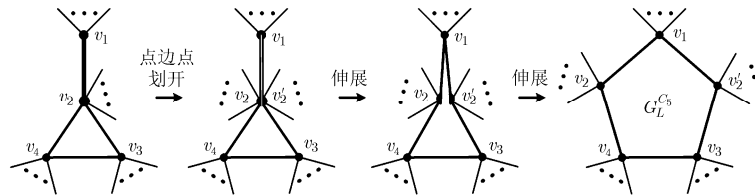


图 19 扩 5-圈型半极大平面图的过程示意图

类型 3 哑铃型子孙图： 设 $Y = \Delta v_1v_3v_2 - \Delta v_4v_5v_2$ 是 G 中的一个哑铃子图。基于 Y 的扩 6-圈型半极大平面图，记作 $G_Y^{C_6}$ ，是指按下列方法获得的半极大平面图：将 Y 中顶点 v_2 从中间划开，使得顶点 v_2 变成两个顶点，分别记作 v_2 与 v'_2 。原来在 Y 左侧与 v_2 关联的边变成与 v_2 关联，原来在 Y 右侧与 v_2 关联的边变成与 v'_2 关联，该过程如图 20 所示，并将顶点对 $\{v_2, v'_2\}$ 称为 $G_Y^{C_6}$ 的扩点对。

设 $G_Y^{C_6}$ 是一个扩 6-圈型半极大平面图，其外圈 $C_6 = v_1v_3v'_2v_5v_4v_2$ ，且 $\{v_2, v'_2\}$ 是 $G_Y^{C_6}$ 的扩点对，如图 20 中的最后一个图示。 $G_Y^{C_6} \in \mathfrak{S}_{v_2, v'_2}^{C_6}$ ，且外圈 $C_6 = v_1v_3v'_2v_5v_4v_2, \{v_2, v'_2\}$ 是 $G_Y^{C_6}$ 的缩点对。如果 $G_Y^{C_6} \cap G_{v_2, v'_2}^{C_6} = C_6 = v_1v_3v'_2v_5v_4v_2v_1$ ，则称 $H = G_Y^{C_6} \cup G_{v_2, v'_2}^{C_6}$ 是图 G 的一个哑铃型子孙图，更详细地，称为图 G 的一个基于 $\{Y, G_{v_2, v'_2}^{C_6}\}$ 的子孙图。

把上述路型、漏斗型和哑铃型子孙图统称为子孙图，在不考虑外圈的长度时，把获得一个图的子孙图的过程也称把一个多米诺构形嵌入在扩圈型半极大平面图上。由上节易知：

$$\left| \mathfrak{S}_{v_2, v'_2}^{C_4} \right| \rightarrow \infty, \left| \mathfrak{S}_{v_2, v'_2}^{C_5} \right| \rightarrow \infty, \left| \mathfrak{S}_{v_2, v'_2}^{C_6} \right| \rightarrow \infty \quad (3)$$

即任一给定的 $\delta(G) \geq 4$ 的极大平面图 G 必有无限多

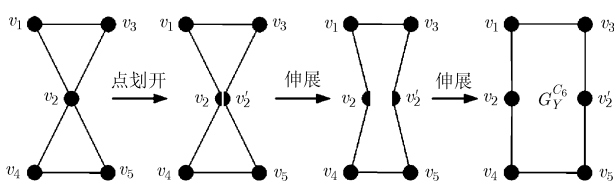


图 20 扩 6-圈型半极大平面图的过程示意图

19 中的最后一个图示。 $G_{v_2, v'_2}^{C_5} \in \mathfrak{S}_{v_2, v'_2}^{C_5}$ ，且外圈 $C_5 = v_1v'_2v_3v_4v_2, \{v_2, v'_2\}$ 是 $G_{v_2, v'_2}^{C_5}$ 的缩点对，如果 $G_L^{C_5} \cap G_{v_2, v'_2}^{C_5} = C_5 = v_1v'_2v_3v_4v_2v_1$ ，则称 $H = G_L^{C_5} \cup G_{v_2, v'_2}^{C_5}$ 是图 G 的一个漏斗型子孙图。更详细地，称为图 G 的一个基于 $\{L, G_{v_2, v'_2}^{C_5}\}$ 的子孙图。

个子孙图。故按照多米诺构形内点数对极大平面图 G 的子孙图进行分类：若多米诺构形内点数为 $t (\geq 1)$ ，则把相应的子孙图 H 称为 G 的第 t 代子孙图，并用 $\zeta^{+t}(G)$ 表示 G 的所有第 t 代的子孙图之集。特别，第 1 代子孙图称为儿子图；第 2 代子孙图称为孙子图；第 3 代子孙图称为重孙图等。

我们用 $\Upsilon^+(G)$ 表示 G 的全体子孙图构成的集合，即

$$\Upsilon^+(G) = \bigcup_{t=1}^{\infty} \zeta^{+t}(G) \quad (4)$$

式中， $\zeta^{+t}(G)$ 只泛泛地给出了极大平面图 G 的第 t 代的所有子孙图。但并未分出具体的多米诺构形。为此，我们在此引入等同子图的概念。设 G 是一个极大平面图， $\text{Aut}(G)$ 是它的自同构群， H, H' 是 G 的两个同构子图。若 $\exists \sigma \in \text{Aut}(G)$ ，使得 $\sigma(H) = H'$ ，则称 H 与 H' 是等同的。

文中用 \mathfrak{S}_G^H 表示极大平面图 G 中所有不等同的子图 H 构成的集合，特别，用 $\mathfrak{S}_G^{P_3}$ 表示 G 中所有不等同的 2-长路 P_3 构成的集合；用 \mathfrak{S}_G^L 表示 G 中所有不等同的漏斗子图 L 构成的集合；用 $\mathfrak{S}_G^{L^*}$ 表示 G 中所有不等同的半封漏斗子图 L^* 构成的集合； \mathfrak{S}_G^Y 表示 G 中所有不等同的哑铃子图 Y 构成的集合； $\mathfrak{S}_G^{Y^*}$ 表示 G 中所有不等同的半封哑铃子图 Y^* 构成的集合； $\mathfrak{S}_G^{Y_*^*}$ 表示 G 中所有不等同的全封哑铃子图 Y_*^* 构成的集合。

基于这些准备，式(4)中 $\zeta^{+t}(G)$ 可以写成

$$\zeta^{+t}(G) = \bigcup_{P_3 \in \mathfrak{S}_G^{P_3}} H_t^{P_3} \bigcup_{L \in \mathfrak{S}_G^L} H_t^L \bigcup_{L^* \in \mathfrak{S}_G^{L^*}} H_t^{L^*} \cdot \bigcup_{Y \in \mathfrak{S}_G^Y} H_t^Y \bigcup_{Y^* \in \mathfrak{S}_G^{Y^*}} H_t^{Y^*} \bigcup_{Y_*^* \in \mathfrak{S}_G^{Y_*^*}} H_t^{Y_*^*} \quad (5)$$

其中， $H_t^{P_3}, H_t^L, H_t^{L^*}, H_t^Y, H_t^{Y^*}, H_t^{Y_*^*}$ 分别表示

基于 G 中 2-长路 P_3 , 漏斗子图 L , 半封漏斗子图 L^* , 哑铃子图 Y , 半封哑铃子图 Y^* 以及全封哑铃子图 Y^* 的 G 的所有第 t 代子孙图集。

4.2 祖先图

设 G 是一个 $\delta(G) \geq 4$ 的极大平面图。 $C_4 = v_1 v_2 v_3 v_2$ 是 G 中一个长度为 4 的圈。如果 C_4 及其内部构成的半极大平面图是以 $\{v_2, v_2'\}$ 为缩点对的多米诺构形 $G_{v_2 v_2'}^{C_4}$, 且 C_4 及其外部构成的半极大平面图, 记作 $G_{P_3}^{C_4}$, 满足 $d_{G_{P_3}^{C_4}}(v_1), d_{G_{P_3}^{C_4}}(v_3) \geq 5$ 。则称 $G_{P_3}^{C_4} \circ \{v_2, v_2'\} = \zeta_{v_2 v_2'}^{-C_4}(G)$ 为 G 的基于多米诺构形 $G_{v_2 v_2'}^{C_4}$ 的祖先图, 也称之为 G 的路型祖先图。

类似地, 若 $C_5 = v_1 v_2' v_3 v_4 v_2$ 是 G 中一个长度为 5 的圈。如果 C_5 及其内部构成的半极大平面图是以 $\{v_2, v_2'\}$ 为缩点对的多米诺构形 $G_{v_2 v_2'}^{C_5}$, 且 C_5 及其外部构成的半极大平面图, 记作 $G_L^{C_5}$, 满足 $d_{G_L^{C_5}}(v_1) \geq 5, d_{G_L^{C_5}}(v_3), d_{G_L^{C_5}}(v_4) \geq 4$ 。则称 $G_L^{C_5} \circ \{v_2, v_2'\} = \zeta_{v_2 v_2'}^{-C_5}(G)$ 为 G 的基于多米诺构形 $G_{v_2 v_2'}^{C_5}$ 的祖先图, 也称之为 G 的漏斗型祖先图。

若 $C_6 = v_1 v_3 v_2' v_5 v_4 v_2$ 是 G 中一个长度为 6 的圈。如果 C_6 及其内部构成的半极大平面图是以 $\{v_2, v_2'\}$ 为缩点对的多米诺构形 $G_{v_2 v_2'}^{C_6}$, 且 C_6 及其外部构成的半极大平面图, 记作 $G_Y^{C_6}$, 满足 $d_{G_Y^{C_6}}(v_1), d_{G_Y^{C_6}}(v_3), d_{G_Y^{C_6}}(v_4), d_{G_Y^{C_6}}(v_5) \geq 4$ 。则称 $G_Y^{C_6} \circ \{v_2, v_2'\} = \zeta_{v_2 v_2'}^{-C_6}(G)$ 为 G 的基于多米诺构形 $G_{v_2 v_2'}^{C_6}$ 的祖先图, 也称之为 G 的哑铃型祖先图。

在不考虑外圈的长度时, 把路型祖先图、漏斗型祖先图和哑铃型祖先图统称为祖先图。

注: 不同于子孙图, 在 $\delta(G) \geq 4$ 的极大平面图 G 中, 基于 G 中一个给定的多米诺构形的祖先图只有一个。

类似于子孙图, 按照多米诺构形 $G_{v_2 v_2'}^{C_i}$ ($i = 4, 5, 6$) 的内点数对极大平面图 G 的祖先图进行层次上的分类。若 $G_{v_2 v_2'}^{C_i}$ 的内点数为 $t (\geq 1)$, 则把相应的祖先图 $\zeta_{v_2 v_2'}^{-C_i}(G)$ 称为 G 的第 t 代祖先图, 或简记为 $\zeta^{-t}(G)$ 。特别, $t = 1$ 的祖先图称为父代图; $t = 2$ 的祖先图称为爷代图; $t = 3$ 的祖先图称为曾祖父图。

显然, \mathfrak{S}_G^H 与 $\text{Aut}(G)$ 息息相关。当 G 的对称性很强时, $|\mathfrak{S}_G^H|$ 却很小。例如, 对正二十面体极大平面图 G , 易证

$$|\mathfrak{S}_G^{P_3}| = |\mathfrak{S}_G^L| = 1, |\mathfrak{S}_G^Y| = 0 \tag{6}$$

而当 $\text{Aut}(G)$ 是单位群时, $|\mathfrak{S}_G^H|$ 比较大。

用 $\Upsilon^-(G)$ 表示 G 的全体祖先图构成的集合, 基于此, 有:

定理 5 设 G 是一个 $\delta(G) \geq 4$ 的极大平面图。则 $|\Upsilon^-(G)|$ 等于 G 中不等同的多米诺构形子图的数目。

作为例子, 在此考察正二十面体 G (见附录中度序列为 555555555555 的 12 阶图) 的祖先图与第 1~3 代子孙图。由于该图中不等同的多米诺构形只有一种: 5-轮。故由定理 5 知它的祖先图只有一个, 如图 21(a)所示。

又由式(6)知, 正二十面体中的不等同路 2-长路与不等同漏斗子图数各为一个, 且无哑铃子图, 故由图 17 与 4.1 节知: 它的第 1~3 代的子孙图共有 9 个, 如图 12(b)~图 12(j)所示。

5 极大平面图的构造方法

前两节给出了构造 $\delta(G) \geq 4$ 的极大平面图 G 的

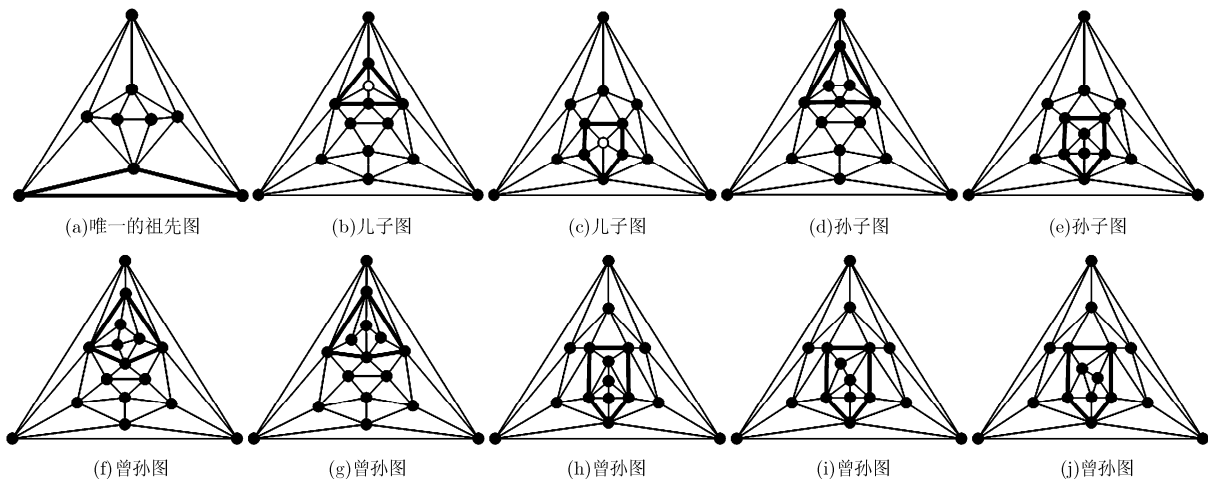


图 21 正 20 面体的祖先图与第 1~3 代子孙图

子孙图的具体方法与步骤。本节的主要贡献是给出构造 n -阶极大平面图的方法与步骤。首先证明了任一 n -阶极大平面图可通过连续扩轮运算获得，换言之，可通过若干次多米诺运算获得；其次给出了可分极大平面图的构造方法与步骤；最后，重点证明了：任一阶数为 $n(\geq 9)$ 极大平面图 G ，要么来自于最小度 ≥ 4 的 $(n-2)$ -阶祖先图，要么来自于最小度 ≥ 4 的 $(n-3)$ -阶祖先图。

5.1 构造的一般理论

定理 6 设 G 是一个 n -阶极大平面图。则可通过不断地实施缩 2-轮、缩 3-轮、缩 4-轮或缩 5-轮运算，使得该图最终收缩成 K_3 。

证明 当 $n = 4$ 时，由于只有一个极大平面图 K_4 ，显然结论成立。假设 $n \geq 4$ ，且顶点数 $\leq n$ 时结论成立，考虑顶点数为 $n+1$ 的情况。对于任意一个阶数为 $n+1$ 的极大平面图 G ，若 G 含有 2 度或 3 度顶点，则收缩该 2 度或 3 度顶点后所得到的图是一个阶数为 n 的极大平面图 $\zeta_2^-(G)$ 或 $\zeta_3^-(G)$ ，由归纳假设，结论成立；若 $\delta(G) = 4$ 或 $\delta(G) = 5$ ，则通过选择某 4 度或 5 度顶点实施缩 4-轮或缩 5-轮运算后所得到的图 $\zeta_4^-(G)$ 或 $\zeta_5^-(G)$ ，它们均是阶数为 $n-1$ 的极大平面图，由归纳假设，它们均可通过不断地实施缩 2-轮、缩 3-轮、缩 4-轮与缩 5-轮运算，使得该图最终收缩成为 K_3 。 证毕

由定理 6 知，每个 n -阶极大平面图 G 均可通过 4 种基本收缩运算可以收缩到 K_3 。当然，沿着对图 G 实施的缩 i -轮运算的逆方向，从 K_3 开始，作相应的扩 i -轮运算，则最终可得到相应的原图 G 。由此，可以推出：

推论 1 任意两个极大平面图 G 和 G' 总可以通过 4 对基本算子，从 G 出发得到 G' 。

5.2 可分极大平面图的构造

设 H_1, H_2 是两个极大平面图， $H_1 \cap H_2 = \Delta_{v_1v_2v_3}$ ，若 $G = H_1 \cup H_2$ 的最小度 ≥ 4 ，则称 G 为可分极大平面图，简称为可分图。由于极大平面图中的每个三角形面均可作为 ∞ -面(即含 ∞ 点的面)，故不妨设 $\Delta_{v_1v_2v_3}$ 总是 H_1 的 ∞ -面，如图 22(a) 所示；并令 $\Delta_{v_1v_2v_3}$ 总为 H_2 的非 ∞ -面，如图 22(b) 所示。故 $G = H_1 \cup H_2$ 可视由一种将 H_1 嵌入于 H_2 的

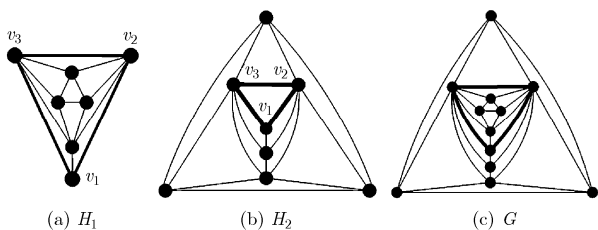


图 22 可分图的嵌入构造过程示意图

$\Delta_{v_1v_2v_3}$ 内的一种嵌入运算得到的极大平面图。

一般地，设 H_1, H_2 是两个极大平面图。 $\Delta_{v_1v_2v_3} \triangleq \Delta_1$ 是 H_1 中的三角形面， $\Delta_{v_1v_2v_3} \triangleq \Delta_2$ 是 H_2 的一个三角形面。所谓基于 $\{\Delta_1, \Delta_2\}$ 的 H_1 与 H_2 的嵌入运算是指，首先对 Δ_2 中的顶点重新标定：顶点 u_i 定义为 $v_i, i = 1, 2, 3$ ，且 H_1 与 H_2 中其余的标定均不相同；进而对标定后的 H_1 与 H_2 施行并运算，所得之图 $G = H_1 \cup H_2$ 是一个可分极大平面图。

注：在对 Δ_2 中的顶点重新标定中，也可选择不同于上述的标定，如 u_1 标定为 v_2 ； u_2 标定为 v_3 ； u_3 标定为 v_1 等。但不同的标定，导致所获得的可分图 $G = H_1 \cup H_2$ 不同。

显然，当 $\delta(H_i) \geq 4, i = 1, 2$ 时，有 $\delta(G) \geq 4$ ；但是，也存在 $\delta(H_i) = 3$ ，但 $\delta(G) \geq 4$ 的情况。如图 22 所示： H_1, H_2 均为最小度 = 3 的极大平面图，且分别只有一个顶点 v_1 的度数为 3，但 $G = H_1 \cup H_2$ 满足 $\delta(G) \geq 4$ 。

一个极大平面图 G 称为递归极大平面图，若它是从 K_4 出发，不断在某些三角面上嵌入一个 3-度顶点得到的极大平面图。用 A_n 表示所有不同构的 n -阶递归极大平面图构成的集合，并令 $\lambda_n = |A_n|$ 。易证，当 $n = 4, 5, 6$ 时， $\lambda_n = 1$ ，对应于 A_4, A_5 与 A_6 中的递归极大平面图如图 23 所示。

易证，一个递归极大平面图至少有 2 个 3 度顶点。把恰有 2 个 3-度顶点的递归极大平面图称为 **(2,2)-型递归极大平面图**。如图 23(b)~(c) 所示的图均为 (2,2) 型递归极大平面图。有关递归极大平面图的系统研究在本系列文章(3)中给出。这里不再赘述。

设 H^* 是一个 (2, 2)-型递归极大平面图或者 K_4 ， $\Delta_{v_1v_2v_3} \triangleq \Delta_1$ 是其中含一个 3-度顶点的三角形面， H_2 是一个最小度 ≥ 4 的极大平面图。所谓将 H^* 嵌入在 H_2 中的某三角形面 Δ_2 中是指基于 $\{\Delta_1, \Delta_2\}$ 的 H^* 与 H_2 的嵌入运算，并定义 $H^* \cup H_2 \triangleq H_2^*$ 。

易证

定理 7 设 H_1, H_2 是两个极大平面图， $H_1 \cap H_2 = \Delta_{v_1v_2v_3}$ 。则 $G = H_1 \cup H_2$ 的最小度 ≥ 4 的充要条件是：对于任意的 $H_i, d_{H_i}(v_1), d_{H_i}(v_2), d_{H_i}(v_3)$ 中至多有一个为 3, H_i 中其余顶点度数均 $\geq 4, i = 1, 2$ 。

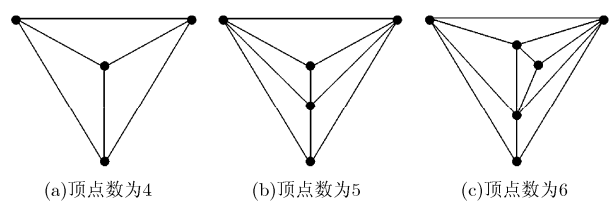


图 23 顶点数分别为 4, 5, 6 的 3 个递归极大平面图

阶数最小的最小度 ≥ 4 的是 6-阶极大平面图，见附录 A 中的第 1 个图；阶数最小且只有一个 3 度顶点的极大平面图是如图 22 中所示的 H_1 。于是由定理 7 知，阶数最小的可分极大平面图的阶数 = $6 + 6 - 3 = 9$ ，其次是 $6 + 7 - 3 = 10$ 。进而，可证：

基于定理 7，现给出构造阶数 $n(\geq 9)$ 可分图的方法与步骤。设 H_i 的阶数为 $n_i(\geq 6)$ ， $i = 1, 2$ ，分如下 2 种情况：

情况 1 $n = n_1 + n_2 - 3$ ：则可用最小度均 ≥ 4 的两个极大平面图 H_1, H_2 来构造 n -阶可分图，其中 n_i 为 H_i 的阶数， $n_i \geq 6$ ， $i = 1, 2$ ，具体步骤如下：

步骤 1 分别找出 H_1 与 H_2 中不等价的三角形面；

步骤 2 将 H_1 中的每个不等价的三角形面嵌入在 H_2 中的每个不同的三角形面中即可。

情况 2 $n < n_1 + n_2 - 3$ ：令 $m = n - n_1 - n_2 + 3$ ， $m = m_1 + m_2$ ， $m_1, m_2 \geq 0$ ， $t_i = m_i + n_i$ ， $i = 1, 2$ 。从而有： $n = t_1 + t_2 - 3$ 。由此可分如下情况讨论：

情况 2.1 $t_1 = n_1$ ，即 $m_1 = 0$ ；

步骤 1 分别找出 H_1 与 H_2 中不等价的三角形面；

步骤 2 把 $(m_2 + 3)$ -阶的 $(2,2)$ -型递归极大平面图 H^* 嵌入在 H_2 中每个不同的三角形面中，或者当 $m_2 = 1$ 时，把 K_4 嵌入在 H_2 中每个不同的三角形面中，所得之图记作 H_2^* ，并将 H_2^* 中含 3 度顶点的三角形面记作 Δ_2 ；

步骤 3 记 H_1 中不等价的三角形面为 Δ_1 ，实施基于 $\{\Delta_1, \Delta_2\}$ 的 H_1 与 H_2^* 的嵌入运算即可；

情况 2.2 $m_i > 0$ ， $i = 1, 2$ 。

步骤 1 分别找出 H_1 与 H_2 中不等价的三角形面；

步骤 2 对 $(m_i + 3)$ -阶的 $(2,2)$ -型递归极大平面图 H^* 嵌入在 H_i 中每个不同的三角形面中，所得之图记作 H_i^* ，当 $m_i = 1$ 时， $H^* = K_4$ ，并将 H_i^* 中含 3 度顶点的三角形面记作 Δ_i ， $i = 1, 2$ ；

步骤 3 实施基于 $\{\Delta_1, \Delta_2\}$ 的 H_1^* 与 H_2^* 的嵌入运算即可。

基于本小节的构造方法，我们给出 10-阶所有可分极大平面图，共有 2 个，其具体的构造方法步骤如下：

由于 $10 = (6 + 7) - 3$ ，而 6-阶与 7-阶的极大平面图各一个，且它们恰只有一个等价的三角形，因此，应用上述情况 1，可构造出一个 10-阶的可分极大平面图，其构造过程如图 24(a) 所示；又由于 $10 = ((6 + 4) - 3) + 6 - 3$ ，故可利用构造上述情况 2 的构造方法构造出另一个 10-阶可分图，其过程如图 24(b)~图 24(c)。容易证明，除了这两个可分图外，再无其它可分图。

按照此方法，我们构造出 11-阶极大平面图中共有 9 个可分图，分别见附录 B 中 11-阶极大平面图中的第 17, 19, 24-28, 30, 32；构造出 12-阶极大平面图中共有 43 个可分图，附录 B 中 12-阶极大平面图中的第 38, 49-52, 58, 62, 64, 68, 70, 72, 74, 81, 83, 84, 86-94, 98-100, 103, 105, 107, 109, 110, 112, 113, 115-117, 119, 120, 122, 125, 127, 129。

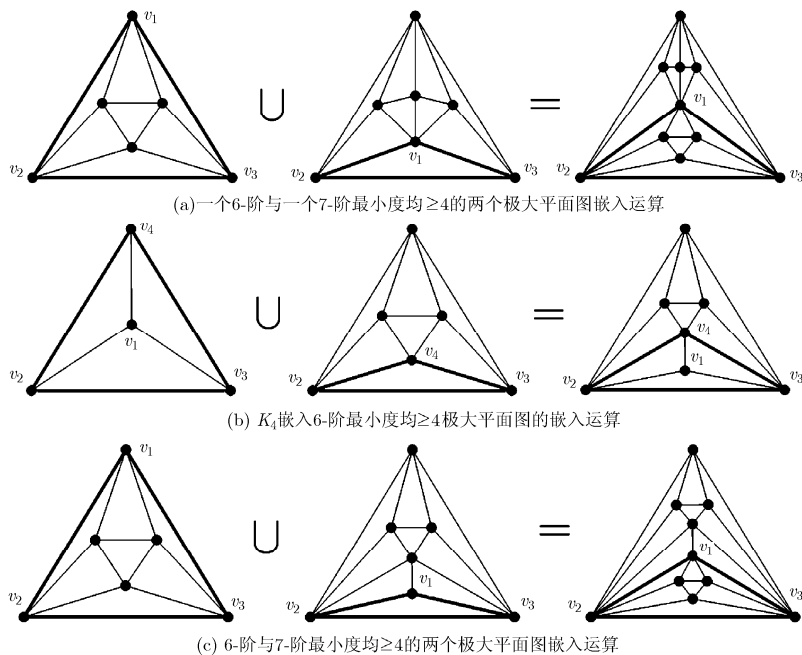


图 24 两个 10-阶可分极大平面图的构造过程示意图

5.3 非可分极大平面图构造基本定理

定理 8 设 G 是一个最小度 ≥ 4 的 $n(\geq 9)$ -阶非可分极大平面图, 则 G 有 $(n-2)$ -阶或 $(n-3)$ -阶祖先图。

证明 设 G 是一个最小度 ≥ 4 的 $n(\geq 9)$ -阶非可分极大平面图. 用 (i, j, t) 标记 G 中三角面 $\Delta v_1 v_2 v_3$, 其中, 顶点 v_1, v_2, v_3 的度数分别为 $i, j, t, i \leq j \leq t$ 。

当 $\delta(G) = 4$, G 中含 4 度顶点的三角面(仍记为 $\Delta v_1 v_2 v_3$)可分如下 3 种类型:

类型 1 $\Delta v_1 v_2 v_3$ 为 $(4, 4, t)$ 型, $t \geq 4$;

此类 $\Delta v_1 v_2 v_3$ 的邻域顶点标记如图 25(a)所示. 具体分如下情况:

情况 1 $t = 4$; 则 G 为 6-阶图或可分图, 矛盾;

情况 2 $t = 5$; 如图 25(b)所示, 则 $d(w_1) \geq 5$, 且 $w_1 w_3 \notin E(G)$, 否则 G 是可分图或者 7-阶图. 若 $d(w_1) = 5$, 则令 u_1 是 $N(w_1)$ 中除 w_2, v_2, v_1, w_4 外的另一个顶点, 如图 25(c)所示. 显然, 有 $d(w_2), d(w_4) \geq 6$, 于是, G 含有一个以 $w_1 w_2 v_3 w_4$ 为外圈, 以 $\{v_1, v_2\}$ 为内点集的基本多米诺构形(w_1, v_3 是缩点对); 若 $d(w_1) \geq 6$, 且 $d(w_3) \geq 5$, 则 $d(w_2), d(w_4) \geq 5$, 故推出以 $w_1 w_2 w_3 w_4 v_1$ 为外圈, 以 $\{v_2, v_3\}$ 为内点集(v_1, w_2 为缩点对)的基本多米诺构形; 若 $d(w_1) \geq 6$, 且 $d(w_3) = 4$, 则 $d(w_2), d(w_4) \geq 6$, 则 G 有一个以 $w_1 w_2 v_3 w_4$ 为外圈, 以 $\{v_1, v_2\}$ 为内点集(v_3, w_1 为缩点对)的基本多米诺构形;

情况 3 $t \geq 6$; 若 $d(w_1) \geq 6$, 则以 v_1 为轮心的 4-轮是 G 的一个多米诺构形(v_2, w_{t-1} 为缩点对); 若 $d(w_1) = 5$, 则 $N(w_1)$ 中有一个顶点(记作 u_1)不属于 $\{v_1, v_2, v_3, w_1, w_2, w_3, \dots, w_{t-1}\}$, 且 $d(w_{t-1}), d(w_2) \geq 5$, 如图 25(d)所示. 若 $d(u_1) \geq 5$, 则 G 有一个基本多米诺构形, 其以 $v_3 v_1 w_{t-1} u_1 w_2$ 为外圈, 以 $\{v_2, w_1\}$ 为内

点集(v_1, w_2 为缩点对), 定理成立; 若 $d(u_1) = 4$, 则 $d(w_{t-1}), d(w_2) \geq 6$, 故 G 有一个基本多米诺构形, 其以 $w_2 v_2 v_3 w_{t-1} u_1$ 为外圈, 以 $\{v_1, w_1\}$ 为内点集(u_1, v_2 为缩点对); 若 $d(w_1) = 4$, 则 G 是可分图, 矛盾。

类型 2 $\Delta v_1 v_2 v_3$ 为 $(4, 5, t)$ 型, $t \geq 5$;

对此情况, $\Delta v_1 v_2 v_3$ 的邻域顶点标记如图 25(e)所示. 具体分如下情况:

情况 1 $t = 5$; 如图 25(f)所示. 若 $d(w_1) = 4$, 则 $\Delta v_1 w_1 v_2$ 为 $(4, 4, 5)$ 型, 由类型 1 知定理成立。

若 $d(w_1) = 5$, 则 $N(w_1)$ 中存在顶点 $u_1 \notin \{v_1, v_2, v_3, w_1, w_2, w_3, w_4\}$, 如图 25(g)所示, 此时 $d(w_5) \geq 5$. 若 $d(w_3) = 4$, 则 $d(w_4), d(w_2) \geq 5$, 此时 G 有以 $w_3 w_4 w_5 v_1 w_1 w_2$ 为外圈, 以 $\{v_2, v_3\}$ 为内点集的基本多米诺构形(v_1, w_3 为缩点对); 若 $d(u_1), d(w_3) \geq 5$, 则 G 有以 $v_3 v_1 w_5 u_1 w_2 w_3$ 为外圈, 以 $\{w_1, v_2\}$ 为内点集的基本多米诺构形(v_1, w_2 为缩点对); 若 $d(w_3) \geq 5$ 且 $d(u_1) = 4$, 则 $d(w_5) \geq 6, d(w_2) \geq 5$, 故以 w_1 为轮心的 5-轮是多米诺构形(v_1, u_1 为缩点对)。

若 $d(w_1) \geq 6$ 且 $d(w_5) = 4$, 则 $\Delta v_1 w_5 w_1$ 属于类型 1. 下面假设 $d(w_1) \geq 6$ 且 $d(w_5) \geq 5$. 此时, 若 $d(w_3) \geq 5$, 则以 v_2 为轮心的 5-轮是多米诺构形(v_1, w_2 为缩点对); 如果 $d(w_3) = 4$, 则 $d(w_4), d(w_2) \geq 5$, 此时 G 有以 $w_3 w_4 w_5 v_1 w_1 w_2$ 为外圈, 以 v_2, v_3 为内点的基本多米诺构形(v_1, w_3 为缩点对)。

情况 2 $t \geq 6$; 分如下情况:

情况 2.1 $d(w_1) \geq 6$; 则以 v_1 为轮心的 4-轮是多米诺构形(v_2, w_t 为缩点对);

情况 2.2 $d(w_1) = 5$; 则 $\Delta v_1 w_1 v_2$ 为 $(4, 5, 5)$ 型, 由类型 2 中情况 2.1 知结论成立;

情况 2.3 $d(w_1) = 4$; 则 $\Delta v_1 w_1 v_2$ 为 $(4, 4, 5)$ 型, 由类型 1 知结论成立。

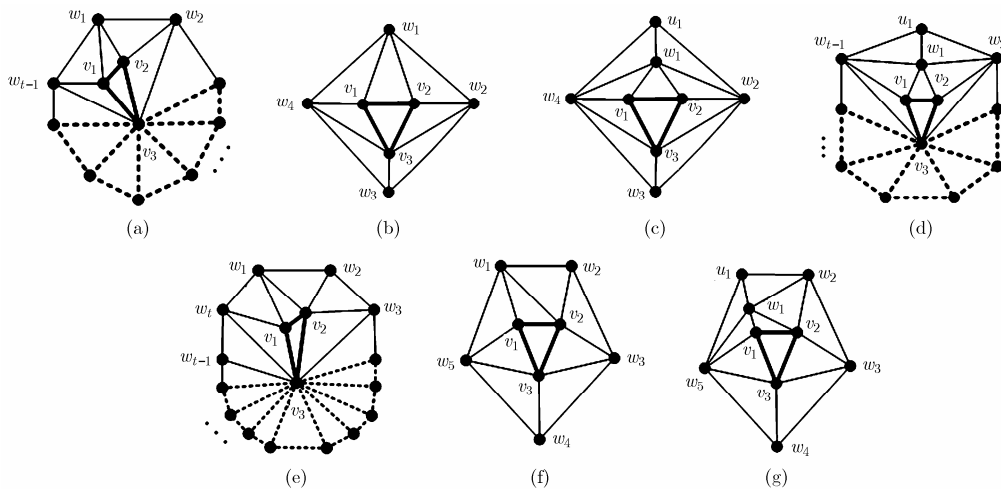


图 25 定理 8 证明示意图

类型 3 $\Delta v_1 v_2 v_3$ 为 $(4, j, t)$ 型, $6 \leq j \leq t$; 令 w_1 ($\neq v_3$) 为 v_1, v_2 的公共邻点。若 $d(w_1) = 4$, 则 $\Delta v_1 w_1 v_2$ 为 $(4, 4, j)$ 型, 由类型 1 知结论成立; 若 $d(w_1) = 5$, 则 $\Delta v_1 w_1 v_2$ 为 $(4, 5, j)$ 型, 由类型 2 知结论成立; 若 $d(w_1) \geq 6$, 则以 v_1 为轮心的 4-轮是多米诺构形。

当 $\delta(G) = 5$ 时, G 中含 5 度顶点的三角面(仍记为 $\Delta v_1 v_2 v_3$)可分为两种类型: $(5, 5, t_1)$ 型, 和 $(5, j, t_2)$ 型, 其中 $t_1 \geq 5, 6 \leq j \leq t_2$ 。相应的证明过程与 $\delta(G) = 4$ 的情况类似, 故略。

综上所述, 本定理成立。 证毕

5.4 非可分极大平面图的构造方法与步骤

基于定理 8, 本小节给出非可分极大平面图构造方法与步骤(在此以构造 $G(n)$ 为例给予说明)。

步骤 1 基于 $G(n-2)$, 构造出所有的第 1 代子孙图, 即过扩 4-轮、扩 5-轮运算生成的极大平面图。其具体步骤如下:

步骤 1.1 找出 $G(n-2)$ 中每个极大平面图中不等同的 2 长路集 \mathfrak{S}_G^P , 漏斗子图集 \mathfrak{S}_G^L ;

步骤 1.2 对 \mathfrak{S}_G^P 中每个图中的每条 2 长路, \mathfrak{S}_G^L 中每个漏斗子图实施扩轮运算即可得到 $G(n-2)$ 中的全部第 1 点子孙图。

步骤 2 基于 $G(n-3)$, 构造出所有的第 2 代子孙图, 采用 4.1 节中的构造方法, 具体步骤如下:

步骤 2.1 找出 $G(n-3)$ 中每个极大平面图中不等同的 2 长路集 \mathfrak{S}_G^P , 漏斗子图集 \mathfrak{S}_G^L , 半封漏斗子图集 $\mathfrak{S}_G^{\tilde{L}}$, 哑铃子图集 \mathfrak{S}_G^Y ; 半封哑铃子图集 $\mathfrak{S}_G^{Y^*}$, 全封哑铃子图集 $\mathfrak{S}_G^{Y^*}$ 。

步骤 2.2 基于 \mathfrak{S}_G^P , 与图 11 中的含 2 个内点第 1 个多米诺构形, 利用路型子孙图构造方法, 构

造出所有可能的路型子孙图;

基于 \mathfrak{S}_G^L , 与图 11 中的含 2 个内点的第 2 个多米诺构形, 利用漏斗型子孙图构造方法, 构造出所有可能的漏斗型子孙图;

基于 $\mathfrak{S}_G^{\tilde{L}}$, 与图 11 中的含 2 个内点的第 2 个多米诺构形, 利用漏斗型子孙图构造方法, 构造出所有可能的漏斗型子孙图;

基于 \mathfrak{S}_G^Y , 与图 11 中的含 2 个内点的第 3 个多米诺构形, 利用哑铃型子孙图构造方法, 构造出所有可能的哑铃型子孙图。

基于 $\mathfrak{S}_G^{Y^*}$, 与图 11 中的含 2 个内点的第 3 个多米诺构形, 利用哑铃型子孙图构造方法, 构造出所有可能的哑铃型子孙图。

基于 $\mathfrak{S}_G^{Y^*}$, 与图 11 中的含 2 个内点的第 3 个多米诺构形, 利用哑铃型子孙图构造方法, 构造出所有可能的哑铃型子孙图。

举例 利用上述方法, 构造 $G(9)$ 过程如下:

由于最小度 ≥ 4 的 7-阶极大平面图只有一个, 如图 26(a)所示, 它是一个双心轮图, 故 \mathfrak{S}_G^P 中含有 3 条 2 长路, 如图 26(a)~图 26(c)中粗线所示; \mathfrak{S}_G^L 中只有 1 个漏斗子图, 如图 26(d)中粗线所示。对图 26(a)~图 26(d)中粗线的对象子图实施相应的扩 4-轮与扩 5-轮运算, 得到相应的 4 个最小度 ≥ 4 的 9-阶极大平面图, 如图 26(a')~图 26(d'), 但图 26(a')与图 26(c')中所示的两个极大平面图是同构的, 故只有 3 个不同构的 9-阶极大平面图。

最小度 ≥ 4 的 6-阶极大平面图也只有一个, 如图 26(e)所示, 其对称性很强, 显然有 $|\mathfrak{S}_G^P| = |\mathfrak{S}_G^L| =$

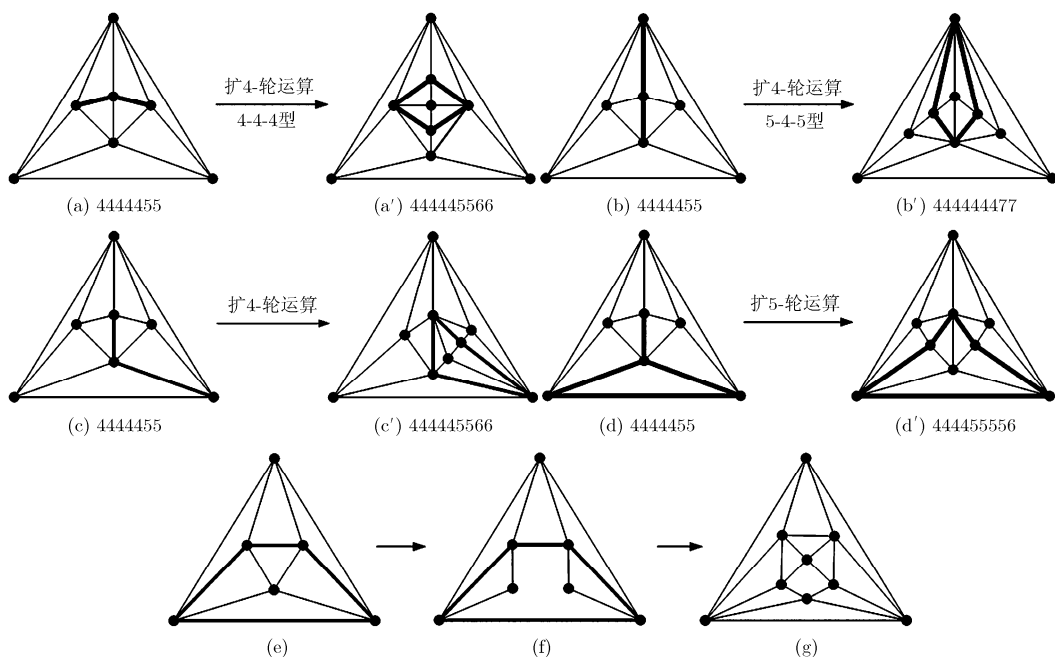


图 26 $G(9)$ 构造过程示意图

$|\mathfrak{S}_G^Y| = 1$ 易证, 对 \mathfrak{S}_G^R 与 \mathfrak{S}_G^L 中对象实施扩圈运算, 再与含两内点的多米诺构形结合给出的 9 阶极大平面图与图 26(a')~图 26(c') 中所示的图同构。故只考虑 \mathfrak{S}_G^Y 中所含唯一全封哑铃的情况, 如图 26(e) 中粗线所示。首先对其施行扩 6-圈, 所得之图如图 26(f) 所示。最后将图 17 中含 2 个内点的 6 圈多米诺构形嵌入在图 26(f) 中所示的半极大平面图中去, 得到如图 26(g) 中所示的 9-阶极大平面图。

至此, 我们已经按照上述构造方法, 构造出了 9 个顶点的全部 4 个非可分极大平面图, 见附录 B。

利用 5.2 节构造可分极大平面图以及 5.3 节构造非可分极大平面图的方法, 在本小节构造出了最小度 ≥ 4 的所有 6~12 阶的极大平面图, 见附录 B。

6 结论与展望

本系列文章(1)中给出了证明四色猜想数学证明的新的思路, 即只需要表征一类称为 4-色漏斗子图型伪唯一 4-色极大平面图的结构与着色特征。这类极大平面图总是与极大平面图中的漏斗子图息息相关。基于此, 文中提出了极大平面图的扩缩运算系统, 不仅与漏斗子图自然关联, 更重要的是: 在后续的文章中将会看到, 此构造方法有机地将图的结构与着色联系起来, 这是优于已有构造方法的关键所在, 也是证明诸如四色猜想、唯一 4-色极大平面图猜想、9-色猜想等难题的一个新思路。

本文的主要贡献是:

(1) 系统建立了一种将着色与结构有机结合的构造极大平面图的新方法—**扩缩运算法**;

(2) 发现了最小度 ≥ 4 的极大平面图中很重要的子图—**多米诺构形**, 并详细地刻画了此类图的结构

特征, 特别给出了构造多米诺构形的方法步骤。此工作是递归性构造极大平面图的基础;

(3) 提出了**祖先图**与**子孙图**, 并详细地刻画了如何构造一个最小度 ≥ 4 极大平面图的祖先图集与子孙图集;

(4) 发现并证明了任一阶数为 $n(\geq 9)$ 的最小度 ≥ 4 的极大平面图的祖先图必含 $(n-2)$ -阶或 $(n-3)$ -阶的祖先图(定理 8)。给出递推性构造 $n(\geq 8)$ 极大平面图的方法与步骤, 并用此方法获得了 6-12-阶所有最小度 ≥ 4 的极大平面图。

特别要说的是: 定理 8 是在后续研究中起到基石作用。

基于本文的工作, 从系列文章(3)开始, 将结构与着色有机结合性地展开研究。

致谢 本文在完成过程中, 与姚兵教授、陈祥恩教授以及吴建良教授, 以及我的 5 位图论专业学生: 刘小青(博士生), 朱恩强(博士后), 李泽鹏(博士后), 王宏宇(博士生)以及周洋洋(硕士生)等进行了多次有益讨论, 在此表示感谢。感谢边凯归副教授, 对英文稿进行了逐字逐句认真修改; 特别感谢北京大学的何新贵院士、余道衡教授对本文的审阅、以及对作者的鼓励、鞭策与支持。

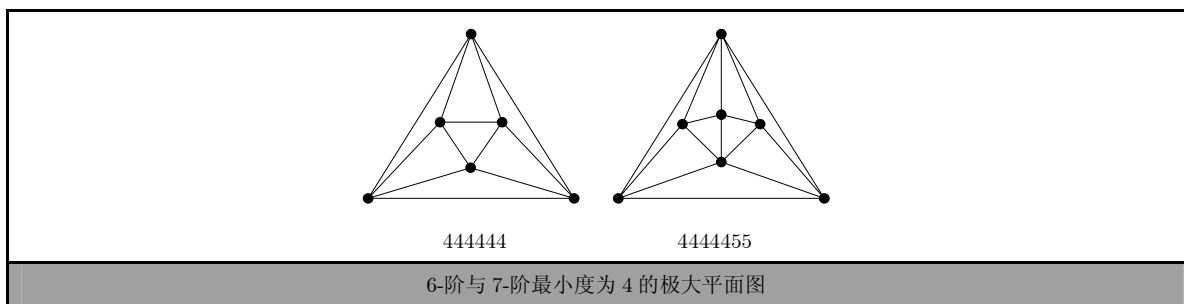
附录 A $\delta(G) \geq 4$ 的 6~23 阶极大平面图的计数表

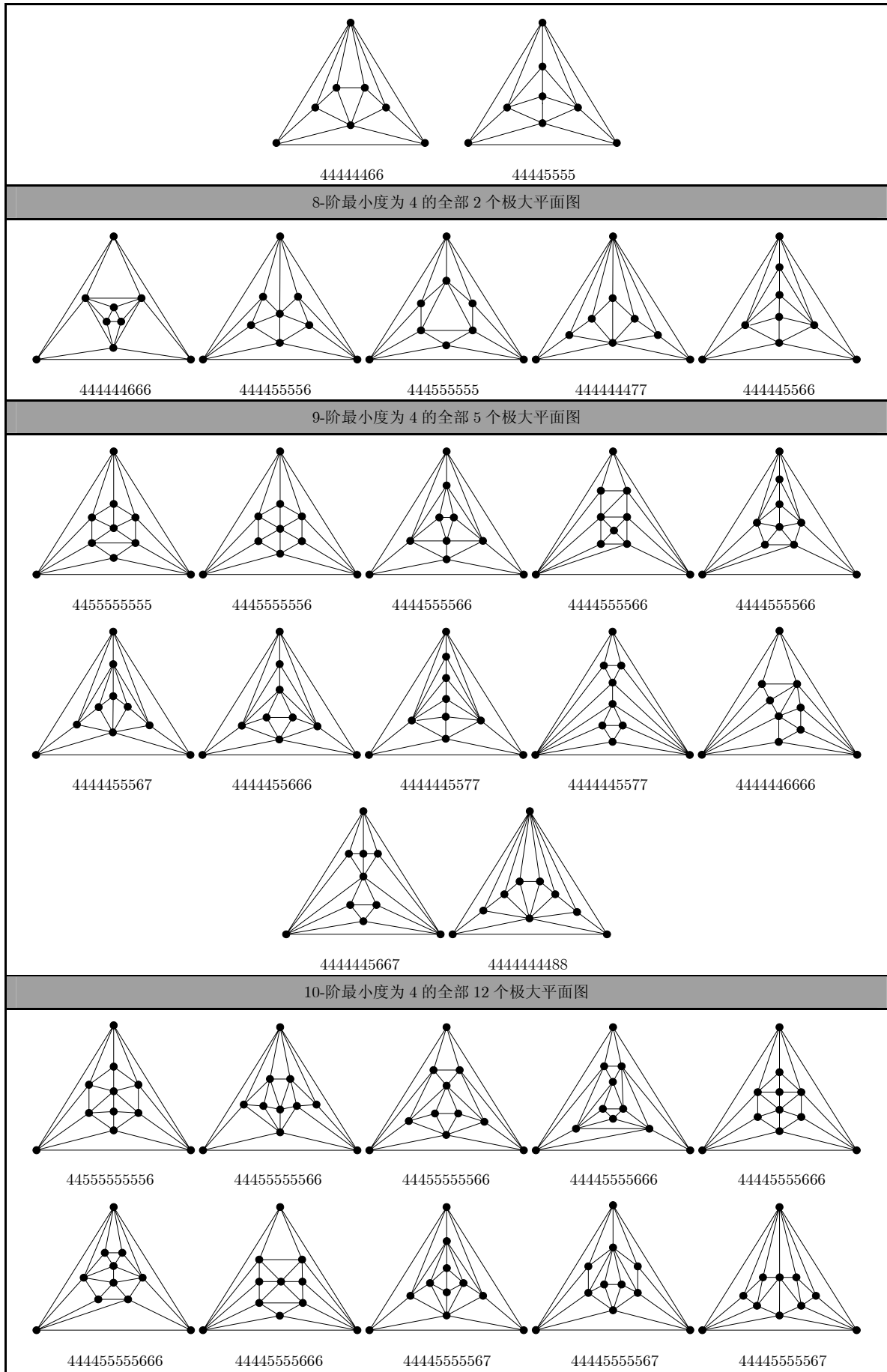
为了证明本节的主要结果, 我们需要知道最小度 $\delta(G) \geq 4$ 的所有 6~12 阶的极大平面图的数目。最小度大于等于 4 的极大平面图的计数问题, 2007 年 BRINKMANN 与 MCKAY 给出一种生成算法^[15]。在此只列举出阶数从 6~23 的计数, 见表 A1。

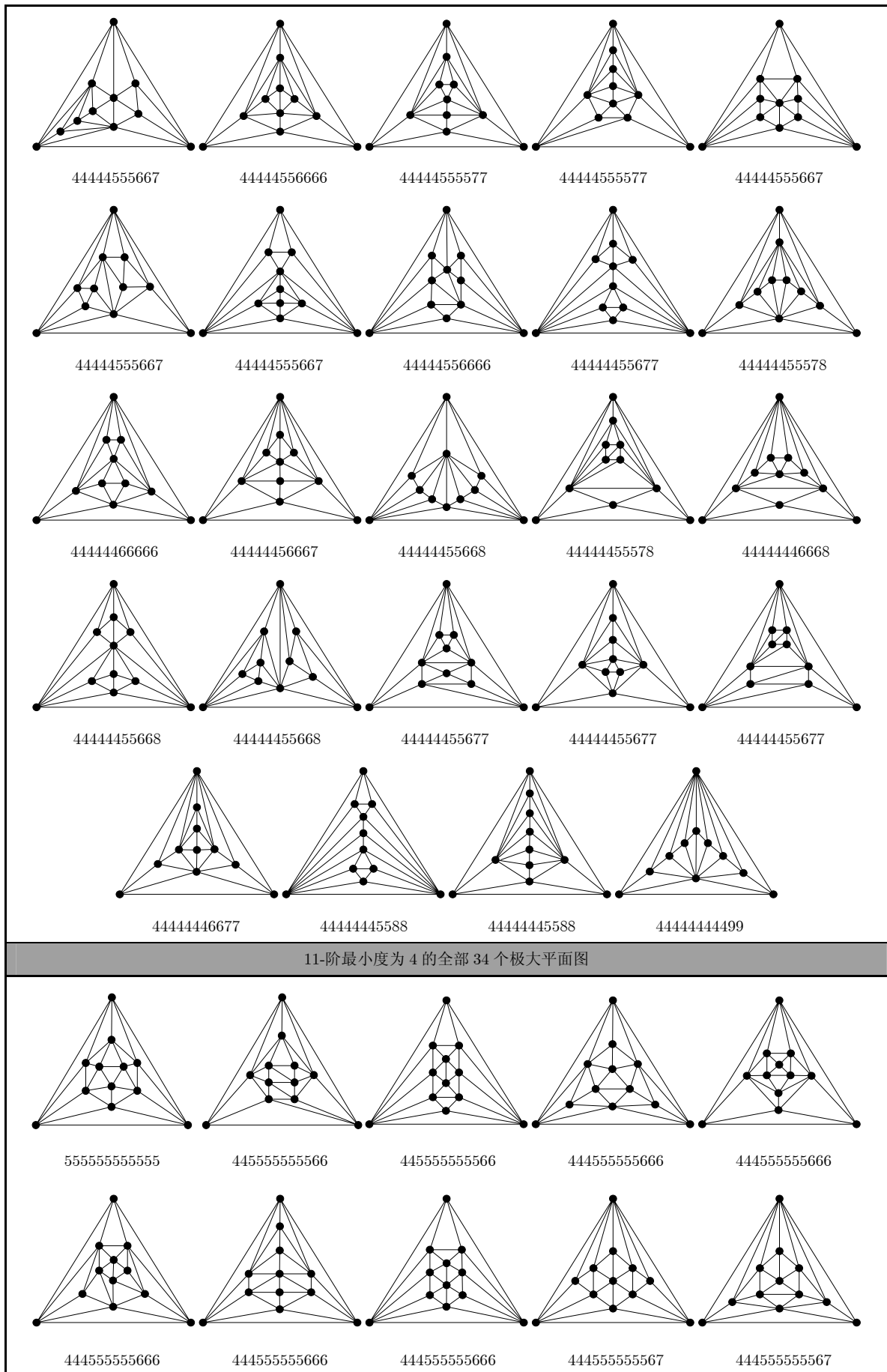
表 A1 满足最小度为 4 的阶数为 6-23 极大平面图的计数表

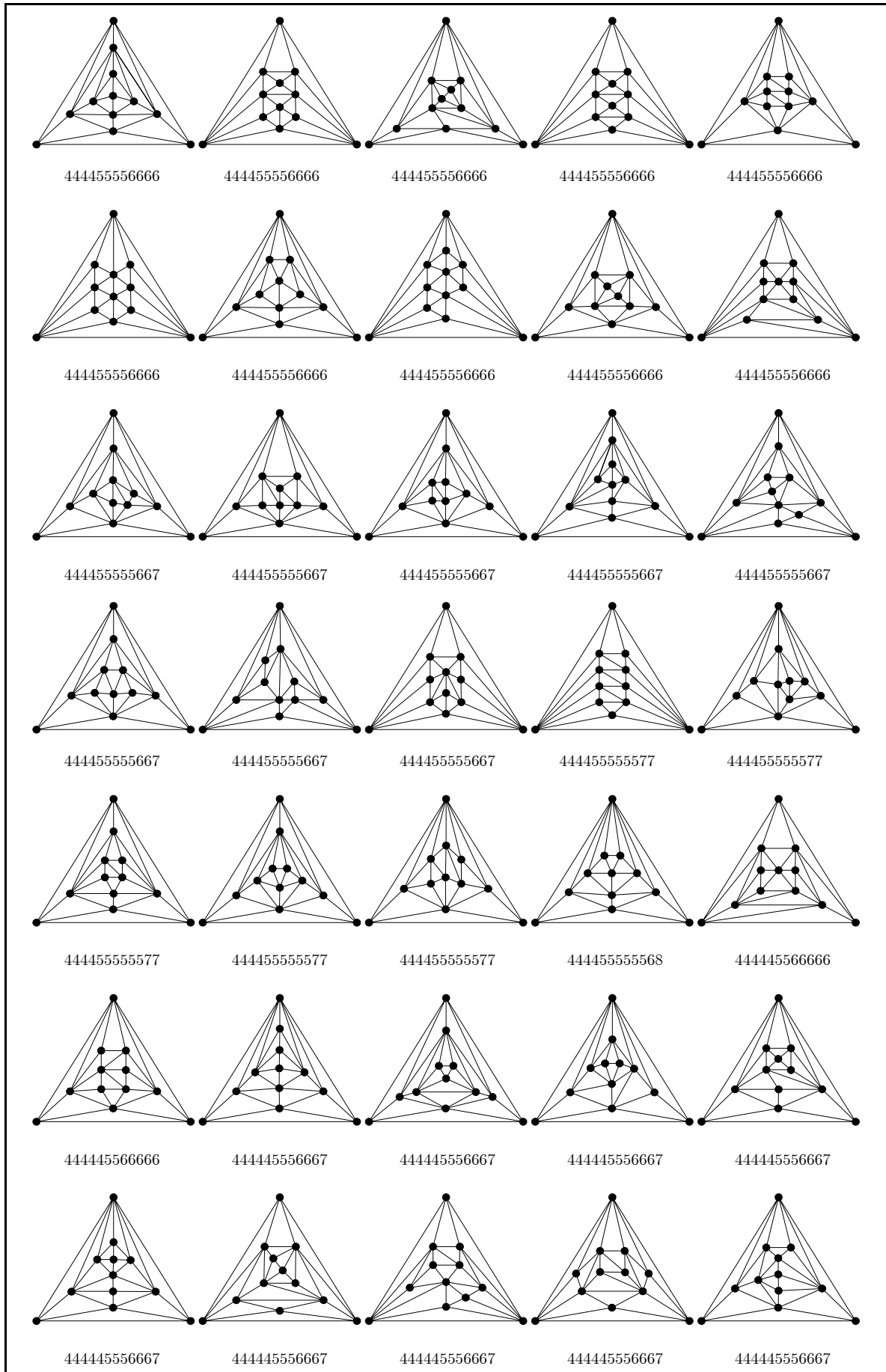
| | | | | | | | |
|------|----------|-----------|------------|-------------|--------|---------|----------|
| 阶数 | 6 | 7 | 8 | 9 | 10 | 11 | 12 |
| 图的数目 | 1 | 1 | 2 | 5 | 12 | 34 | 130 |
| 阶数 | 13 | 14 | 15 | 16 | 17 | 18 | 19 |
| 图的数目 | 525 | 2472 | 12400 | 65619 | 357504 | 1992985 | 11284042 |
| 阶数 | 20 | 21 | 22 | 23 | | | |
| 图的数目 | 64719885 | 375126827 | 2194439398 | 12941995397 | | | |

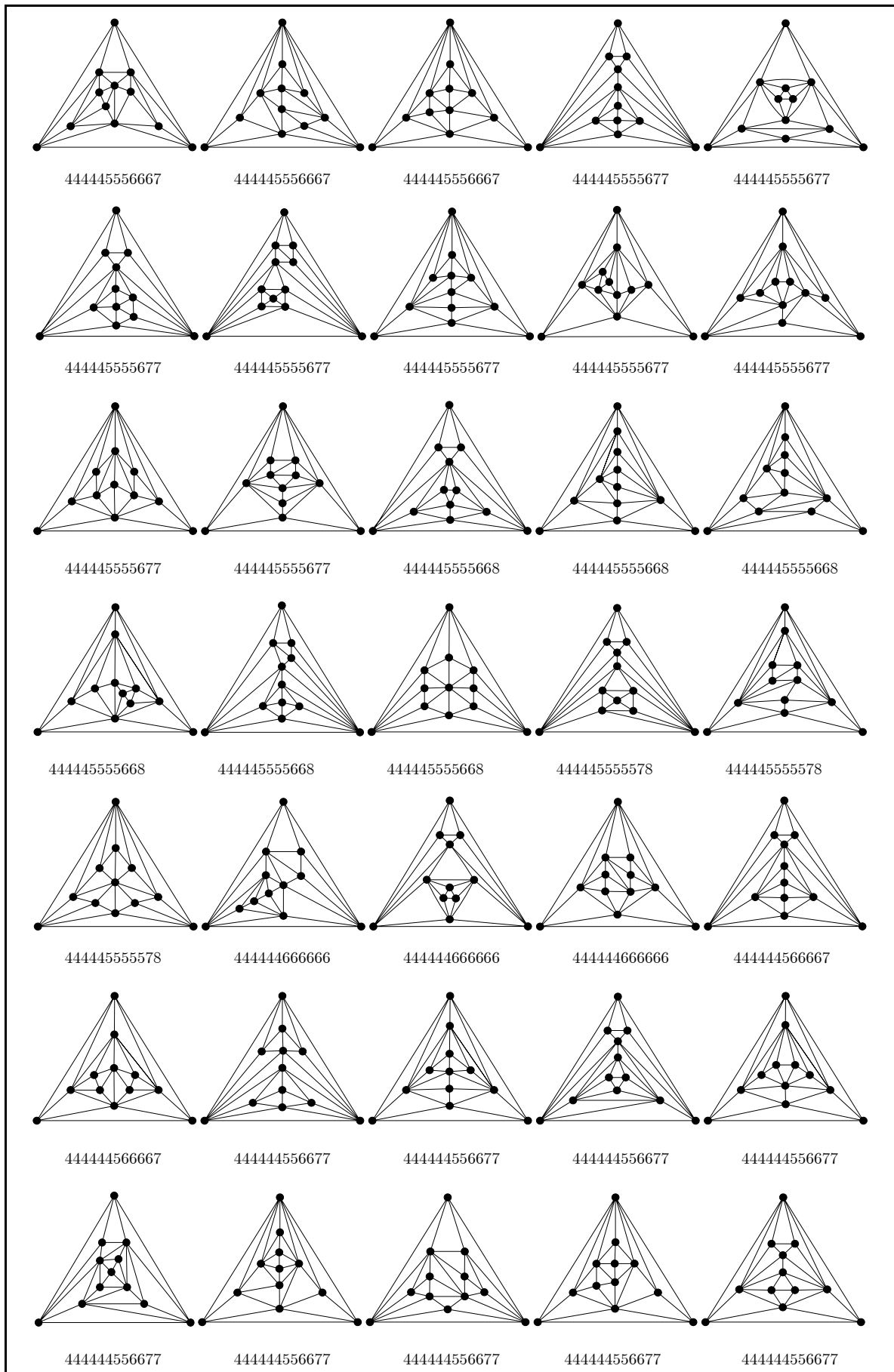
附录 B $\delta(G) \geq 4$ 的顶点数为 6~12 的所有极大平面图(图 B1)

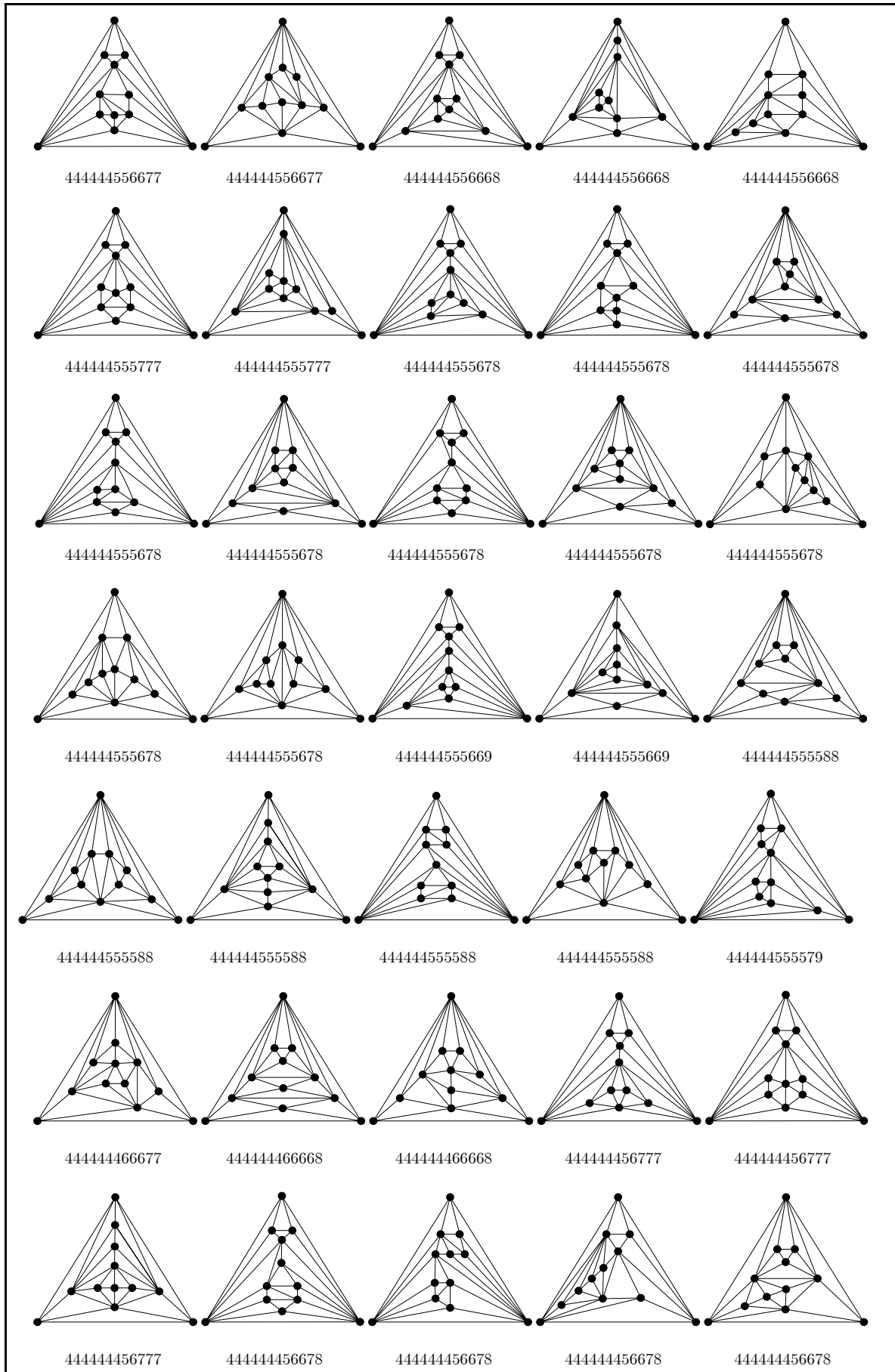












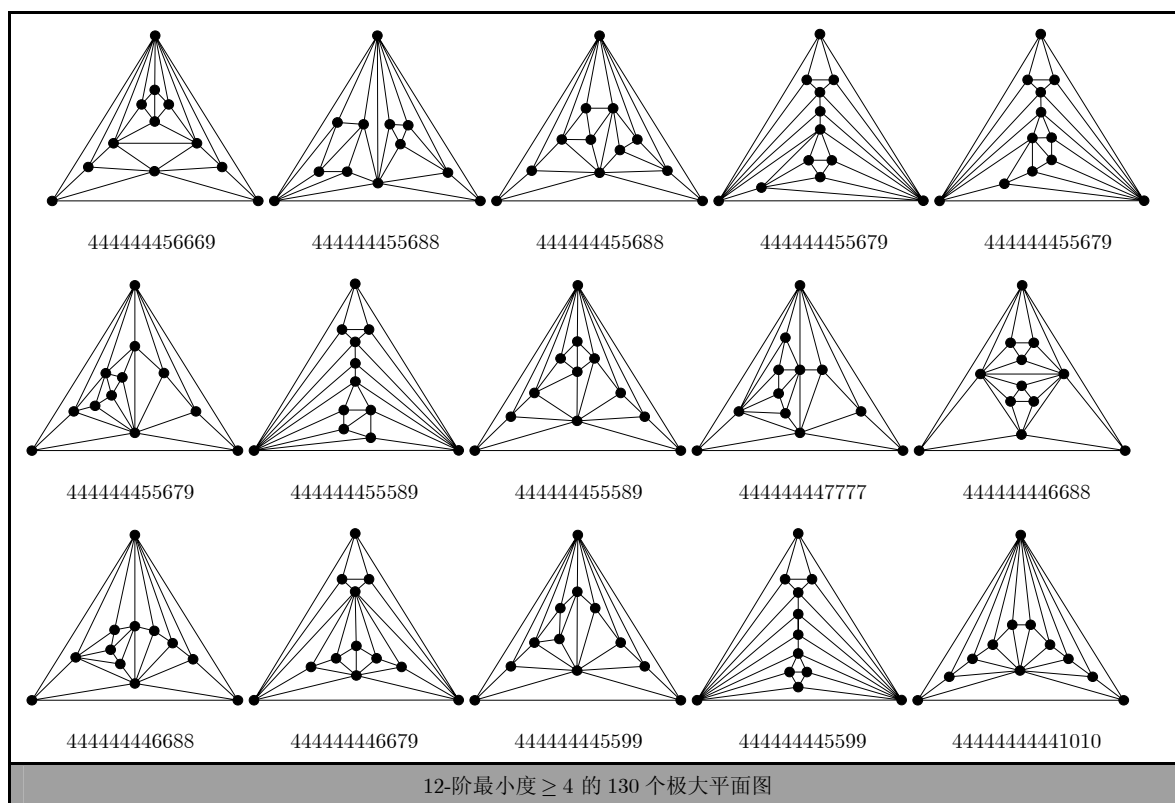


图 B1

参 考 文 献

- [1] APPEL K and HAKEN W. The solution of the four-color map problem[J]. *Science American*, 1977, 237(4): 108-121. doi: 10.1038/scientificamerican1077-108.
- [2] APPEL K and HAKEN W. Every planar map is four colorable, I: Discharging[J]. *Illinois Journal of Mathematics*, 1977, 21(3): 429-490.
- [3] APPEL K, HAKEN W, and KOCH J. Every planar map is four-colorable, II: Reducibility[J]. *Illinois Journal of Mathematics*, 1977, 21(3): 491-567.
- [4] EBERHARD V. Zur Morphologie Der Polyeder, Mit Vielen Figuren Im Text[M]. Leipzig: Benedictus Gotthelf Teubner, 1891: 14-68.
- [5] 王邵文. 构造极大平面图的圈加点法[J]. *北京机械工业学院学报*, 2000, 15(1): 26-29.
WANG Shaowen. Method of cycle add-point to construct a maximum plate graph[J]. *Journal of Beijing Institute of Machinery*, 2000, 15(1): 26-29.
- [6] 王邵文. 构造极大平面图的三种方法[J]. *北京机械工业学院学报*, 1999, 14(1): 16-22.
WANG Shaowen. Three methods to construct maximum plain graph[J]. *Journal of Beijing Institute of Machinery*, 1999, 14(1): 16-22.
- [7] BARNETTE D. On generating planar graphs[J]. *Discrete Mathematics*, 1974, 7(3-4): 199-208. doi: 10.1016/0012-365X(74)90035-1.
- [8] BUTLER J W. A generation procedure for the simple 3-polytopes with cyclically 5-connected graphs[J]. *Journal of the Mechanical Behavior of Biomedical Materials*, 1974, 26(2): 138-146.
- [9] BATAGELJ V. An inductive definition of the class of all triangulations with no vertex of degree smaller than 5[C]. *Proceedings of the Fourth Yugoslav Seminar on Graph Theory*, Novi Sad, 1983: 15-24.
- [10] WAGNER K. Bemerkungen zum vierfarbenproblem[J]. *Jahresbericht der Deutschen Mathematiker-Vereinigung*, 1936, 46: 26-32.
- [11] BRINKMANN G and MCKAY B D. Construction of planar triangulations with minimum degree 5[J]. *Discrete Mathematics*, 2005, 301: 147-163. doi: 10.1016/j.disc.2005.06.019.
- [12] MCKAY B D. Isomorph-free exhaustive generation[J]. *Journal of Algorithms*, 1998, 26(2): 306-324. doi: 10.1006/jagm.1997.0898.
- [13] AVIS D. Generating rooted triangulations without repetitions[J]. *Algorithmica*, 1996, 16(6): 618-632.
- [14] NAKANO S. Efficient generation of triconnected plane triangulations[J]. *Computational Geometry*, 2004, 27(2): 109-122.

- [15] BRINKMANN G and MCKAY B. Fast generation of planar graphs[J]. *MATCH Communications in Mathematical and in Computer Chemistry*, 2007, 58(58): 323–357.
- [16] BRINKMANN G and MCKAY B D. The program plantri [OL]. <http://cs.anu.edu.au/~bdm/plantri>.
- [17] NEGAMI S and NAKAMOTO A. Diagonal transformations of graphs on closed surfaces[J]. *Science Reports of the Yokohama National University. Section I. Mathematics, Physics, Chemistry*, 1994, 40(40): 71–96.
- [18] KOMURO H. The diagonal flips of triangulations on the sphere[J]. *Yokohama Mathematical Journal*, 1997, 44(2): 115–122.
- [19] MORI R, NAKAMOTO A, and OTA K. Diagonal flips in Hamiltonian triangulations on the sphere[J]. *Graphs and Combinatorics*, 2003, 19(3): 413–418. doi: 10.1007/s00373-002-0508-6.
- [20] GAO Z C, URRUTIA J, and WANG J Y. Diagonal flips in labeled planar triangulations[J]. *Graphs and Combinatorics*, 2004, 17(4): 647–656. doi: 10.1007/s003730170006.
- [21] BOSE P, JANSSENS D, VAN RENSSSEN A, *et al.* Making triangulations 4-connected using flips[C]. Proceedings of the 23rd Canadian Conference on Computational Geometry, Toronto, 2014, 47(2): 187–197 doi: 10.1016/j.comgeo.2012.10.012.
- [22] 许进. 极大平面图的结构与着色理论(1): 色多项式递推公式与四色猜想[J]. *电子与信息学报*, 2016, 38(4): 763–779. doi: 10.11999/JEIT160072.
- XU Jin. Theory on the structure and coloring of maximal planar graphs(1): recursion formula of chromatic polynomial and four-color conjecture[J]. *Journal of Electronics & Information Technology*, 2016, 38(4): 763–779. doi: 10.11999/JEIT160072.
- [23] BONDY J A and MURTY U S R. *Graph Theory*[M]. Springer, 2008: 5–46.
- [24] XU Jin, LI Zepeng, and ZHU Enqiang. On purely tree-colorable planar graphs[J]. *Information Processing Letters*, 2016, 116(8): 532–536. doi: 10.1016/j.ipl.2016.03.011.
- 许进: 男, 1959年生, 教授, 主要研究领域为图论与组合优化、生物计算机、社交网络与信息安全等.

Theory on Structure and Coloring of Maximal Planar Graphs

(2) Domino Configurations and Extending-Contracting Operations

XU Jin*

(Key Laboratory of High Confidence Software Technologies, Peking University, Beijing 100871, China)

(School of Electronics Engineering and Computer Science, Peking University, Beijing 100871, China)

Abstract: The first paper of this series of articles revealed that Four-Color Conjecture is hopefully proved mathematically by investigating a special class of graphs, called the 4-chromatic-funnel, pseudo uniquely-4-colorable maximal planar graphs. To characterize the properties of such class of graphs, a novel technique, “extending-contracting operation”, is proposed which can be used to construct maximal planar graphs. The essence of this technique is to study a special kind of configurations, domino configurations. In this paper, a necessary and sufficient condition for a planar graph to be a domino configuration is constructively given, on the basis of which it is proposed to construct the ancestor-graphs and descendent-graphs of a graph. Particularly, it is proved that every maximal planar graph with order $n(\geq 9)$ and minimum degree ≥ 4 has an ancestor-graph of order $(n-2)$ or $(n-3)$. Moreover, an approach is put forward to construct maximal planar graphs recursively, by which all maximal planar graphs with order 6~12 and minimum degree ≥ 4 are constructed. The extending-contracting operation constitutes the foundation in this series of articles.

Key words: Maximal planar graphs; Extending-contracting operations; Domino configurations; Ancestor-graphs; Descendent-graphs; Recursive construction approach

CLC index: O157.5

Document code: A

DOI: 10.11999/JEIT160224

1 Introduction

In mathematics, there are three remarkable conjectures: FERMAT's Conjecture (FERMAT's Last Theorem), GOLDBACH's Conjecture, and Four-Color Conjecture. The primary reason why these conjectures are widely known is the easy understanding of them. Specifically, FERMAT's Conjecture claims that no three positive integers x, y and z that satisfy the equation $x^n + y^n = z^n$ for any integer $n > 3$, GOLDBACH Conjecture says that every even integer greater than 2 can be written as the sum of two primes, and Four-Color Conjecture states that every map in the world can be colored with four colors such that no two adjacent regions, sharing a common boundary, receive the same color. Clearly, these conjectures are readily comprehensible for people, even for those who receive an education at only junior high school level. In particular, Four-Color Conjecture is

much more understandable, which is possible to be understood by uneducated persons. To compare with the description of Four-Color Conjecture, the approach to confirm it is considerably difficult. In 1976, APPLE and HAKEN declared that they had got a computer-assisted proof of Four-Color Conjecture^[1-3], but this result is still not satisfying in mathematics. Therefore, finding a mathematical method to concisely solve the Four-Color Conjecture is still open. Given that the studying object of Four-Color Conjecture can be confined to maximal planar graphs, we are necessary to investigate the structural properties and construction methods of such class of graphs.

In fact, as early as 1891, EBERHARD^[4] had begun a deep research on the construction problem of maximal planar graphs, and devised an operational system to generate maximal planar graphs. We use $\langle K_4; \Phi = \{\varphi_1, \varphi_2, \varphi_3\} \rangle$ to denote this system, where K_4 , Φ , and $\varphi_1, \varphi_2, \varphi_3$ are called original object, operation set, and generating operations, respectively (see Fig. 1).

For a maximal planar graph G and a cycle C of G , if the interior of C contains no vertices and all the interior faces of C are triangles, then

Received: 2016-01-24; Accepted: 2016-04-21; Online published: 2016-04-26

*Corresponding author: XU Jin jxu@pku.edu.cn

Foundation Items: The National 973 Program of China (2013CB329600), The National Natural Science Foundation of China (61372191, 61472012, 61472433, 61572046, 61502012, 61572492, 61572153, 61402437)

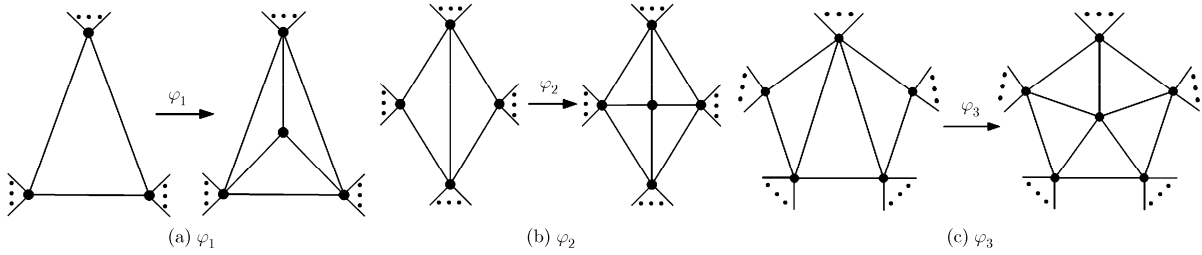


Fig. 1 Three generating operations used by EBERHARD to construct maximal planar graphs

C is called a purely-chordcycle. The interior edges of a purely-chord cycle are referred to as chords of C . For the ease of description, we view triangles in maximal planar graphs as purely-chord cycles. By using this definition, EBERHARD's construction approach is to delete all chords of a purely-chordcycle C with the length k ($= 3, 4, 5$), then add a new vertex inside C and connect it to all vertices of C .

From 1999 to 2000, WANG^[5,6] independently proposed a similar method as that of EBERHARD to construct maximal planar graphs. On the basis of EBERHARD's method, he extend the length of purely-chord cycles from 3, 4, 5 to arbitrary $k \geq 3$.

After EBERHARD's work, the research on

this topic advanced little for almost a century, and drew our attention again in 1974 with the study of constructing all 5-connected maximal planar graphs by BARNETTE^[7] and BUTLER^[8], independently. Different from EBERHARD's operational system, BARNETTE and BUTLER's operational system is $\langle Z_{20}; \Phi = \{\varphi_4, \varphi_5, \varphi_6\} \rangle$, in which the original object Z_{20} is the icosahedron and the operation set is $\{\varphi_4, \varphi_5, \varphi_6\}$ (see Fig. 2; the ellipses attached to the vertices in the description of the generating operations denote any number (zero or more) of edges satisfying $\delta = 5$). In short, BARNETTE and BUTLER's method starts with the icosahedron and uses the operations φ_4, φ_5 , and φ_6 to generate 5-connected maximal planar graphs.

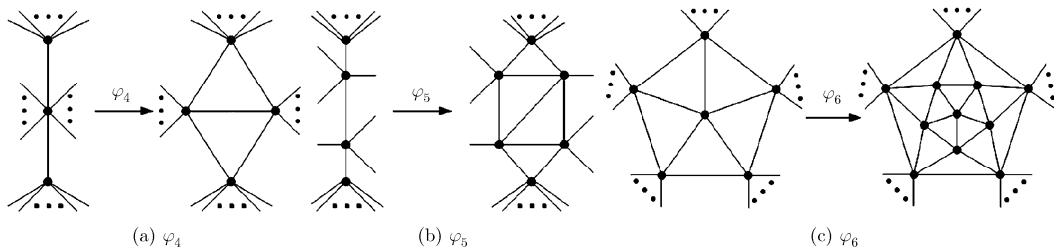


Fig. 2 BARNETTE and BUTLER's operations

In 1983, BATAGELJ^[9] improved the method of BARNETTE and BUTLER by changing one of the operations. Specifically, he used a new generating operation φ_7 instead of φ_6 and kept the remaining parts unchanged. The new operational system is denoted by $\langle Z_{20}; \Phi = \{\varphi_4, \varphi_5, \varphi_7\} \rangle$, where φ_7 is called the flip operation (Fig.3).

The research of flip operation has been a long history. This concept was introduced by WAGNER^[10] in 1936. Up to now, the flip operation has been studied very thoroughly, so we will give a specific discussion about it in the following paragraph.

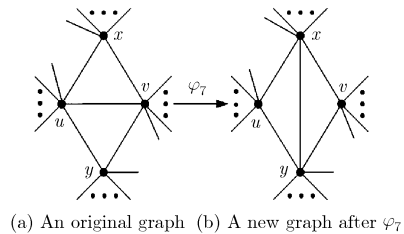


Fig. 3 The edge flip operation

In 2005, further works were done by BRINKMANN and MCKAY^[11] in terms of BARNETTE, BUTLER, and BATAGELJ's conclusions. They gave an efficient method to construct all simple maximal planar graphs of

minimum degree 5. Moreover, they pointed out the restrictions using $\varphi_4, \varphi_5, \varphi_6$, and φ_7 to construct the maximal planar graphs with minimum degree 5, which contain separating 3-cycles, 4-cycles, and 5-cycles respectively, and gave an algorithm to construct the graphs on computers. Particularly, by constructive method, they listed the number of maximal planar graphs of minimum degree 5 with orders from 12 to 40, where the numbers of 3-connected, 4-connected, and 5-connected 40-vertex maximal planar graphs of minimum degree 5 are 8469193859271, 7488436558647, and 5925181102878, respectively. Note that they used the canonical construction path method proposed by MCKAY^[12] in 1998, to avoid the generation of isomorphic copies in his computer program.

The study on algorithms for generating maximal planar graphs also inspires many scholars' interests. In 1996, AVIS^[13] gave an $O(r \cdot f(n, r))$ -time algorithm for generating all r -rooted 3-connected maximal planar graphs on n vertices by the reverse search technique. First, construct an n -vertex canonical maximal planar graph (contains exactly two vertices of degree $n - 1$); then generate all r -rooted 3-connected maximal planar graphs of order n by means of flip operations.

In 2004, NAKANO^[14] gave a simple algorithm to generate all 3-connected r -rooted plane triangulations with at most n vertices. He showed that all 3-connected rooted plane triangulations with exactly n vertices and exactly r vertices on the outer face can be generated in $O(r \cdot f(n, r))$ time without duplications. In 2007, BRINKMANN and MCKAY^[15] introduced the Plantri-operational rule based on the canonical configuration path^[12], and gave the program plantri^[16].

Let G be a maximal planar graph, and $\Delta_{uvx}, \Delta_{uvy}$ be the two triangles in G that have the common edge $e = uv$. An edge flip operation is to delete the edge e from G and add a new edge $e' = xy$ to the graph satisfying that the resulting graph is still a maximal planar graph. The edge e is called flippable (see Fig. 3).

It is clear that edge flip operation transforms a maximal planar graph into another one with the same number of edges. Naturally, this raises a

question: can an arbitrary n -vertex maximal planar graph be transformed into a given n -vertex maximal planar graph through a finite sequence of flips? In 1936, WAGNER^[10] first addressed this question with the positive answer. Although the number of n -vertex maximal planar graphs is exponential in n , WAGNER avoided the issue of graph isomorphism by converting a maximal planar graph into a canonical maximal planar graph, and proved that any given maximal planar graph can be transformed into a given n -vertex maximal planar graph by at most $2n^2$ edge flips.

After that there are lots of scholars working on this topic, and improving the upper bound. In 1993, NEGAMI and NAKAMOTO^[17] proved that any given n -vertex maximal planar graph could be converted into the canonical maximal planar graph via n^2 edge flips. KOMURO^[18] proved that any two n -vertex maximal planar graphs can be transformed into mutually through at most $8n - 54$ (or $8n - 48$) edges flips for $n \geq 13$ (or $n \geq 7$). MORI^[19] *et al.* showed that any Hamiltonian maximal planar graph on n vertices could be transformed into a canonical maximal planar graph by at most $2n - 10$ edge flips, preserving the existence of HAMILTON cycle. He also proved that any n -vertex maximal planar graph could be made 4-connected by at most $n - 4$ edge flips, and any two maximal planar graphs on n vertices could be converted into each other by at most $6n - 30$ edge flips.

In 2001, GAO *et al.*^[20] proved that every maximal planar graph on n vertices contains at least $n - 2$ flippable edges and that there exist some maximal planar graphs that contain at most $n - 2$ flippable edges. Moreover, he showed that there were at least $2n + 3$ flippable edges in a maximal planar graph G if $\delta(G) \geq 4$, and the bound was tight in certain cases.

In 2001, BOSE *et al.*^[21] showed that a maximal planar graph on $n (\geq 6)$ vertices could become 4-connected by at most $\lfloor (3n - 6)/5 \rfloor$ edge flips, and any two maximal planar graphs on n vertices could be transformed into each other by at most $5.2n - 32.8$ edge flips.

The above review the construction methods and algorithms. By the existing methods of generating maximal planar graphs, it is very hard to associate the structure with coloring. In this paper, we introduce a novel technique, extending-contracting operation, to construct maximal planar graphs. Our method can well associate the structure of a maximal planar graph with its coloring. We prove that any two maximal planar graphs can be transformed into each other by four pairs of basic extending-contracting operators. The essence of this technique is to study a special kind of configurations, domino configurations. To characterize the properties of such class of configurations, we propose an operational system to generate all of the domino configurations, on the basis of which a method is proposed to construct all of the ancestor-graphs and descendent-graphs of a graph. Particularly, we show that every maximal planar graph with order $n (\geq 11)$ and minimum degree ≥ 4 has an ancestor-graph of order $(n-2)$ or $(n-3)$. Moreover, we give an approach to construct separable maximal planar graphs.

Notice that, to prove Four-Color Conjecture according to the idea proposed in the first paper of this series of articles^[22], we need to use the extending-contracting operational system introduced in this article.

From coloring perspective, adding or deleting vertices of degree 3 in a 4-colorable maximal planar graph has no effect on the study of relation between structure and coloring. Therefore, unless otherwise stated, graphs considered in this paper are assumed to be a maximal planar graph with minimum degree ≥ 4 . As an example for illustrating the extending-contracting operational system, all maximal planar graphs with order 6~12 and minimum degree ≥ 4 are constructed in this paper.

All graphs considered in this paper are finite, simple and undirected. For a given graph G , we use $V(G)$, $E(G)$, $d_G(v)$, and $N_G(v)$ to denote the vertex set, the edge set, the degree of v , and the neighborhood of v in G (the set of neighbors of v), respectively, which can be written as V , E , $d(v)$, and $N(v)$ for short. The order of G is the

number of its vertices. A graph $H = (V', E')$ is a subgraph of G if $V' \subseteq V$ and $E' \subseteq E$. For a subgraph H of G , if $uv \in E(G) \Leftrightarrow uv \in E(H)$ for any $u, v \in V'$, then H is called an induced subgraph of G or a subgraph of G induced by V' , denoted by $G[V']$. Two graphs G and H are disjoint if they have no vertex in common. By starting with a disjoint union of G and H , and adding edges joining every vertex of G to every vertex of H , one obtains the join of G and H , denoted by $G \vee H$. We write K_n and C_n for the complete graph and cycle of order n , respectively. The join $C_n \vee K_1$ of a cycle and a single vertex is referred to as a wheel, denoted by W_n (the examples W_3, W_4, W_5 are shown in Fig. 4), where C_n is called the wheel-cycle of W_n and the vertex of K_1 is called the wheel-center of W_n . If $V(K_1) = \{x\}$, we also denote by C^x the wheel-cycle of W_n .

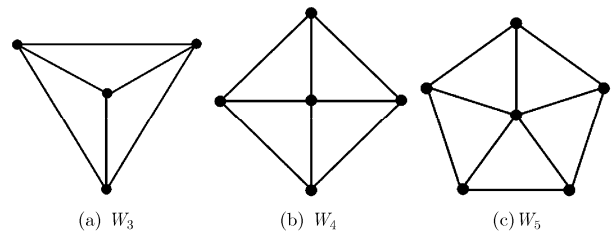


Fig. 4 Three wheels W_3, W_4 , and W_5

A graph is said to be planar if it can be drawn in the plane so that its edges intersect only at their ends. Such a drawing is called a planar embedding of the graph. Any planar graph considered in the paper is assumed one of its planar embedding. A maximal planar graph is a planar graph to which no new edges can be added without violating planarity. A triangulation is a planar graph in which every face is bounded by three edges (including its infinite face). It can be easily proved that maximal planar graphs are triangulations, and vice versa. A graph is separable if one of its proper induced subgraph is a maximal planar graph, otherwise, it is non-separable.

Let G^C be a planar graph, and C be the boundary of infinite face of G^C . If all the faces of

G^C are bounded by three edges except its infinite face, then we call G^C and C a semi-maximal planar graph and the outer cycle of G^C , respectively.

The definitions and notations not mentioned here can be found in Refs. [22,23].

2 Basic Extending-contracting Operational System

In this section, we introduce the basic extending-contracting operational system. This system consists of two parts: operating objects and basic operators, where the operating objects are maximal planar graphs; the basic operators include four pairs of operators: the extending i -wheel operation and the contracting i -wheel operations, $i = 2, 3, 4, 5$. The function of this system is: starting with K_3 , we can generate any given maximal planar graph by using the four pairs of operators repeatedly.

The extending 2-wheel operation consists of 2 steps: (1)add a new edge between two adjacent vertices, which will generate a 2-parallel edge (namely a 2-cycle, a cycle of order 2); (2)add a new vertex in the face of the 2-cycle and connecting the new vertex to the two vertices of the 2-cycle. Naturally, the object of extending 2-wheel operation is an edge of a maximal planar graph, see Fig. 6(a).

For a graph with 2-wheels, the contracting 2-wheel operation is to delete the wheel-center of a 2-wheel and the two edges incident with the wheel-center, and then delete one of the parallel edges of the 2-cycle. The procedures of extending and contracting 2-wheel operations are shown in Fig. 5.

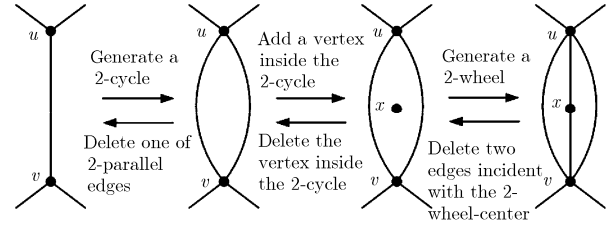


Fig. 5 The procedures of extending and contracting 2-wheel operations

The extending 3-wheel operation is to add a new vertex in a certain face of the maximal planar graph, and connect it to the three vertices of the face, respectively. The object of extending 3-wheel operation is a triangle of a maximal planar graph, see Fig. 6(b). The contracting 3-wheel operation is to delete a certain 3-degree vertex and its incident edges.

Let G be a maximal planar graph, and $P_3 = v_1v_2v_3$ be 2-path (a path of length 2) in G . The extending 4-wheel operation on path P_3 consists of two steps: (1)to replace P_3 by a 4-cycle $v_1v_2v_3v'_2$. That is, split the vertex v_2 into two vertices v_2 and v'_2 , split the edges v_1v_2 into two edges v_1v_2 , $v_1v'_2$, and split v_2v_3 into v_2v_3 , v'_2v_3 . All edges (incident with v_2) on the left of P_3 in G are incident with v_2 and all edges (incident with v_2) on the right of P_3 in G are incident with v'_2 , so that the obtained new graph would be planar. This process is shown in Fig. 7 (see the first to the fourth graph); (2)to add a new vertex in the face $v_1v_2v_3v'_2$, and connect it to vertices v_1, v'_2, v_3, v_2 respectively, see the fifth graph in Fig. 7.

The contracting 4-wheel operation includes three steps: (1)to delete a certain 4-degree vertex and the edges incident with it; (2)to identify a pair of the non-adjacent vertices; (3)to delete one of 2-parallel edges if there exists 2-parallel edges in

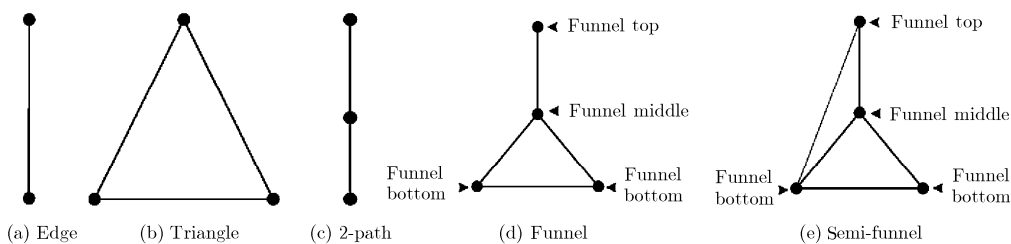


Fig. 6 The objects of basic extending wheel operations and semi-funnel

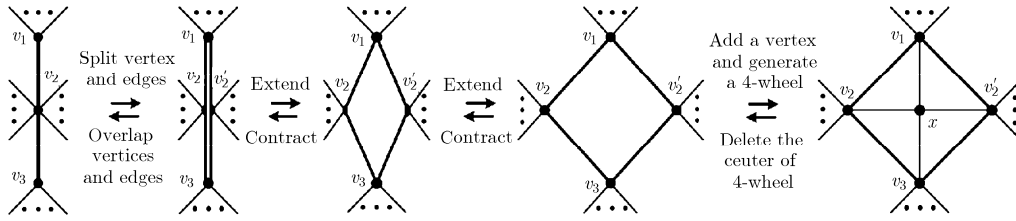


Fig. 7 The procedures of extending and contracting 4-wheel operations

the obtained new graph, and no vertex in the face of 2-parallel edges. This procedure is shown in Fig. 7 (see the fifth to the first graph).

The graph shown in Fig. 6(d) is called a funnel, denoted by L , where the 1-degree vertex is the top of the funnel, the 3-degree vertex is the middle of the funnel, and the two 2-degree vertices are the bottoms of the funnel. As the middle and two bottoms of L are vertices of a triangle, we also write L by $L = v - \Delta$, where v is the top of L . If we add an edge between the top and one of bottoms of the funnel, then we call the new graph a semi-funnel (see Fig. 6(e)). Let H be an induced subgraph of G . We call H a funnel (or semi-funnel) subgraph if H is isomorphic to a funnel (or a semi-funnel). The semi-funnel subgraph is one of objects to construct ancestor-graphs or descendent-graphs of a graph.

For a maximal planar graph G , the extending 5-wheel operation and the contracting 5-wheel operation are similar to the extending 4-wheel operation and the contracting 4-wheel operation. The difference between the 5-wheel and 4-wheel operations is that an extending 5-wheel operation is on a funnel, while an extending 4-wheel operation is on a 2-path. Fig. 8 presents graphical illustrations of definitions of extending and contracting 5-wheel operations. Specifically, the extending 5-wheel operation on a funnel L includes two steps: (1) to replace L by a 5-cycle $v_1v_2v_3v_4v_2'$. That is, split the vertex v_2 into two vertices v_2 and v_2' , and

split the edge v_1v_2 into two edges v_1v_2, v_1v_2' . All edges (incident with v_2) on the left of L in G are incident with v_2 and all edges (incident with v_2) on the right of L in G are incident with v_2' , satisfying that the obtained new graph is also planar; (2) to add a new vertex in the face of the 5-cycle $v_1v_2v_3v_4v_2'$, and connect it to vertices v_1, v_2', v_3, v_4, v_2 respectively. The contracting 5-wheel operation is to: (1) delete a certain 5-degree vertex and the edges incident with it; (2) identify a pair of the non-adjacent vertices; (3) then delete one of 2-parallel edges if there exists 2-parallel edges in the obtained new graph, and no vertex in the face.

Let ζ_i^+ and ζ_i^- denote the extending i -wheel operation and the contracting i -wheel operation for $i = 2, 3, 4, 5$, respectively, and let $\Psi = \{\zeta_2^-, \zeta_2^+, \zeta_3^-, \zeta_3^+, \zeta_4^-, \zeta_4^+, \zeta_5^-, \zeta_5^+\}$ denote the set of all the basic operators given above, where $\zeta_2^-, \zeta_2^+, \zeta_3^-, \zeta_3^+$ are called intermediate operators, $\zeta_4^-, \zeta_4^+, \zeta_5^-, \zeta_5^+$ are called final operators. For a maximal planar graph G , we denote by $\zeta_i^+(G)$ and $\zeta_i^-(G)$ the resulting graphs after implementing an extending i -wheel operation and a contracting i -wheel operation for $i = 2, 3, 4, 5$, respectively. Without taking into account the value of i in the extending and contracting i -wheel operation, we use $\zeta^-(G)$ and $\zeta^+(G)$ to replace $\zeta_i^-(G)$ and $\zeta_i^+(G)$ simply; in addition, we use $\zeta^{m+}(G)$ and $\zeta^{m-}(G)$ to denote the resulting graphs after implementing m contracting

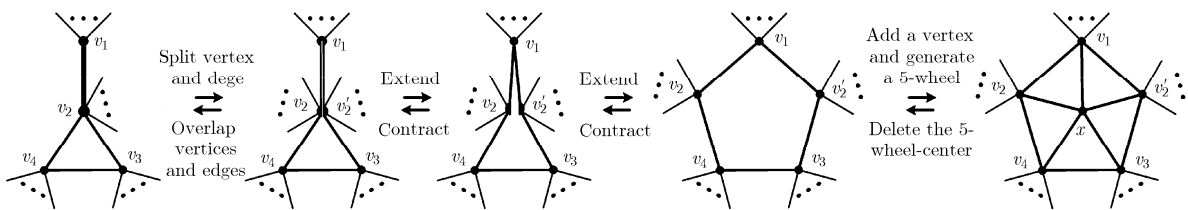


Fig. 8 The procedures of extending and contracting 5-wheel operations

Operations and m extending operations respectively, where $m \geq 2$.

Obviously, for a non-separable maximal planar graph G with $\delta \geq 4$, we can see that both $\zeta^-(G)$ and $\zeta^+(G)$ are maximal planar graph, while they are possible to be separable, or have minimum degree 2 or 3. No matter what the degrees of them are, the following result holds.

Theorem 1 Let G be a maximal planar graph with order n and minimum degree ≥ 4 . Then

$$|\zeta_2^-(G)| = |\zeta_3^-(G)| = |V(G)| - 1 = n - 1 \quad (1)$$

$$|\zeta_4^-(G)| = |\zeta_5^-(G)| = |V(G)| - 2 = n - 2 \quad (2)$$

Theorem 1 can be easily obtained, and we leave the proof to the reader.

3 Domino Extending-contracting Operational System

3.1 Consecutive extending-contracting operation and domino extending-contracting operation

The previous section introduces four pairs of basic extending and contracting operators, which can generate maximal planar graphs. More importantly, the method proposed can associate structure with coloring easily. Starting with K_3 , we can generate any given maximal planar graph using this system. Generally, to generate a desired graph we need to implement many times of extending and contracting operations. We refer to such a sequence of extending and contracting operations as a consecutive extending-contracting operation.

Recall that the maximal planar graphs considered in this paper are assumed to be those with minimum degree at least 4. Therefore, if the minimum degree of $\zeta^+(G)$ or $\zeta^-(G)$ is 2 or 3, then we need to further implement extending or contracting operations repeatedly until we obtain a graph with $\delta \geq 4$ or K_4 .

Let G be a maximal planar graph with

$\delta \geq 4$, and W_4 (or W_5) be a 4-wheel (or 5-wheel). Let $\zeta^-(G)$ be the graph resulting from contracting 4-wheel (or 5-wheel) operation on W_4 or W_5 . If $\delta_{\zeta^-(G)} \geq 4$, then we call such a contracting 4-wheel (or 5-wheel) operation a domino contracting wheel operation. If $\delta_{\zeta^-(G)} = 2$ or 3, then we continue to implement a contracting 2-wheel or 3-wheel operation, and denote the resulting graph by $\zeta^{2-}(G)$. If $\delta_{\zeta^{2-}(G)} \geq 4$, we refer to these two successive contracting wheel operations as a domino contracting wheel operation. If $\delta_{\zeta^{2-}(G)} = 2$ or 3, then we implement contracting 2-wheel or 3-wheel operations repeatedly until a K_4 or a graph $\zeta^{m-}(G)$ with $\delta_{\zeta^{m-}(G)} \geq 4$ is obtained. If $\delta_{\zeta^{m-}(G)} \geq 4$, we refer to these m contracting wheel operations as a domino contracting wheel operation; if $\zeta^{m-}(G) \cong K_4$, we call G a dominoable maximal planar graph. Fig. 9(a) shows a dominoable maximal planar graph G of order 9, and Fig. 9(b) is $\zeta^-(G)$ that is obtained from Fig. 9(a) by implementing one contracting 4-wheel operation on the 4-wheel (marked by bold lines in Fig. 9(a)), in the process of which u, v are identified. As there exists two 2-degree vertices in $\zeta^-(G)$, we implement contracting 2-wheel operations on the two 2-degree vertices respectively. The resulting graph $\zeta^{3-}(G)$ is shown in Fig. 9(c), which has minimum degree 3. Therefore, we continually conduct contracting wheel operations till the resulting graph is K_4 or the one with minimum degree ≥ 4 . The process of a domino contracting wheel operation on G is illustrated in Fig. 9(a)~9(d).

Let G be a maximal planar graph with $\delta \geq 4$, and P_3 (or L) be a 2-path (or funnel subgraph). If $\zeta^+(G)$ is the resulting graph by

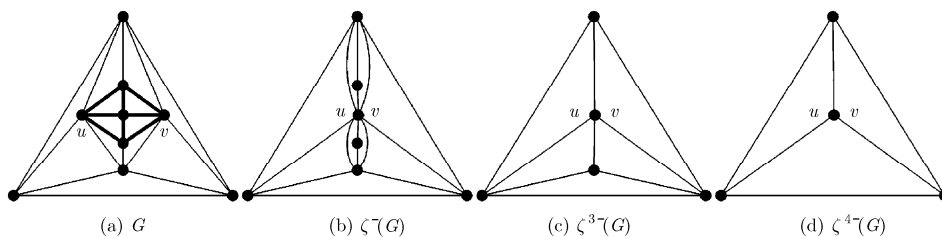


Fig. 9 A dominoable maximal planar graph of order 9

conducting an extending 4-wheel (or 5-wheel) operation on P_3 (or L), then we call the extending 4-wheel (or 5-wheel) operation a domino extending wheel operation. If $\zeta^+(G)$ is the resulting graph by conducting an extending 2-wheel (or 3-wheel) operation, then the minimum degree of $\zeta^+(G)$ is 2 or 3. We continue to implement an extending wheel operation on $\zeta^+(G)$, and denote the resulting graph by $\zeta^{2+}(G)$. If $\delta_{\zeta^{2+}(G)} \geq 4$, we refer to these two consecutive extending wheel operations as a domino extending wheel operation; if $\delta_{\zeta^{2+}(G)} = 2$ or 3, then we need to continually implement extending wheel operations. Let m be the total number of extending wheel operations. If $\zeta^{m+}(G)$ has minimum degree ≥ 4 , then we refer to these m extending wheel operations as a domino extending wheel operation. Examples for domino extending wheel operations are given in the following subsection.

3.2 Domino extending-contracting operations with inner vertices ≤ 3 and domino configuration

Let G be a maximal planar graph with $\delta \geq 4$, and $\zeta^{m+}(G)$ be the resulting graph by conducting one domino extending wheel operation based on G , which includes m extending wheel operations. The structural change from G to $\zeta^{m+}(G)$ is related closely with a subgraph, called domino configuration. In the following, we discuss this configuration in detail for $m = 1, 2, 3$.

When $m = 1$, $\zeta^+(G)$ is obtained by one extending 4-wheel or 5-wheel operation on G . In this case, we call the 4-wheel or 5-wheel a domino configuration, where the object of extending wheel operations is a 2-path or funnel, see Fig. 10.

Suppose $\zeta^+(G)$ is a maximal planar graph of minimum degree ≥ 4 , and $W_4 = x - v_1v_2v_3v_2'$ is a 4-wheel subgraph of $\zeta^+(G)$, shown in Fig. 10(a),

where $d_{\zeta^+(G)}(v_1), d_{\zeta^+(G)}(v_3) \geq 6$. We use G to denote the resulting graph by conducting contracting wheel operation on W_4 . Obviously, $\delta(G) \geq 4$. Therefore, we can obtain G from $\zeta^+(G)$ by conducting only one domino contracting wheel operation. We then call the W_4 in $\zeta^+(G)$ a domino configuration. Analogously, if $W_5 = x - v_1v_2v_3v_4v_2'$ is a 5-wheel in $\zeta^+(G)$ and $d_{\zeta^+(G)}(v_1) \geq 6, d_{\zeta^+(G)}(v_3) \geq 5, d_{\zeta^+(G)}(v_4) \geq 5$, as Shown in Fig. 10(b), then one contracting wheel operation on W_5 is also a domino contracting wheel operation, where v_2, v_2' are identified. Accordingly, we call the 5-wheel W_5 in $\zeta^+(G)$ a domino configuration.

When $m = 2$, we can obtain $\zeta^{2+}(G)$ by implementing extending 24-wheel operation (that is, implement ζ_2^+ first and then ζ_4^+ . Other definitions are defined in the same way), extending 34-wheel operation, extending 25-wheel operation or extending 35-wheel operation (there exist two types: one is I-type extending 35-wheel operation, in which the wheel-center in the process of extending 3-wheel is the top of funnel in extending 5-wheel; see Fig. 11(d). The other is II-type extending 35-wheel operation, in which the wheel-center in the process of extending 3-wheel is one bottom of funnel in extending 5-wheel; see Fig. 11(e)). In this case, we refer to the subgraph induced by the vertices set of two wheel-centers and their neighbors in $\zeta^{2+}(G)$ as a domino configuration, where the objects before extending wheel operation can be a 2-path, funnel or dumbbell subgraph (two triangles with exactly one common vertex); see Fig. 11.

Remark Domino configurations induced by extending 25-wheel, 34-wheel and 35-wheel operations respectively are isomorphic.

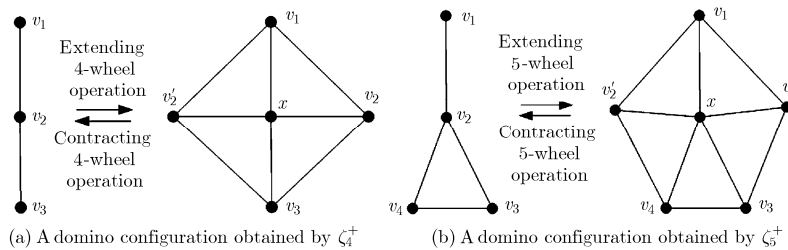


Fig. 10 Two domino configurations with one vertex inside the infinite face

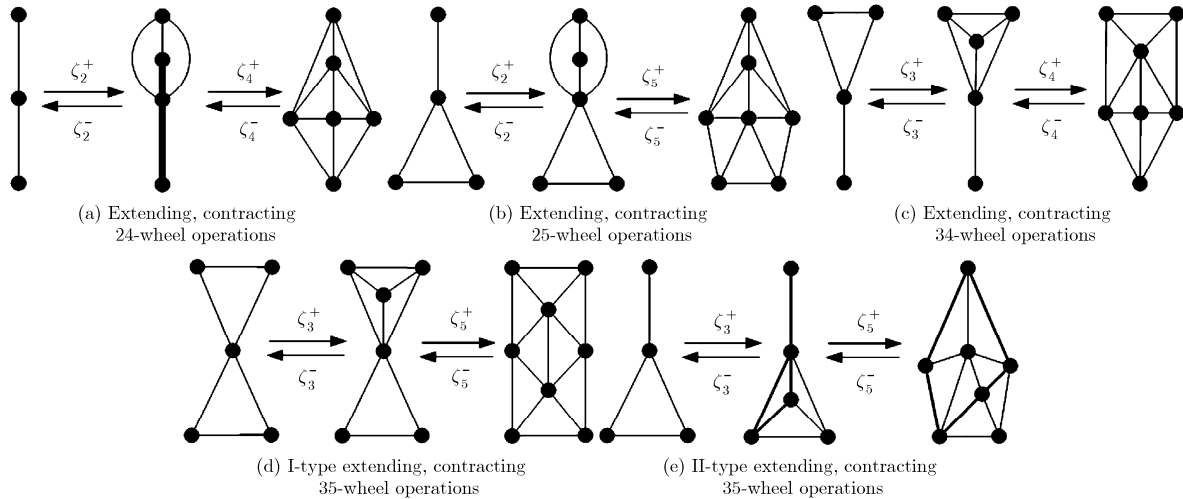


Fig. 11 Domino configurations with two vertices inside the infinite face

Therefore, the number of domino configurations including two wheel-centers is 3.

Analogously, the number of domino contracting wheel operations that involve two wheel-centers is in total five: contracting 24-wheel operation, contracting 25-wheel operation, contracting 34-wheel operation, I-type contracting 35-wheel operation, and II-type contracting 35-wheel operation, respectively; see Fig. 11. It is not hard to obtain the necessary conditions for implementing these five kinds of domino contracting wheel operations. For example, the necessary condition for implementing contracting 24-wheel operation is all vertices in the outer cycle of the corresponding configuration have degree at least 6, except two ones which are identified in the process of contracting 4-wheel operation.

When $m=3$, $\zeta^{3+}(G)$ can be obtained from G by conducting extending 224-wheel operation, 234-wheel operation, 334-wheel operation (two types: one is non-adjacent extending 334-wheel operation, in which two wheel-centers in the process of extending 3-wheel are not adjacent; see Fig. 12(c); the other is adjacent extending 334-wheel operation, in which the two wheel-centers in the process of extending 3-wheel are adjacent; see Fig. 12(d)), extending 235-wheel operation (two types: one is adjacent extending 235-wheel operation, in which two wheel-centers in the process of ζ_2^+ and ζ_3^+ are adjacent; see Fig. 12(e); the other is non-adjacent extending 235-wheel

operation, in which the two wheel-centers in the process of ζ_2^+ and ζ_3^+ are not adjacent; see Fig. 12(f)), or extending 335-wheel operation (three types: non-adjacent extending 335-wheel operation, asymmetric and adjacent extending 335-wheel operation, and symmetric and adjacent extending 335-wheel operation; see Fig. 12(g)~12(i)). In this case, we refer to the subgraph of $\zeta^{3+}(G)$ induced by the vertex set of the three wheel-centers and their neighbors, in the process of extending wheel operation, as a domino configuration, where the object of the above extending operations can be a 2-path, funnel or dumbbell subgraph. We refer to the non-adjacent extending 334-wheel operation as dumbbell transformation, which will play a key role on the study of pure tree-coloring graphs^[24]; see the third paper of this series of articles that will discuss about the dumbbell transformation in details.

Remark Domino configurations induced by extending 334-wheel and 235-wheel operations are isomorphic, by extending 234-wheel and 335-wheel operations are isomorphic. Therefore, the number of domino configurations that contain three wheel-centers is 7.

Similarly, there are 9 kinds of domino contracting wheel operations involving three wheel-centers: contracting 224-wheel operation, contracting 234-wheel operation, non-adjacent contracting 334-wheel operation, adjacent contracting 334-wheel operation, adjacent

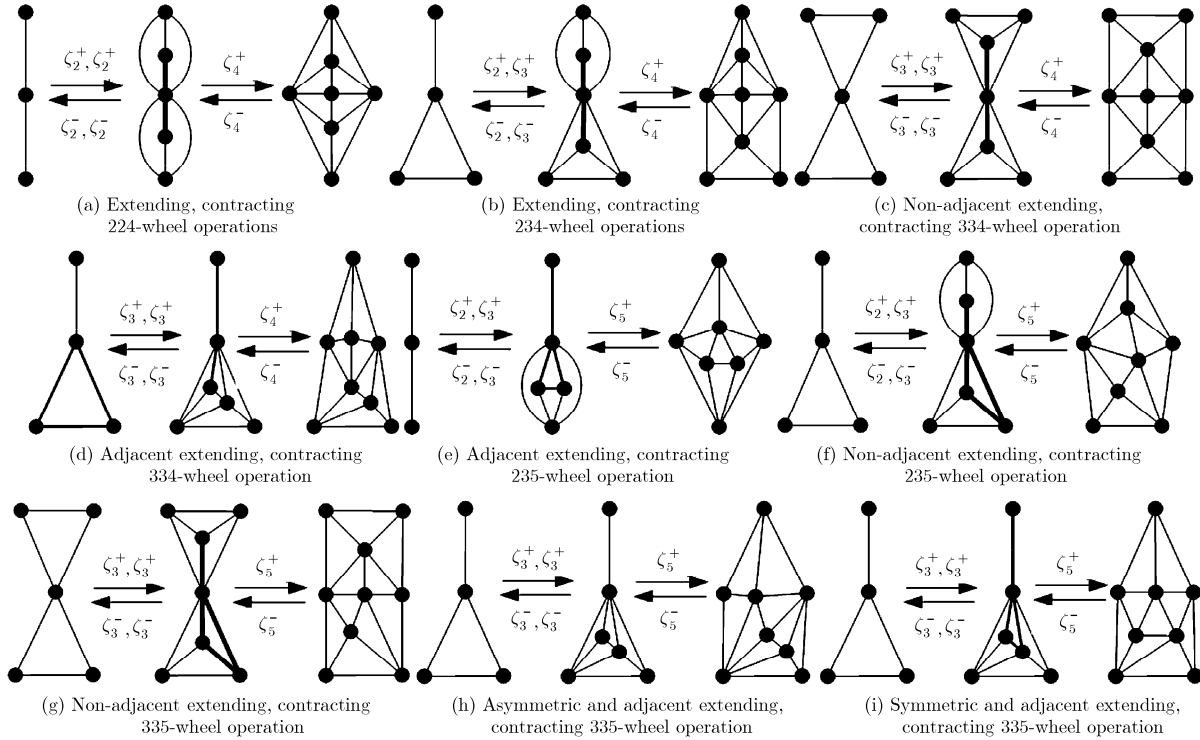


Fig. 12 Seven domino configurations with three vertices inside the infinite face

contracting 235-wheel operation, non-adjacent contracting 235-wheel operation, non-adjacent contracting 335-wheel operation, asymmetric and adjacent contracting 335-wheel operation, symmetric and adjacent contracting 335-wheel operation; see Fig. 12. The necessary conditions for implementing these operations can also be deduced easily, so we are not going to repeat them in detail.

To sum up, there are in total a number of 12 domino configurations with 1~3 wheel-centers. For convenience, we list all of them in Fig. 16. In what follows, the wheel-centers in a domino configuration are also called inner vertices of the domino configuration, and the 5 domino configurations illustrated in the first two lines in Fig. 17 are also called basic domino configurations.

3.3 The set of objects of domino extending wheel operations

Let G be a maximal planar graph with $\delta \geq 4$. Suppose that $P_3 = v_1v_2v_3$ is a 2-path and $L = u_1 - \Delta u_2u_3u_4$ is a funnel subgraph. If v_1 and v_3 are adjacent in P_3 , or u_1 is adjacent to one of bottoms of L , then the resulting graph by conducting one extending 4-wheel operation on P_3 or 5-wheel operation on L is separable. So, when

we only conduct one extending wheel operation, we demand that v_1 and v_3 are not adjacent in P_3 , and u_1 is not adjacent to any bottom of L . However, when we conduct $m(\geq 2)$ extending wheel operations, the situation will be different.

Remark 1 Let G be a maximal planar graph with $\delta \geq 4$, and $P_3 = v_1v_2v_3$ be a 2-path of G such that v_1 and v_3 are adjacent. For any $m \geq 1$, when implementing m extending wheel operations on P_3 , we obtain a separable graph $\zeta^{m+}(G)$ that has a maximal planar proper subgraph with infinite face $\Delta v_1v_2v_3$.

Remark 2 Let G be a non-separable maximal planar graph with $\delta \geq 4$. Suppose that $L = v_1 - \Delta v_2v_3v_4$ is a funnel subgraph of G , in which v_1 and v_3 are adjacent. For any $m \geq 2$, when implementing m extending wheel operations on L , we obtain a non-separable graph $\zeta^{m+}(G)$. Examples of this remark are shown in Figs. 13(g)~13(j).

Remark 3 Let G be a non-separable maximal planar graph with $\delta \geq 4$. Suppose that $Y = \Delta v_1v_2u - \Delta uv_3v_4$ is a dumbbell of G , as shown in Fig. 13(c). No matter whether or not v_1 is

adjacent to v_3 and v_2 is adjacent to v_4 , we will obtain a non-separable graph $\zeta^{m+}(G)$ by implementing $m(\geq 2)$ extending wheel operations on Y ; see Figs. 13(k) and 13(l).

Based on these three remarks, it is easy to know that there are in total 6 objects in domino extending wheel operations; see Figs. 13(a)~ 13(f).

3.4 General definition of domino configurations

In Subsection 3.2, we showcased all domino configurations containing 1~3 inner vertices. A question naturally arises: what is the structure of a domino configuration when it contains $m \geq 4$ inner vertices? To answer this question, we give a general definition of the domino configuration, and characterize properties of such a class of graphs in this subsection. First, we give three examples to illustrate the processes of domino contacting wheel operations on domino configurations with $m \geq 4$ inner vertices, shown in Fig. 14.

Note that for any domino configuration with 1~3 inner vertices given in Subsection 3.2 or more than 3 inner vertices obtained by implementing domino extending wheel operation, there are the following properties. At least one of 4-wheel W_4 or 5-wheel W_5 in the domino configuration satisfy: (1) let x be the wheel-center of W_4 or W_5 , then there exists a pair of non-adjacent vertices u, v on C^x such that $\{u, v\} \subset V(C)$; (2) when conducting one domino contracting wheel operation on W_4 or W_5 , in which u, v are identified, we can obtain a 2-path, funnel or dumbbell.

Based on the above discussions, we introduce the general definition of domino configurations as follows. Let G be a maximal planar graph with minimum degree at least 4, and G^C be a semi-maximal planar subgraph of G with outer cycle C . We call G^C a domino configuration if there exists a 4-wheel W_4 or a 5-wheel W_5 in G^C satisfying: (1) let x be the wheel-center of W_4 or W_5 . Then there exists a pair of non-adjacent vertices u, v on C^x such that $\{u, v\} \subset V(C)$; (2) when conducting a domino contracting wheel operation on W_4 or W_5 , in which u, v are identified, we can obtain a graph without any wheels. Here, we call u, v the contracted vertices of G^C , and call x the initial contracted wheel-center of G^C .

Suppose G^C is a domino configuration, and x is the initial contracted wheel-center. We use $X(x)$ to denote the set of inner vertices of G^C . Moreover, when there is no scope for confusion, we also write $X(x)$ as X simply.

It is easy to see that every domino configuration G^C can be contracted into a 2-path, a funnel or a dumbbell subgraph, which implies that the length of C is 4, 5 or 6. So, we have the following theorem.

Theorem 2 Let G be a maximal planar graph with $\delta_G \geq 4$, and G^C be a domino configuration of G with contracted vertices u, v . Then,

- (1) G^C can be contracted into a 2-path, a

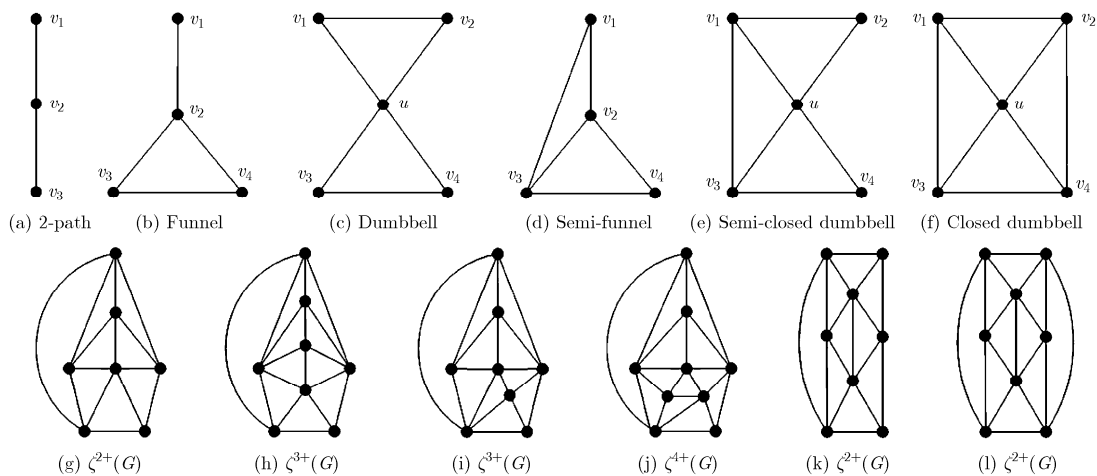


Fig. 13 Sixobject subgraphs that are extended in domino extending wheel operations and examples

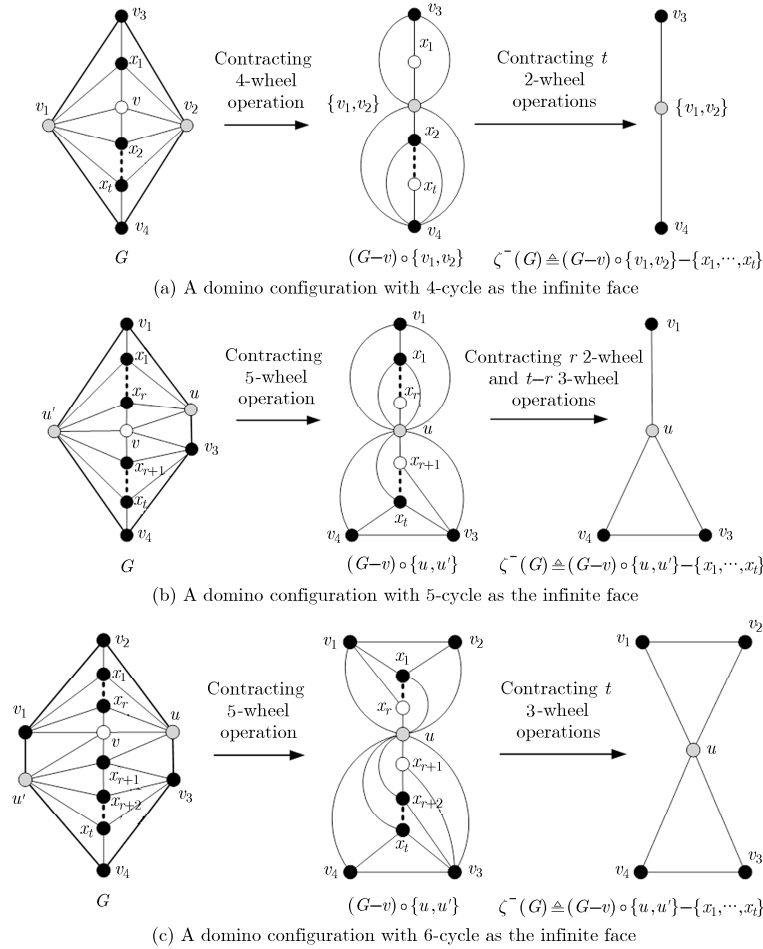


Fig. 14 Three domino configurations with ≥ 4 inner vertices

funnel, or a dumbbell subgraph by conducting a domino contracting operation where u, v are contracted vertices;

(2) $4 \leq |C| \leq 6$.

Based on Theorem 2, we further have the following result.

Lemma 1 Let G^C be a domino configuration with contracted vertices u, v .

(1) When $|V(C)| = 4$, let $C = uz_1vz_2u$. Then $d_{G^C}(z_1) \leq 4$; $d_{G^C}(z_2) \leq 4$;

(2) When $|V(C)| = 5$, let $C = uz_1vz_2z_3u$. Then $d_{G^C}(z_1) \leq 4$; $d_{G^C}(z_2)$ or $d_{G^C}(z_3) = 3$.

(3) When $|V(C)| = 6$, let $C = uz_1z_2vz_3z_4u$. Then $d_{G^C}(z_1)$ or $d_{G^C}(z_2) = 3$; $d_{G^C}(z_3)$ or $d_{G^C}(z_4) = 3$.

Proof For (1), to the contrary we assume $d_{G^C}(z_1) \geq 5$. Let u, y_1, \dots, y_l, v be the $l \geq 3$ neighbors of z_1 one by one in G^C . Let x be the

initial contracted wheel-center of G^C . Then G^C can be contracted into a 2-path by conducting a domino contracting operation. It is easy to see that all degrees of y_1, \dots, y_l are ≥ 3 in $G^C[V(C) \cup \{y_1, \dots, y_l\}]$. Suppose that in the process of the above domino contracting wheel operation y is the first vertex in $\{y_1, \dots, y_l\}$ to be contracted. We use $\zeta^-(G^C)$ to denote the graph just before the wheel with wheel-center y is contracted during the domino contracting wheel operation. When $y = y_1$ or y_l , it has that y_2 or y_{l-1} is adjacent to x_v^u in $\zeta^-(G^C)$, where x_v^u is the new vertex after identifying u and v . Thus, y_2 is adjacent to u , or y_{l-1} is adjacent to v in G^C ; that is, $d_{G^C}(y_2) = 3$ or $d_{G^C}(y_{l-1}) = 3$, which contradicts the fact that G^C is a domino configuration. Therefore, $d_{G^C}(z_1) \leq 4$. By the same token, we also have $d_{G^C}(z_2) \leq 4$.

For (2), we present an analogous proof of that

for (1). We have that $d_{G^C}(z_1) \leq 4$. Obviously, $d_{G^C}(z_2)$ and $d_{G^C}(z_3) \geq 3$. Assume that $d_{G^C}(z_2) \geq 4$ and $d_{G^C}(z_3) \geq 4$. Let u, y_1, \dots, y_l, v be the l neighbors of z_2 or z_3 , one by one in G^C , where y_r is the common neighbor of z_2 and z_3 , $2 \leq r \leq l-1$, $l \geq 3$. Then in $G^C[V(C) \cup \{y_1, \dots, y_l\}]$, the degree of y_r is 4, and all degrees of $\{y_1, \dots, y_l\} \setminus \{y_r\} \geq 3$. Suppose that in the process of the above domino contracting operation y is the first vertex to be contracted in $\{y_1, \dots, y_l\}$. Similar to the proof of (1), it follows that there is a 3-degree vertex in G^C , and a contradiction. Hence, $d_{G^C}(z_2) = 3$ or $d_{G^C}(z_3) = 3$.

For (3), analogously to the proof of (2), we can deduce that $d_{G^C}(z_1) = 3$ or $d_{G^C}(z_2) = 3$, $d_{G^C}(z_3) = 3$ or $d_{G^C}(z_4) = 3$. So the result holds.

Theorem 3 follows from Lemma 1 directly.

Theorem 3 Let G^C be a domino configuration with initial contracted wheel-center x and contracted vertices u, v .

(1) If $P_3 = uz_1v$ is a 2-path on C , where z_1 and x are not adjacent, then $G^C - z_1$ is a domino configuration with initial contracted wheel-center x and contracted vertices u, v ;

(2) If $P_4 = uz_2z_3v$ is a 3-path on C , where neither z_2 nor z_3 is adjacent to x . If $d_{G^C}(z_2) = d_{G^C}(z_3) = 3$, then $G^C - \{z_2, z_3\}$ is a domino configuration with initial contracted wheel-center x and contracted vertices u, v ; if $d_{G^C}(z_2) = 3$, $d_{G^C}(z_3) \geq 4$, then $G^C - z_2$ is a domino configuration with initial contracted wheel-center x and contracted vertices u, v .

3.5 Properties of domino configurations

In order to characterize domino configurations,

we first introduce four operators, $\tau_1, \tau'_1, \tau_2, \tau_3$, called generated operations of domino configurations.

Suppose that G^C is a domino configuration with contracted vertices u, v . The τ_1 operator of G^C is to select a 2-path $P = uyv$ on C , and then add a new vertex z in the exterior of C and connect z to u, y, v respectively. The resulting graph obtained from G^C by implementing τ_1 is denoted by $\tau_1(G^C)$.

The τ'_1 operator of G^C is to select a 2-path $P = xyv$ on C , where $x \notin \{u, v\}$, and then add a new vertex z in the exterior of C and connect this vertex to x, y, v respectively. The resulting graph obtained from G^C by implementing τ'_1 is denoted by $\tau'_1(G^C)$.

The τ_2 operator of G^C is to select a 2-path $P = uyv$ on C , and then add two adjacent vertices z_1, z_2 in the exterior of C and connect z_1 to u , z_2 to v , and y to z_1 and z_2 , respectively. The resulting graph obtained from G^C by implementing τ_2 is denoted by $\tau_2(G^C)$.

The τ_3 operator of G^C is to select a 3-path $P = uy_1y_2v$ on C , and then add a new vertex z in the exterior of C and connect this vertex to u, y_1, y_2, v respectively. The resulting graph obtained from G^C by implementing τ_3 is denoted by $\tau_3(G^C)$. The specific processes of $\tau_1, \tau'_1, \tau_2, \tau_3$ are shown in Figs. 15(a)~15(d).

Based on the above four operators, we built an operational system to generate domino configurations, denoted by $\langle \{W_4, W_5\}; \Gamma \rangle$, where $\Gamma = \{\tau_1, \tau'_1, \tau_2, \tau_3\}$. This system aims to generate all domino configurations based on W_4 and W_5 by using $\tau_1, \tau'_1, \tau_2, \tau_3$ repeatedly. For example, starting with W_4 , we can obtain $\tau_3\tau_2\tau_1\tau_3\tau_2\tau_1(W_4)$, shown in Fig. 16(a) by implementing $\tau_1, \tau_2, \tau_3, \tau_1, \tau_2, \tau_3$ successively; starting with W_5 , we can obtain

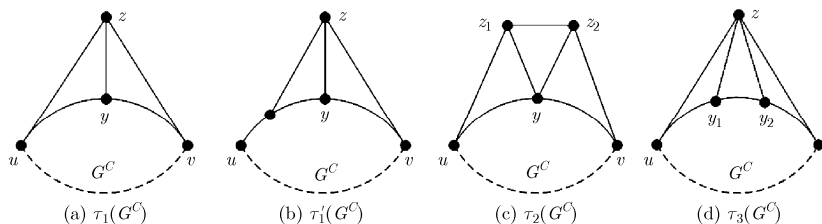


Fig. 15 Four kinds of generated operations of domino configurations

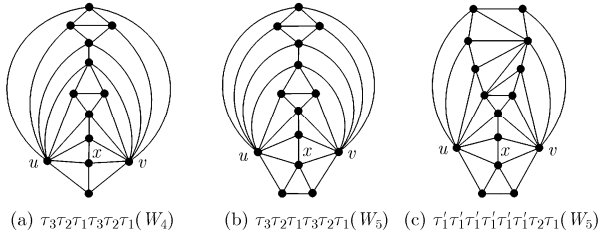


Fig. 16 Threedomino configurations

$\tau_3\tau_2\tau_1\tau_3\tau_2\tau_1(W_5)$ shown in Fig. 16(b), by implementing $\tau_1, \tau_2, \tau_3, \tau_1, \tau_2, \tau_3$ successively; starting with W_5 , we can obtain $\tau_1'\tau_1'\tau_1'\tau_1'\tau_1'\tau_2\tau_1(W_5)$ shown in Fig. 16(c), by implementing $\tau_1, \tau_2, \tau_1', \tau_1', \tau_1', \tau_1', \tau_1'$ successively.

Note that for any configuration G^C with the contracted vertices u, v , there exist the following facts.

Fact 1 Implementing one τ_1 is the same as conducting one extending 2-wheel operation, thus, G^C is a domino configuration iff $\tau_1(G^C)$ is a domino configuration. The length of the boundary of infinite face of $\tau_1(G^C)$ is equal to that of G^C , that is, $|V(\tau_1(C))| = |V(C)|$, where $\tau_1(C)$ is the boundary of infinite face of $\tau_1(G^C)$, similarly hereinafter.

Fact 2 Implementing one τ_1' is the same as conducting one extending 3-wheel operation. Thus, G^C is a domino configuration iff $\tau_1'(G^C)$ is a domino configuration. The length of the boundary

of infinite face of $\tau_1'(G^C)$ is equal to that of G^C , that is, $|V(\tau_1'(C))| = |V(C)|$.

Fact 3 Implementing one τ_2 is the same as conducting one extending 3-wheel operation. So G^C is a domino configuration iff $\tau_2(G^C)$ is a domino configuration. Here, $|V(\tau_2(C))| = |V(C)| + 1$.

Fact 4 Implementing one τ_3 operator is the same as conducting one extending 23-wheel operation. Hence, G^C is a domino configuration iff $\tau_3(G^C)$ is a domino configuration. Here, $|V(\tau_3(C))| = |V(C)| - 1$.

Theorem 4 Any domino configuration can be generated by $\langle \{W_4, W_5\}; \Gamma \rangle$.

Proof The proof is by inducing the number t of inner vertices of a domino configuration G^C .

When $t=2, 3$, by the foregoing discussion (in Subsection 3.2), there are in total three domino configurations with 2 inner vertices (see Fig. 11 or line 2 in Fig. 17). Moreover, all the domino configurations with 1~3 inner vertices are illustrated in Fig. 17.

By implementing τ_1 and τ_2 on W_4 , respectively, we obtain the first and second domino configurations with two inner vertices, shown in line 2 of Fig. 17; by implementing τ_1, τ_1', τ_2 , and τ_3 on W_5 , respectively, we get the second and third domino configurations (in line 2 of Fig. 17) which contain two inner vertices, and the last

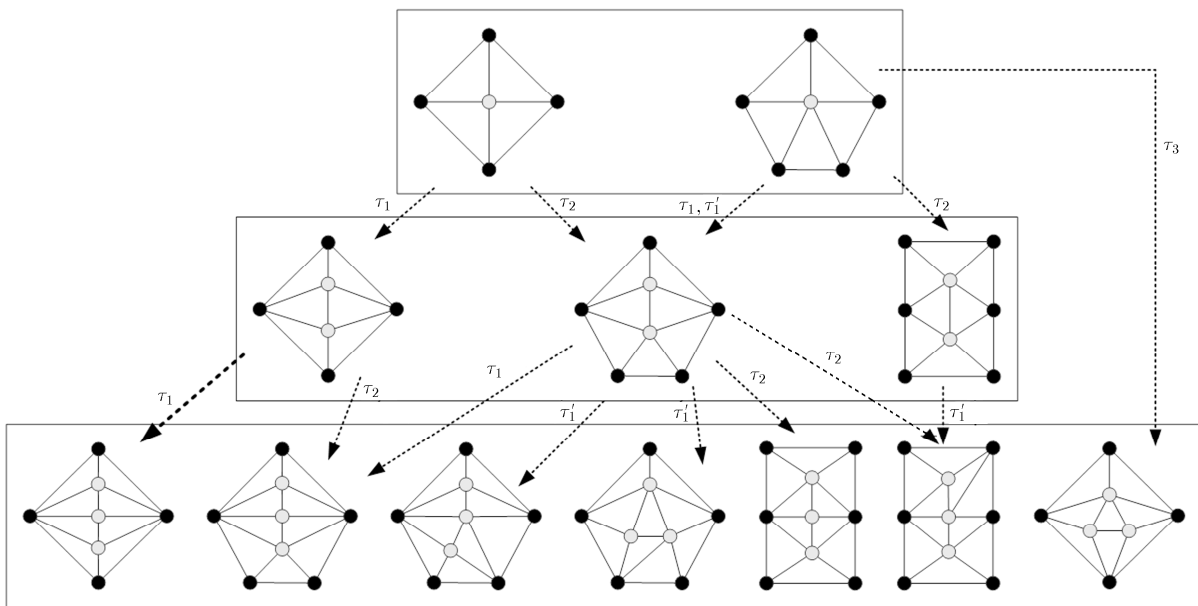


Fig. 17 All the domino configurations with 1-3 inner vertices

domino configuration (in line 3 of Fig. 17) which contain three inner vertices.

In Fig. 17, we get the first and second domino configurations (in line 3) with three inner vertices by conducting τ_1 and τ_2 to the first graph in line 2. In addition, we can get the second, third, fourth, fifth, and sixth domino configurations (in line 3) with 3 inner vertices by implementing operations $\tau_1, \tau'_1, \tau'_1, \tau_2$, and τ_2 on the second graph in line 2, respectively. Note that in the process of these operations, the involved contracted vertices are different. If we conduct τ'_1 on the third graph in line 2, then we can also obtain the sixth graph in line 3.

Hence, the result holds for $t=2, 3$.

Suppose that the result holds for $t = n (\geq 3)$. We now consider the case of $t = n + 1$. Let u, v be the contracted vertices of G^C . According to Lemma 1, we need to consider the following three cases.

Case 1 $|V(C)| = 4$

Let $C = uz_1vz_2u$. Then $d_{G^C}(z_1) \leq 4, d_{G^C}(z_2) \leq 4$, and there is at least one vertex among z_1, z_2 that is not adjacent to the initial contracted wheel-center x . Without loss of generality, assume z_1 is not adjacent to x . If $d_{G^C}(z_1)=3$, then $G^C - z_1$ is a domino configuration according to Theorem 4. Thus, by the induction hypothesis, $G^C - z_1$ can be generated by $\langle\{W_4, W_5\}; \Gamma\rangle$. Notice that $G^C = \tau_1(G^C - z_1)$, that is, G^C can be generated by $\langle\{W_4, W_5\}; \Gamma\rangle$.

If $d_{G^C}(z_1)=4$, then $G^C - z_1$ is a domino configuration, which can be generated by $\langle\{W_4, W_5\}; \Gamma\rangle$. Notice that $\tau_3(G^C - z_1)=G^C$. So G^C can be generated by $\langle\{W_4, W_5\}; \Gamma\rangle$.

Case 2 $|V(C)| = 5$

Let $C = uz_1vz_2z_3u$. Then $d_{G^C}(z_1) \leq 4, d_{G^C}(z_2) = 3$ or $d_{G^C}(z_3) = 3$. Without loss of generality, assume that $d_{G^C}(z_2) = 3$. Similar to Case 1, we can prove that $G^C - z_2$ is a domino configuration, which can be generated by $\langle\{W_4, W_5\}; \Gamma\rangle$. Note that $G^C = \tau'_1(G^C - z_2)$. So G^C can be generated

by $\langle\{W_4, W_5\}; \Gamma\rangle$.

Case 3 $|V(C)| = 6$

Let $C = uz_1z_2vz_3z_4u$. Then $d_{G^C}(z_1) = 3$ or $d_{G^C}(z_2) = 3$, and $d_{G^C}(z_3) = 3$ or $d_{G^C}(z_4) = 3$. Without loss of generality, we assume that z_1 is not adjacent to the initial contracted wheel-center, and $d_{G^C}(z_1)=3$. Similar to Case 1, we can see that $G^C - z_1$ is a domino configuration, which can be generated by $\langle\{W_4, W_5\}; \Gamma\rangle$. Therefore, G^C can be generated by $\langle\{W_4, W_5\}; \Gamma\rangle$, since $G^C = \tau'_1(G^C - z_1)$.

Hence, the conclusion holds.

Theorem 4 provides a method for generating domino configurations, by which any given domino configuration can be generated from W_4, W_5 . The domino configuration is the core of extending-contracting operational system of maximal planar graphs.

4 Ancestor-graphs and Descendent-graphs

In regard to the construction of maximal planar graphs, we need to consider two basic problems. (1)Where is a maximal planar graph from? More specifically, given a maximal planar graph G , what are the characteristics of the maximal planar graphs generating G by using extending wheel operation? (2)How many non-isomorphic maximal planar graphs can be generated from a given one? In order to solve these two problems, we need to use Theorem 4 as a key technique. For this, we introduce the concepts of ancestor-graphs and descendent-graphs.

Suppose that G is a maximal planar graph with $\delta_G \geq 4$. If it can be obtained from another maximal planar graph $\zeta^-(G)$ with $\delta_{\zeta^-(G)} \geq 4$ and lower order, then we call $\zeta^-(G)$ an ancestor-graph of G , while G is referred to as a descendent-graph of $\zeta^-(G)$. Accordingly, for a maximal planar graph G with $\delta_G \geq 4$, if $\zeta^+(G)$ is a maximal planar graph with $\delta_{\zeta^+(G)} \geq 4$ which is obtained from G by implementing extending wheel operations, then G is the ancestor-graph of $\zeta^+(G)$, and $\zeta^+(G)$ is the descendent-graph of G . Now we give their definitions in details.

4.1 Descendent-graphs

For a domino configuration G^C , we use $G_{v_2v_2}^{C_4}$, $G_{v_2v_2}^{C_5}$, and $G_{v_2v_2}^{C_6}$ to denote the domino configurations with outer cycles' length 4, 5, and 6, respectively. We also denote by $\mathfrak{S}_{v_2,v_2}^{C_4}$, $\mathfrak{S}_{v_2,v_2}^{C_5}$, and $\mathfrak{S}_{v_2,v_2}^{C_6}$ the set of all domino configurations with outer cycles' length 4, 5 and 6, respectively, where v_2, v_2' are the contracted vertices of G^C . Similarly, descendent-graphs of G are classified into the following three types.

(1)Path-type descendent-graphs

Let $P_3 = v_1v_2v_3$ be a 2-path of G . The extending-4-cycle-type semi-maximal planar graph of G based on P_3 , denoted by $G_{P_3}^{C_4}$, is the resulting graph obtained by the following actions: replace P_3 by a 4-cycle $C_4 = v_1v_2'v_3v_2$; that is, spilt the vertex v_2 into two vertices v_2 and v_2' , split v_1v_2 into two edges v_1v_2 and v_1v_2' , and split v_2v_3 into v_2v_3 and $v_2'v_3$ respectively. All edges (incident with v_2) on the left of P_3 in G are incident with v_2 , and all edges (incident with v_2) on the right of P_3 in G are incident with v_2' , such that the resulting graph is still planar. This process is shown in Fig. 18, where v_2 and v_2' are called extended vertices of $G_{P_3}^{C_4}$.

Suppose that $G_{v_2v_2}^{C_4} \in \mathfrak{S}_{v_2,v_2}^{C_4}$, $C_4 = v_1v_2'v_3v_2$, and v_2, v_2' are contracted vertices of $G_{v_2v_2}^{C_4}$; see the last graph in Fig. 18. If $G_{P_3}^{C_4} \cap G_{v_2v_2}^{C_4} = C_4 = v_1v_2'v_3v_2v_1$,

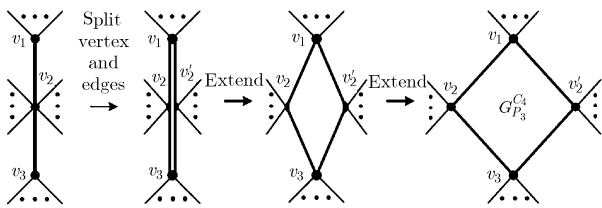


Fig. 18 The process of constructing an extending-4-cycle-type semi-maximal planar graph

then we refer to $G_{P_3}^{C_4} \cup G_{v_2v_2}^{C_4}$ as a path-type descendent-graph of G , or a descendent-graph of G based on $\{P_3, G_{v_2v_2}^{C_4}\}$ specifically.

(2)Funnel-type descendent-graphs

Let $L = v_1 - \Delta v_2v_3v_4$ be a funnel of G . The extending-5-cycle-type semi-maximal planar graph of G based on L , denoted by $G_L^{C_5}$, is the resulting graph obtained by conducting the following procedures: replace L by a 5-cycle $v_1v_2v_3v_4v_2'$; that is, spilt the vertex v_2 into two vertices v_2 and v_2' , and split the edge v_1v_2 into two edges v_1v_2 and v_1v_2' . All edges (incident with v_2) on the left of L in G are incident with v_2 , and all edges (incident with v_2) on the right of L in G are incident with v_2' , satisfying that the resulting graph is still planar. This process is shown in Fig. 19, where v_2 and v_2' are called extended vertices of $G_L^{C_5}$.

Suppose that $G_{v_2v_2}^{C_5} \in \mathfrak{S}_{v_2,v_2}^{C_5}$, $C_5 = v_1v_2'v_3v_4v_2$, and v_2, v_2' are contracted vertices of $G_{v_2v_2}^{C_5}$. If $G_L^{C_5} \cap G_{v_2v_2}^{C_5} = C_5 = v_1v_2'v_3v_4v_2v_1$, then we refer to $G_L^{C_5} \cup G_{v_2v_2}^{C_5}$ as a funnel-type descendent-graph of G , or a descendent-graph of G based on $\{L, G_{v_2v_2}^{C_5}\}$.

(3)Dumbbell-type descendent-graphs

Let $Y = \Delta v_1v_3v_2 - \Delta v_4v_5v_2$ be a dumbbell of G . The extending-6-cycle-type semi-maximal planar graph of G based on Y , denoted by $G_Y^{C_6}$, is the resulting graph obtained by the following actions: replace Y by a 6-cycle $v_1v_3v_2'v_5v_4v_2$; that is, spilt the vertex v_2 into two vertices v_2 and v_2' . All the edges (incident with v_2) on the left of Y in G are incident with v_2 , and all edges (incident with v_2) on the right of Y in G are incident with v_2' , such that the resulting graph is still planar.

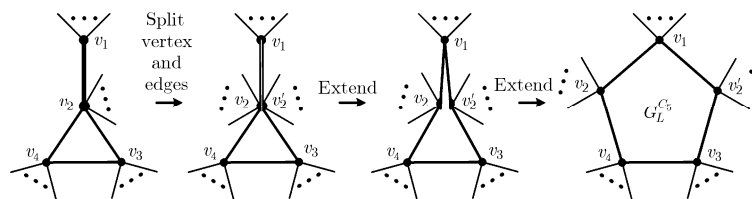


Fig. 19 The process of constructing an extending-5-cycle-type semi-maximal planar graph

This process is shown in Fig. 20, where v_2 and v_2' are called extended vertices of $G_Y^{C_6}$.

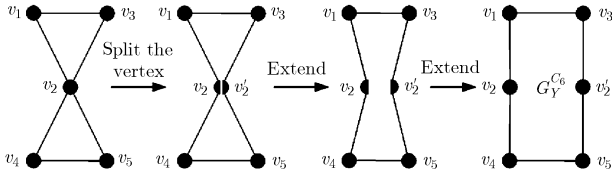


Fig. 20 The process of constructing an extending -6-cycle-type semi-maximal planar graph

Suppose that $G_{v_2 v_2'}^{C_6} \in \mathfrak{S}_{v_2, v_2'}^{C_6}$, $C_6 = v_1 v_3 v_2' v_5 v_4 v_2$ and v_2, v_2' are contracted vertices of $G_{v_2 v_2'}^{C_6}$. If $G_Y^{C_6} \cap G_{v_2 v_2'}^{C_6} = C_6 = v_1 v_3 v_2' v_5 v_4 v_2$, then we refer to $G_Y^{C_6} \cup G_{v_2 v_2'}^{C_6}$ as a dumbbell-type descendent-graph of G , or a descendent-graph of G based on $\{Y, G_{v_2 v_2'}^{C_6}\}$.

We collectively refer to the three types of descendent-graphs as descendent-graphs. Without taking the length of outer cycle into account, we also call the process of deriving a descendent-graph from a graph as embedding a domino configuration in an extending-cycle-type semi-maximal planar graph. By the discussion in the last section, we have that

$$|\mathfrak{S}_{v_2, v_2'}^{C_4}| \rightarrow \infty, |\mathfrak{S}_{v_2, v_2'}^{C_5}| \rightarrow \infty, |\mathfrak{S}_{v_2, v_2'}^{C_6}| \rightarrow \infty \quad (3)$$

The above formula means that every maximal planar graph G with $\delta(G) \geq 4$ has infinite amount of descendent-graphs. So the descendent-graphs of G can be classified by the number of inner vertices of domino configurations. Generally, if there are $t (\geq 1)$ inner vertices in the domino configuration, then we call the corresponding descendent-graph H a t -th descendent-graph of G , and use $\zeta^{+t}(G)$ to denote the set of all t -th descendent-graphs of G . Particularly, the 1-st, 2-nd and 3-rd descendent-graphs are also called the son-graph, grandson-graph, and great-grandson-graph, respectively.

Let $\Upsilon^+(G)$ denote the set of all descendent-graphs of G , then

$$\Upsilon^+(G) = \bigcup_{t=1}^{\infty} \zeta^{+t}(G) \quad (4)$$

In Equation (4), $\zeta^{+t}(G)$ only presents all the

generic t -th descendent-graphs of G , while the specific types of the involved domino configuration are not given. To address this issue, we introduce the concept of identical subgraph. Suppose that G is a maximal planar graph, and H, H' are two isomorphic subgraphs of G . Let $\text{Aut}(G)$ be the automorphism group of G . We say that H is identical to H' , if $\exists \sigma \in \text{Aut}(G)$ satisfies $\sigma(H) = H'$; Otherwise, H is non-identical to H' .

Throughout this paper, we denote by \mathfrak{S}_G^H the set of all non-identical subgraphs of G . In particular, we use $\mathfrak{S}_G^{P_3}, \mathfrak{S}_G^L, \mathfrak{S}_G^{L^*}, \mathfrak{S}_G^Y, \mathfrak{S}_G^{Y^*}$, and $\mathfrak{S}_G^{Y_*^*}$ to denote the sets of all non-identical 2-path P_3 , funnel subgraph L , semi-funnel subgraph L^* , dumbbell subgraph Y , semi-closed dumbbell subgraph Y^* and closed dumbbell subgraph Y_*^* of G , respectively.

With these conventions, $\zeta^{+t}(G)$ in Equation (4) can be written as

$$\zeta^{+t}(G) = \bigcup_{P_3 \in \mathfrak{S}_G^{P_3}} H_t^{P_3} \bigcup_{L \in \mathfrak{S}_G^L} H_t^L \bigcup_{L^* \in \mathfrak{S}_G^{L^*}} H_t^{L^*} \cdot \bigcup_{Y \in \mathfrak{S}_G^Y} H_t^Y \bigcup_{Y^* \in \mathfrak{S}_G^{Y^*}} H_t^{Y^*} \bigcup_{Y_*^* \in \mathfrak{S}_G^{Y_*^*}} H_t^{Y_*^*} \quad (5)$$

where $H_t^{P_3}, H_t^L, H_t^{L^*}, H_t^Y, H_t^{Y^*}$, and $H_t^{Y_*^*}$ denote the sets of all the t -th descendent-graphs of G based on 2-path P_3 , funnel subgraph L , semi-funnel subgraph L^* , dumbbell subgraph Y , semi-closed dumbbell subgraph Y^* , and closed dumbbell subgraph Y_*^* , respectively.

4.2 Ancestor-graphs

Let G be a maximal planar graph with $\delta(G) \geq 4$. Suppose that $C_4 = v_1 v_2' v_3 v_2$ is a 4-cycle of G . If the subgraph of G induced by C_4 and its interior, denoted by $G_{v_2 v_2'}^{C_4}$, is a domino configuration with contracted vertices v_2, v_2' , and the subgraph of G induced by C_4 and its exterior, denoted by $G_{P_3}^{C_4}$, satisfies that $d_{G_{P_3}^{C_4}}(v_1) \geq 5, d_{G_{v_2 v_2'}^{C_4}}(v_3) \geq 5$, then we call $G_{P_3}^{C_4} \circ \{v_2, v_2'\} = \zeta_{v_2 v_2'}^{-}(G)$ the ancestor-graph of G based on $G_{v_2 v_2'}^{C_4}$, or the path-type ancestor-graph of G .

Similarly, suppose that $C_5 = v_1 v_2' v_3 v_4 v_2$ is a 5-cycle of G . If the semi-maximal planar graph induced by C_5 and its interior is a domino

Configuration $G_{v_2v_2}^{C_5}$ with contracted vertices v_2, v_2' , and $d_{G_L^{C_5}}(v_1) \geq 5, d_{G_L^{C_5}}(v_3), d_{G_L^{C_5}}(v_4) \geq 4$ where $G_L^{C_5}$ is the semi-maximal planar graph induced by C_5 and its exterior, then we call $G_L^{C_5} \circ \{v_2, v_2'\} = \zeta_{G_{v_2v_2}^{C_5}}^-(G)$ the ancestor-graph of G based on $G_{v_2v_2}^{C_5}$, or the funnel-type ancestor-graph of G .

Let $C_6 = v_1v_3v_2'v_5v_4v_2$ be a 6-cycle of G . If the semi-maximal planar graph consisting of C_6 and its interior is a domino configuration $G_Y^{C_6}$ with contracted vertices v_2, v_2' , and $d_{G_Y^{C_6}}(v_1), d_{G_Y^{C_6}}(v_3), d_{G_Y^{C_6}}(v_4), d_{G_Y^{C_6}}(v_5) \geq 4$ in which $G_Y^{C_6}$ is the semi-maximal planar graph consisting of C_6 and its exterior, then we refer to $G_Y^{C_6} \circ \{v_2, v_2'\} = \zeta_{G_{v_2v_2}^{C_6}}^-(G)$ as the ancestor-graph of G based on $G_{v_2v_2}^{C_6}$, or the dumbbell-type ancestor-graph of G .

When ignoring the length of outer cycle of domino configurations, the above three types of ancestor-graphs are collectively called ancestor-graphs.

Remark For a maximal planar graph G with $\delta(G) \geq 4$, different from its descendent-graphs, there is only one ancestor-graph based on a given domino configuration.

For a maximal planar graph G , similar to its descendent-graphs, the ancestor-graphs can also be classified according to the number of inner vertices

of domino configurations $G_{v_2v_2}^{C_i}, (i = 4, 5, 6)$. Generally, we call $\zeta_{G_{v_2v_2}^{C_i}}^-(G)$ the t -th ancestor-graph of G (also denoted by $\zeta^{+t}(G)$ simply), if $\zeta_{G_{v_2v_2}^{C_i}}^-(G)$ has $t (\geq 1)$ inner vertices. In particular, the 1-st, 2-nd and 3-rd ancestor-graphs are also called the father-graph, grandfather-graph, and great-grandfather-graph, respectively.

Obviously, \mathfrak{S}_G^H is closely related to $\text{Aut}(G)$. The more likely G has a symmetric structure, the smaller the size of $|\mathfrak{S}_G^H|$ is. For instance, let G be the icosahedron graph. Then

$$|\mathfrak{S}_G^{R_3}| = |\mathfrak{S}_G^L| = 1, |\mathfrak{S}_G^Y| = 0 \tag{6}$$

In contrast, when $\text{Aut}(G)$ is a unit group, the size of $|\mathfrak{S}_G^H|$ is very large.

Let $\Upsilon^-(G)$ denote the set of all ancestor-graphs of G . Then we have the following results.

Theorem 5 Suppose that G is a maximal planar graph with $\delta(G) \geq 4$. Then $|\Upsilon^-(G)|$ is equal to the number of all non-identical domino configurations of G .

As an illustration, we take the icosahedron for instance (see the graph of order 12 and degree sequence 555555555555 shown in Appendix B). Since icosahedron contains only one non-identical domino configuration, the 5-wheel, it follows that icosahedron has only one ancestor-graph according to Theorem 5; see Fig. 21(a).

In addition, by Equation (6), we can see that icosahedron contains one non-identical 2-path, one

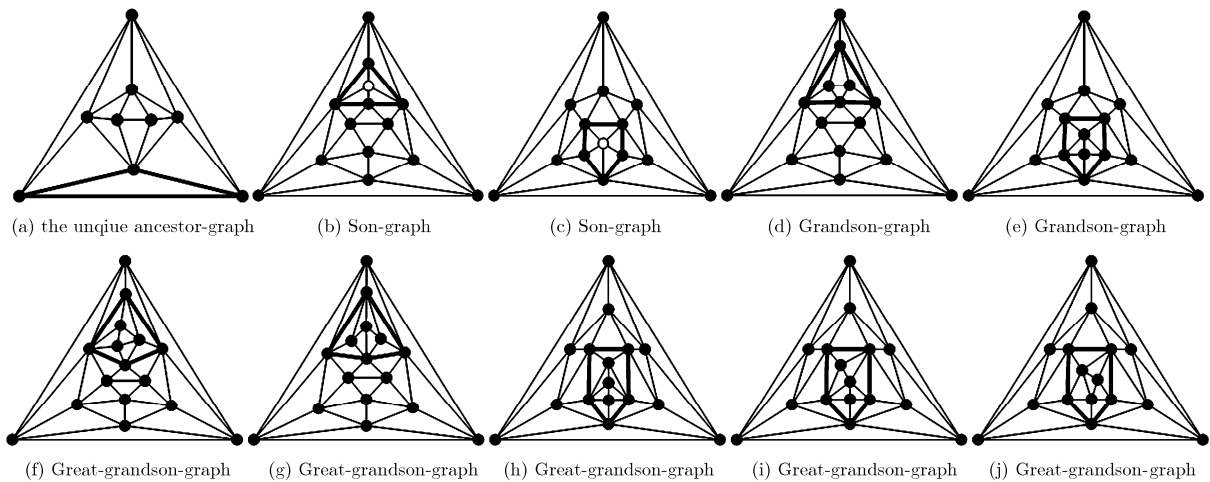


Fig. 21 The icosahedron together with its ancestor-graph and the 1-3rd descendent-graphs

non-identical funnel subgraph and no dumbbell subgraph. Therefore, according to Fig. 17 and discussions in Subsection 4.1, it has that the number of the 1~3rd descendent-graphs of icosahedron is 9; see Figs. 12(b)~12(j).

5 Methods to Generate Maximal Planar Graphs

The previous two sections give methods to construct ancestor-graphs and descendent-graphs of a maximal planar graph G with $\delta(G) \geq 4$. This section is devoted to considering how to construct a maximal planar graph of order n . First, we prove that every maximal planar graph can be generated from another one by a sequence of extending wheel operations, in other words, by some domino extending wheel operations. Then we describe how to construct a separable maximal planar graph. Finally, we show that any maximal planar graph with order $n (\geq 11)$ and minimum degree ≥ 4 has an ancestor-graph of order $(n - 2)$ or $(n - 3)$.

5.1 General theory on constructing graphs

Theorem 6 Suppose that G is a maximal planar graph of order n . Then G can be contracted to K_3 by implementing a series of contracting i -wheel operations for $i=2, 3, 4, 5$.

Proof The proof is by inducing the number n . When $n = 4$, there is only one maximal planar graph K_4 . So the conclusion is true. Suppose that the conclusion holds for $n \leq p (p \geq 4)$, which means that any maximal planar graph with order at most p can be contracted to K_3 by implementing contracting 2-wheel, 3-wheel, 4-wheel, and 5-wheel operations, repeatedly.

Now we consider the case when $n = p + 1$. For any maximal planar graph G of order $p + 1$, if G has a 2-degree or 3-degree vertex, then we will get a maximal planar graph with order p , $\zeta_2^-(G)$ or $\zeta_3^-(G)$, by deleting a 2-degree or a 3-degree vertex and its incident edges. According to the induction hypothesis, the conclusion holds. If $\delta(G) = 4$ or 5, then properly implementing a contracting 4-wheel operation or a contracting 5-wheel operation for some 4-degree or 5-degree vertex, we will get a graph $\zeta_4^-(G)$ or $\zeta_5^-(G)$, which is a maximal planar graph of order $p - 1$. On the basis of the induction

hypothesis, they can be contracted to K_3 by a series of contracting i -wheel operations for $i = 2, 3, 4, 5$. Hence, the conclusion holds.

According to Theorem 6, we can see that every maximal planar graph of order n can be contracted to K_3 by implementing four basic contracting wheel operations repeatedly. Accordingly, if we trace back to the reverses of contracting i -wheel operations of graph G , then by starting with K_3 and conducting the corresponding extending i -wheel operations, we can get the original graph G . So, the following corollary holds.

Corollary 1 Any two maximal planar graphs can be transformed into each other by implementing the four pairs of contracting and extending operations.

5.2 Construction of separable maximal planar graphs

Let H_1 and H_2 be maximal planar graphs, $H_1 \cap H_2 = \Delta_{v_1v_2v_3}$. If $G = H_1 \cup H_2$ has minimum degree at least 4, then G is called separable maximal planar graph, or separable graph for short. Since every triangle face of a maximal planar graph can be regarded as ∞ -face of the graph, we without loss of generality assume that $\Delta_{v_1v_2v_3}$ is always the ∞ -face of H_1 ; see Fig. 22(a), while assume that $\Delta_{v_1v_2v_3}$ is always the interior face of H_2 ; see Fig. 22(b). Thus, $G = H_1 \cup H_2$ can be considered to be the resulting maximal planar graph by embedding H_1 in the interior face $\Delta_{v_1v_2v_3}$ of H_2 , where the process of embedding a graph in one face of another graph is referred to as an embedding operation.

Suppose that H_1 and H_2 are two maximal planar graphs, $\Delta_{v_1v_2v_3} \triangleq \Delta_1$ and $\Delta_{v_1v_2v_3} \triangleq \Delta_2$ are triangle faces of H_1 and H_2 , respectively. The embedding operation of H_1 and H_2 based on $\{\Delta_1, \Delta_2\}$ is to relabel Δ_2 first; that is, define u_i as v_i for $i = 1, 2, 3$, and all the other vertices in H_1 and H_2 are labeled differently. Then, implement an union operation of H_1 and H_2 , by which the resulting graph $G = H_1 \cup H_2$ is a separable maximal planar graph.

Remark In the process of relabeling Δ_2 , u_i can also be defined in other ways. For example, u_1 ,

u_2 , and u_3 can be relabeled by v_2 , v_3 , and v_1 , respectively. Of course, we will obtain different separable graphs by relabeling Δ_2 in different ways.

Obviously, when $\delta(H_i) \geq 4, i = 1, 2$, it has that $\delta(G) \geq 4$. However, when $\delta(H_i) = 3$, it may exist that $\delta(G) \geq 4$. For example, H_1, H_2 are maximal planar graphs with minimum degree 3, $H_1 \cup H_2 = \Delta v_1 v_2 v_3$, while $G = H_1 \cup H_2$ has minimum degree ≥ 4 ; see Fig. 22.

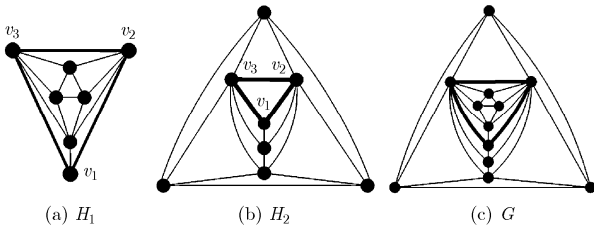


Fig. 22 The process of an embedding operation to generate a separable graph

Let G be a maximal planar graph. We call G a recursive maximal planar graph, if it can be obtained from K_4 by embedding a 3-degree vertex in some triangular face continuously. We write A_n as the set consisting of all non-isomorphic recursive maximal planar graphs of order n . Let $\lambda_n = |A_n|$. Obviously, $A_4 = A_5 = A_6 = 1$. The corresponding recursive maximal planar graphs are shown in Fig. 23.

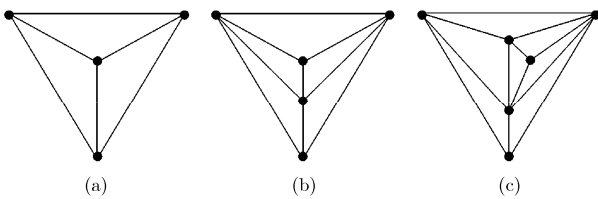


Fig. 23 Three recursive maximal planar graphs

It is easy to prove that every recursive maximal planar graph has at least two vertices of degree 3. A recursive maximal planar graph is called a (2,2)-type recursive maximal planar graph if it contains only two vertices of 3-degree. For example, graphs shown in Figs. 23(b) and 23(c) are (2,2)-type recursive maximal planar graphs. An in-depth research on recursive maximal planar graphs is given in Ref. [24].

Suppose that H^* is K_4 or a (2,2)-type recursive maximal planar graph with a triangle face $\Delta v_1 v_2 v_3 \triangleq \Delta_1$, where one of vertex in Δ_1 is a 3-degree vertex. Let H_2 be a maximal planar graph of minimum degree ≥ 4 . Embedding H^* in the triangle face Δ_2 of H_2 means that an embedding operation of H^* and H_2 based on $\{\Delta_1, \Delta_2\}$, denoted by $H^* \cup H_2 \triangleq H_2^*$.

It is easy to see that the following result holds.

Theorem 7 Suppose that H_1 and H_2 are two maximal planar graphs, $H_1 \cap H_2 = \Delta v_1 v_2 v_3$. Then $G = H_1 \cup H_2$ is a maximal planar graph with minimum degree ≥ 4 iff for any $H_i, i = 1, 2$, there is at most one 3-degree vertex in $\Delta v_1 v_2 v_3$ and all the other vertices in H_i have degree ≥ 4 .

The smallest maximal planar graph with minimum degree ≥ 4 has six vertices; see the first graph in Appendix B. The smallest maximal planar graph with exactly one 3-degree vertex is the graph shown in Fig. 22(a). Thus, by Theorem 7, the smallest separable maximal planar graph has an order of 9 ($6 + 6 - 3 = 9$). Further, according to Theorem 7, we give a method to generate any separable graph with order $n \geq 9$ as follows.

Let H_i be a maximal planar graph of order $n_i (\geq 6), i = 1, 2$. We need to consider the following two cases for constructing separable maximal planar graphs.

Case 1 $n = n_1 + n_2 - 3$

In this case, we can construct a separable graph of order n using H_1 and H_2 , two maximal planar graphs with minimum degree at least 4, by the following steps, where H_i has order $n_i (\geq 6), i = 1, 2$.

Step 1 Find out all the non-identical triangle faces of H_1 and H_2 , respectively;

Step 2 For every non-identical triangle face of H_1 , embed it in every non-identical triangle face of H_2 , and the resulting graphs are our desired ones.

Case 2 $n < n_1 + n_2 - 3$

Let $m = n - n_1 - n_2 + 3, m = m_1 + m_2, m_1, m_2 \geq 0, t_i = m_i + n_i, i = 1, 2$. So, $n = t_1 + t_2 - 3$. We need to further consider two subcases:

Subcase 2.1 $t_1 = n_1$. Then $m_1 = 0$

Step 1 Find out all the non-identical triangle faces of H_1 and H_2 ;

Step 2 If $m_2 = 1$, then embed K_4 in every non-identical triangle face of H_2 ; if $m_2 \neq 1$, then embed the (2,2)-type recursive maximal planar graph H^* of order $(m_2 + 3)$ in every non-identical triangle face of H_2 . Denote the resulting graph by H_2^* , and let Δ_2 be a triangle face of H_2^* with a 3-degree vertex;

Step 3 For any triangle face of H_1 , denoted by Δ_1 , implement an embedding operation of H_1 and H_2^* based on $\{\Delta_1, \Delta_2\}$ respectively. Then, the resulting graphs are the desired ones.

Subcase 2.2 $m_i > 0, i = 1, 2$

Step 1 Find out all the non-identical triangle faces of H_1 and H_2 ;

Step 2 For $i = 1, 2$, embed the (2,2)-type recursive maximal planar graph H^* of order $(m_i + 3)$ in every non-identical triangle face of H_i . Denote the resulted graph by H_i^* . When $m_i = 1$, we have $H^* = K_4$. Let Δ_i be a triangle face of H_i^* with a 3-degree vertex;

Step 3 For each H_1^* and H_2^* , implement an embedding operation based on $\{\Delta_1, \Delta_2\}$ respectively. The resulting graphs are the ones we desired.

By the above method, we construct all of the two separable maximal planar graphs of order 10 as

follows.

Note that $10 = (6 + 7) - 3$, and there is only one maximal planar graph of order i for $i = 6, 7$. In addition, one can readily confirm that each of the two maximal planar graphs of order 6 or 7 has only one non-identical triangle. Therefore, according to Case 1, we can construct a separable maximal planar graph of order 10; see Fig. 24(a). Additionally, since $10 = ((6 + 4) - 3) + 6 - 3$, by using the steps given in Case 2, we can construct another separable maximal planar graph of order 10; see Figs. 24(b) and 24(c). It is easy to prove that there are only two separable maximal planar graphs of order 10.

By using this method, we can construct all the nine separable maximal planar graphs of order 11; see the 17, 19, 24~28, 30, 32nd graphs among maximal planar graphs of order 11 in Appendix B. Similarly, all forty-three separable maximal planar graphs of order 12 are also constructed; see the 38, 49~52, 58, 62, 64, 68, 70, 72, 74, 81, 83, 84, 86~94, 98~100, 103, 105, 107, 109, 110, 112, 113, 115~117, 119, 120, 122, 125, 127, 129th graphs among maximal planar graphs of order 12 in Appendix B.

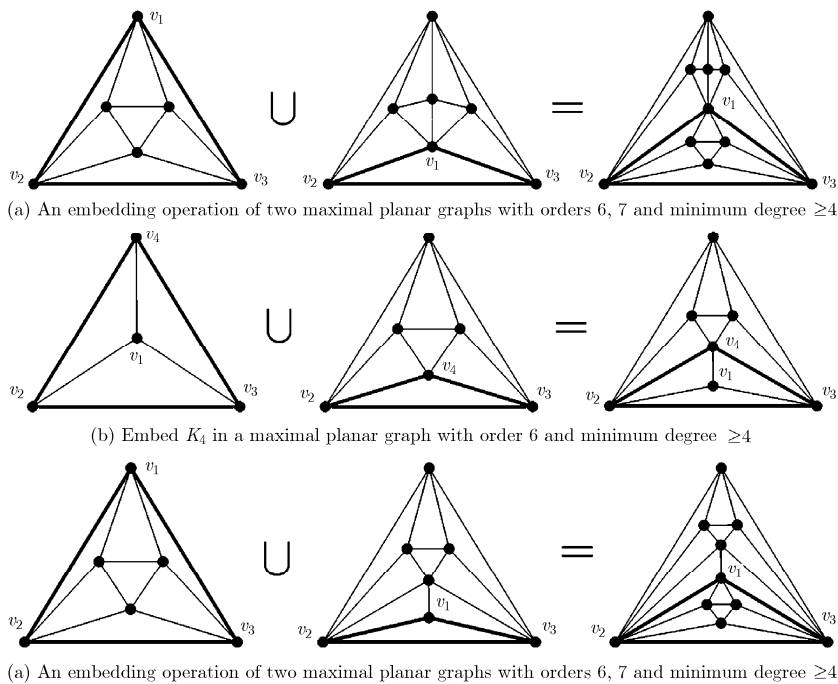


Fig. 24 Processes of constructing two separable maximal planar graphs of order 10

5.3 Basic theorem on constructing non-separable maximal planar graphs of minimum degree ≥ 4

Theorem 8 Suppose that G is a non-separable maximal planar graph with order $n (\geq 9)$ and minimum degree ≥ 4 . Then G has an ancestor-graph of order $(n-2)$ or $(n-3)$.

Proof Let G be an arbitrary non-separable maximal planar graph with order $n (\geq 9)$ and minimum degree ≥ 4 . Denote by (i, j, t) , $i \leq j < t$, a triangle $\Delta v_1 v_2 v_3$ of G , such that the degrees of v_1, v_2 and v_3 are i, j , and t , respectively.

When $\delta(G) = 4$, let $\Delta v_1 v_2 v_3$ be a $(4, j, t)$ triangle, where $4 \leq j < t$. We distinguish three types in terms of the values of j and t .

Type 1 $\Delta v_1 v_2 v_3$ is $(4, 4, t)$, $t \geq 4$

The neighbors of v_1, v_2 , and v_3 are denoted by w_1, w_2, \dots, w_{t-1} in clockwise, as shown in Fig. 25(a). We then further deal with three cases as follows.

Case 1 $t = 4$. Then, G is a graph of order 6 or separable, and a contradiction.

Case 2 $t = 5$; see Fig. 25(b). Then $d(w_1) \geq 5$ and $w_1 w_3 \notin E(G)$; otherwise, G is separable or a graph with order 7. If $d(w_1) = 5$, let u_1 be the neighbor of w_1 different from w_2, v_2, v_1, w_4 , see Fig. 25(c). Obviously, $d(w_2), d(w_4) \geq 6$, and G has a basic domino configuration with outer cycle $w_1 w_2 v_3 w_4$ and inner vertices v_1, v_2 (w_1, v_3 are contracted vertices). If $d(w_1) \geq 6$ and $d(w_3) \geq 5$, then we have $d(w_2), d(w_4) \geq 5$, and G has a basic domino configuration with outer cycle $w_1 w_2 w_3 w_4 v_1$

and inner vertices v_2, v_3 (v_1, w_2 are contracted vertices). If $d(w_1) \geq 6$ and $d(w_3) = 4$, then $d(w_2), d(w_4) \geq 6$, and G has a basic domino configuration with outer cycle $w_1 w_2 v_3 w_4$ and inner vertices v_1, v_2 (v_3, w_1 are contracted vertices).

Case 3 $t \geq 6$. If $d(w_1) \geq 6$, then the 4-wheel with wheel-center v_1 is a domino configuration (v_2, w_{t-1} are contracted vertices). If $d(w_1) = 5$, then w_1 has a neighbor, denoted by u_1 not in $\{v_1, v_2, v_3, w_1, w_2, w_3, \dots, w_{t-1}\}$, and clearly $d(w_{t-1}), d(w_2) \geq 5$; see Fig. 25(d). If $d(u_1) \geq 5$, then G has a basic domino configuration with outer cycle $v_3 v_1 w_{t-1} u_1 w_2$ and inner vertices v_2, w_1 (v_1, w_2 are contracted vertices); if $d(u_1) = 4$, then $d(w_{t-1}), d(w_2) \geq 6$. Therefore, G has a basic domino configuration with outer cycle $w_2 v_2 v_3 w_{t-1} u_1$ and inner vertices v_1, w_1 (u_1, v_2 are contracted vertices). If $d(w_1) = 4$, then G is separable, and a contradiction.

Type 2 $\Delta v_1 v_2 v_3$ is $(4, 5, t)$, $t \geq 5$

The neighbors of v_1, v_2 , and v_3 in this situation are shown in Fig. 25(e).

Case 1 $t = 5$; see Fig. 25(f). If $d(w_1) = 4$, then $\Delta v_1 v_1 v_2$ is $(4, 4, 5)$, and by Type 1 the result holds.

If $d(w_1) = 5$, then w_1 has a neighbor u_1 not in $\{v_1, v_2, v_3, w_1, w_2, w_3, w_4\}$; see Fig. 25(g). Obviously, $d(w_5) \geq 5$. If $d(w_3) = 4$, then $d(w_4), d(w_2) \geq 5$, and G has a basic domino configuration with outer cycle $w_3 w_4 w_5 v_1 w_1 w_2$ and inner vertices v_2, v_3 (v_1, w_3 are contracted vertices). If $d(u_1), d(w_3) \geq 5$,

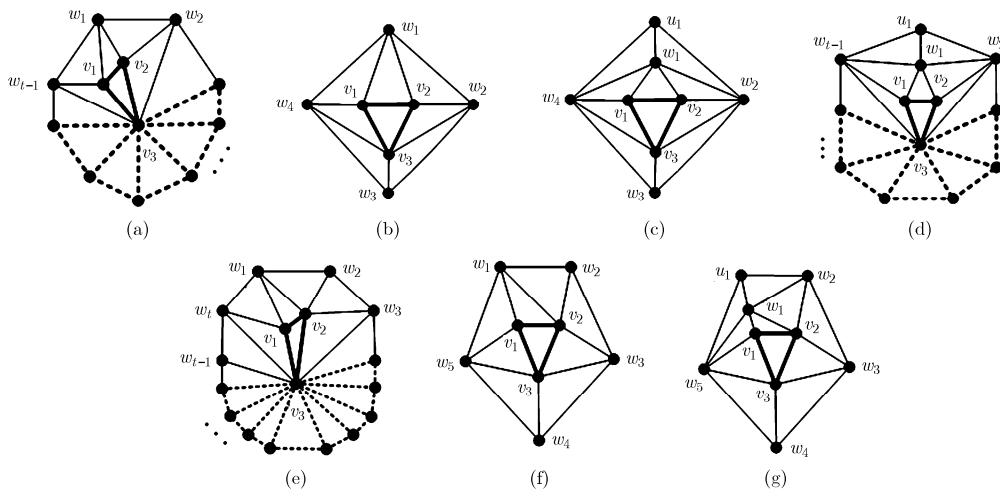


Fig. 25 The schematic for the proof of Theorem 8

then G has a basic domino configuration with outer cycle $v_3v_1w_5u_1w_2w_3$ and inner vertices w_1, v_2 (v_1, w_2 are contracted vertices). If $d(w_3) \geq 5$ and $d(u_1) = 4$, then we have $d(w_5) \geq 6$ and $d(w_2) \geq 5$. Therefore, the 5-wheel with wheel-center w_1 is a domino configuration (v_1, u_1 are contracted vertices).

If $d(w_1) \geq 6$ and $d(w_5) = 4$, then $\Delta v_1w_5w_1$ is of the Type 1. Therefore, we only need to consider the case that $d(w_1) \geq 6$ and $d(w_5) \geq 5$. Then, when $d(w_3) \geq 5$, the 5-wheel with wheel-center v_2 is a domino configuration (v_1, w_2 are contracted vertices); when $d(w_3) = 4$, we have $d(w_4), d(w_2) \geq 5$, and there is a basic domino configuration in G with outer cycle $w_3w_4w_5v_1w_2$ and inner vertices v_2, v_3 (v_1, w_3 are contracted vertices).

Case 2 $t \geq 6$. In this case, if $d(w_1) \geq 6$, then the 4-wheel with wheel-center v_1 is a domino configuration (v_2, w_1 are contracted vertices); if $d(w_1) = 5$, then $\Delta v_1w_1v_2$ is (4,5,5), by Subcase 2.1 in Type 2, the result holds; if $d(w_1) = 4$, then $\Delta v_1w_1v_2$ is (4,4,5), which belongs to Type 1.

Type 3 $\Delta v_1v_2v_3$ is (4, j , t), $6 \leq j \leq t$. Let w_1 be a common neighbor of v_1 and v_2 different from v_3 . If $d(w_1) = 4$ or 5, then $\Delta v_1w_1v_2$ is a (4,4, j) or (4,5, j) triangle, which belongs to Type 1 or Type 2. If $d(w_1) \geq 6$, then the 4-wheel with wheel-center v_1 is a domino configuration.

When $\delta(G) = 5$, the triangles with a 5-degree vertex in G can be distinguished into two types: (5,5, t_1) and (5, j , t_2), where $t_1 \geq 5$, $6 \leq j \leq t_2$. Analogously to the proof of $\delta(G) = 4$, we can also show that there is a basic domino configuration in G .

Hence, the theorem holds.

5.4 A recursive method to generate non-separable maximal planar graphs with order n and minimum degree ≥ 4

Based on the Theorem 8, this section will present an approach to construct non-separable maximal planar graphs recursively. Suppose that $G(n)$ is the set of all non-identical and non-separable maximal planar graphs with order n and minimum degree ≥ 4 . Now, we generate all of graphs in $G(n)$ by the following.

Step 1 For every $H \in G(n-2)$, construct all of its 1-st descendent-graphs; That is, implement

an extending 4-wheel or 5-wheel operation in H . The specific procedures are as follows.

Step 1.1 For every H in $G(n-2)$, find out $\mathfrak{S}_H^{P_3}$ and \mathfrak{S}_H^L , the set of non-identical 2-paths and the set of funnels.

Step 1.2 For every H in $G(n-2)$, implement once extending wheel operation on every 2-path in $\mathfrak{S}_H^{P_3}$ and funnel in \mathfrak{S}_H^L , respectively. We can obtain all the 1-st descendent-graphs of H .

Step 2 For every H in $G(n-3)$, construct all of its 2-nd descendent-graphs by the methods given in Subsection 4.1. The specific procedures are as follows.

Step 2.1 For every H in $G(n-3)$, find out the sets of non-identical 2-paths, funnels, semi-funnels, dumbbells, semi-closed dumbbells, and closed dumbbells, denoted by $\mathfrak{S}_H^{P_3}$, \mathfrak{S}_H^L , $\mathfrak{S}_H^{L^*}$, \mathfrak{S}_H^Y , $\mathfrak{S}_H^{Y^*}$, and $\mathfrak{S}_H^{Y^*}$, respectively.

Step 2.2 For every H in $G(n-3)$, we conduct the following operations. Based on $\mathfrak{S}_H^{P_3}$ and the first domino configuration that contains two inner vertices (in Fig. 11), we construct all the path-type descendent-graphs of H with order n ; Based on \mathfrak{S}_H^L and the second domino configuration that contains two inner vertices (in Fig. 11), we construct all the funnel-type descendent-graphs of H with order n . Based on $\mathfrak{S}_H^{L^*}$ and the second domino configuration that contains two inner vertices (in Fig. 11), we construct all the funnel-type descendent-graphs of H with order n . Based on \mathfrak{S}_H^Y and the third domino configuration that contains two inner vertices (in Fig. 11), we construct all the dumbbell-type descendent-graphs of H with order n ; Based on $\mathfrak{S}_H^{Y^*}$ and the third domino configuration that contains two inner vertices (in Fig. 11), we construct all the dumbbell-type descendent-graphs of H with order n . Based on $\mathfrak{S}_H^{Y^*}$ and the third domino configuration that contains two inner vertices (in Fig. 11), we construct all the dumbbell-type descendent-graphs of H with order n .

We illustrate the process of constructing $G(9)$ as follows.

Notice that there is only one non-separable maximal planar graph of minimum degree ≥ 4 and order 7, denoted by G ; see Fig. 26(a). It is easy to see that $|\mathfrak{S}_G^P| = 3$ and $|\mathfrak{S}_G^Y| = 1$ (the bold lines in Figs. 26(a)~26(d)). Thus, if we implement an extending wheel operation on every 2-path in \mathfrak{S}_G^P and funnel in \mathfrak{S}_G^L , respectively, then we can obtain four maximal planar graphs with order 9 and minimum degree ≥ 4 ; see Figs. 26(a')~26(d'), in which two graphs shown in Fig. 26(a') and Fig. 26(c') are isomorphic.

In addition, one can readily confirm that $G(6)$ contains only one graph, denoted also by G , see Figs. 26(e). This graph has strongly symmetrical characteristic, that is, $|\mathfrak{S}_G^P| = |\mathfrak{S}_G^L| = |\mathfrak{S}_G^{Y*}| = 1$, $|\mathfrak{S}_G^{L*}| = |\mathfrak{S}_G^{L'}| = |\mathfrak{S}_G^{Y*'}| = 0$. Based on the elements (paths and funnels) in \mathfrak{S}_G^P and \mathfrak{S}_G^L , we can construct three descendent-graphs of G with order 9. These three graphs are isomorphic to the graphs shown in Figs. 26(a') ~ 26(c'), respectively. Moreover, if we try to construct descendent-graphs of G with order 9 based on the unique closed dumbbell in \mathfrak{S}_G^{Y*} , then we will get the graph shown in Figs. 26(g).

Above all, we construct all of the four non-isomorphism and non-separable maximal planar graphs with minimum degree ≥ 4 and order 9; see Fig. 26 or Appendix B.

By using the methods on how to generate separable and non-separable maximal planar graphs, prescribed in Subsections 5.2 and 5.4, we construct all of the maximal planar graphs with order 6~12 and minimum degree ≥ 4 . These graphs are listed in Appendix B.

6 Conclusion and Propection

The first paper of this series of articles revealed that the Four-Color Conjecture can be hopefully proved mathematically by investigating a special class of graphs, called the 4-chromatic-funnel pseudo uniquely-4-colorable maximal planar graphs. The 4-coloring of this kind of graphs is closely related to the funnel subgraphs in the graphs. Based on these observations, we introduce the extending-contracting operational system. This system not only correlates with funnel subgraphs naturally, but also associates the structure with 4-coloring of a maximal planar graph closely (see the later paper of this series of articles). This is the essential advantage over the existing methods, and also a novel idea to solve hard problems, such as Four-Color Conjecture, Uniquely Four-Colorable Planar Graphs Conjecture, Nine-Color Conjecture, etc.

The main contributions of this paper are as follows.

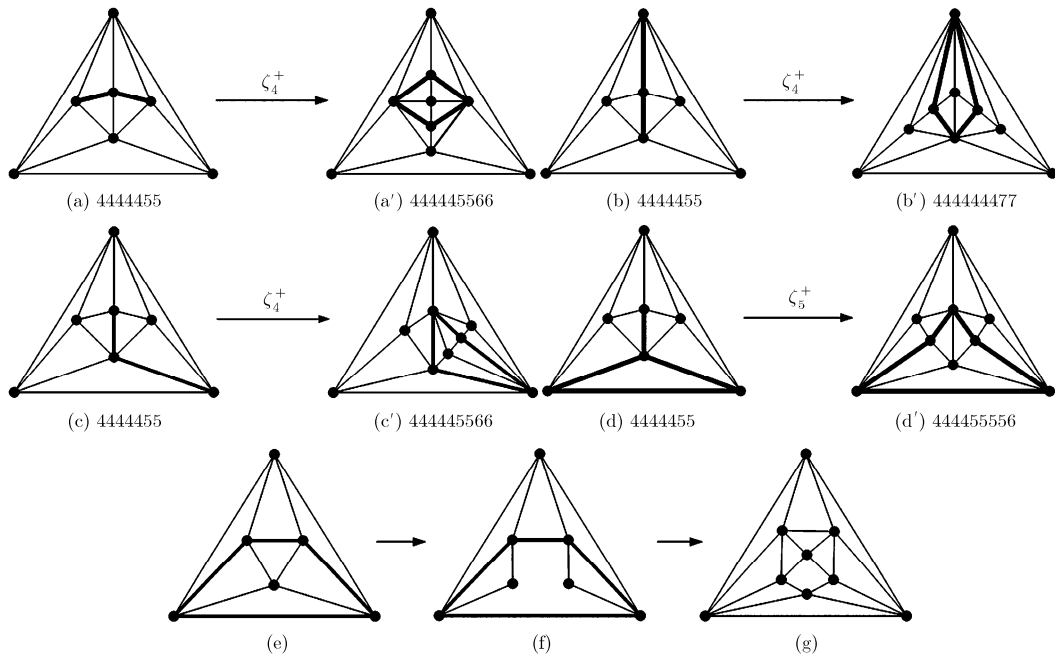


Fig. 26 Procedures of constructing $G(9)$

(1)A new method, called extending-contracting operation, is established to generate maximal planar graphs, which can connect the structure and coloring of an arbitrary maximal planar graph closely.

(2)A useful class of subgraphs in maximal planar graphs of minimum degree ≥ 4 is observed and studied. We characterize the structures of these graphs in depth and propose an approach to construct them. This work is the foundation to construct maximal planar graphs recursively.

(3)We introduce the definitions of ancestor-graphs and descendent-graphs of a maximal planar graph of minimum degree ≥ 4 , and propose a method to construct them.

(4)It is proved that every maximal planar graph with order $n (\geq 11)$ and minimum degree ≥ 4 has an ancestor-graph of order $(n - 2)$ or $(n - 3)$ (Theorem 8), based on which a recursive method is given to construct maximal planar graphs of order $n (\geq 8)$. As examples, all maximal planar graphs with order 6~12 and minimum degree ≥ 4 are constructed.

Note that Theorem 8 is the foundation for our subsequent study. Based on the work Shown in this paper, starting from the third paper of this series of articles, we will demonstrate the combination of

structures and 4-colorings of maximal planar graphs.

Acknowledgements The author would like to gratefully acknowledge the efforts of discussions with and communications from many colleagues, among them Professors YAO Bing, CHEN Xiangen, WU Jianliang, and my students LIU Xiaoqing, ZHU Enqiang, LI Zepeng, WANG Hongyu, and ZHOU Yangyang. Many thanks to Associate Professor BIAN Kaigui who revised the English version carefully. Finally, I would especially like to thank the Academician HE Xingui and Processor YU Daoheng in Peking University for their reviews, selfless supports and encouragements to accomplish this study.

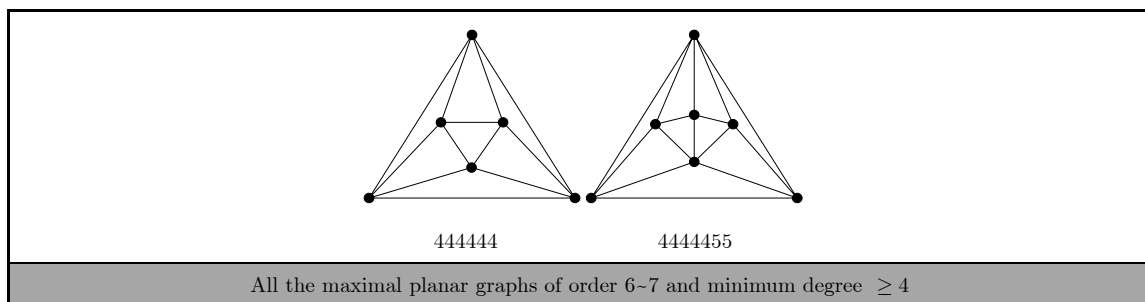
Appendix A Table of the number of all maximal planar graphs of order 6~23 and minimum degree ≥ 4

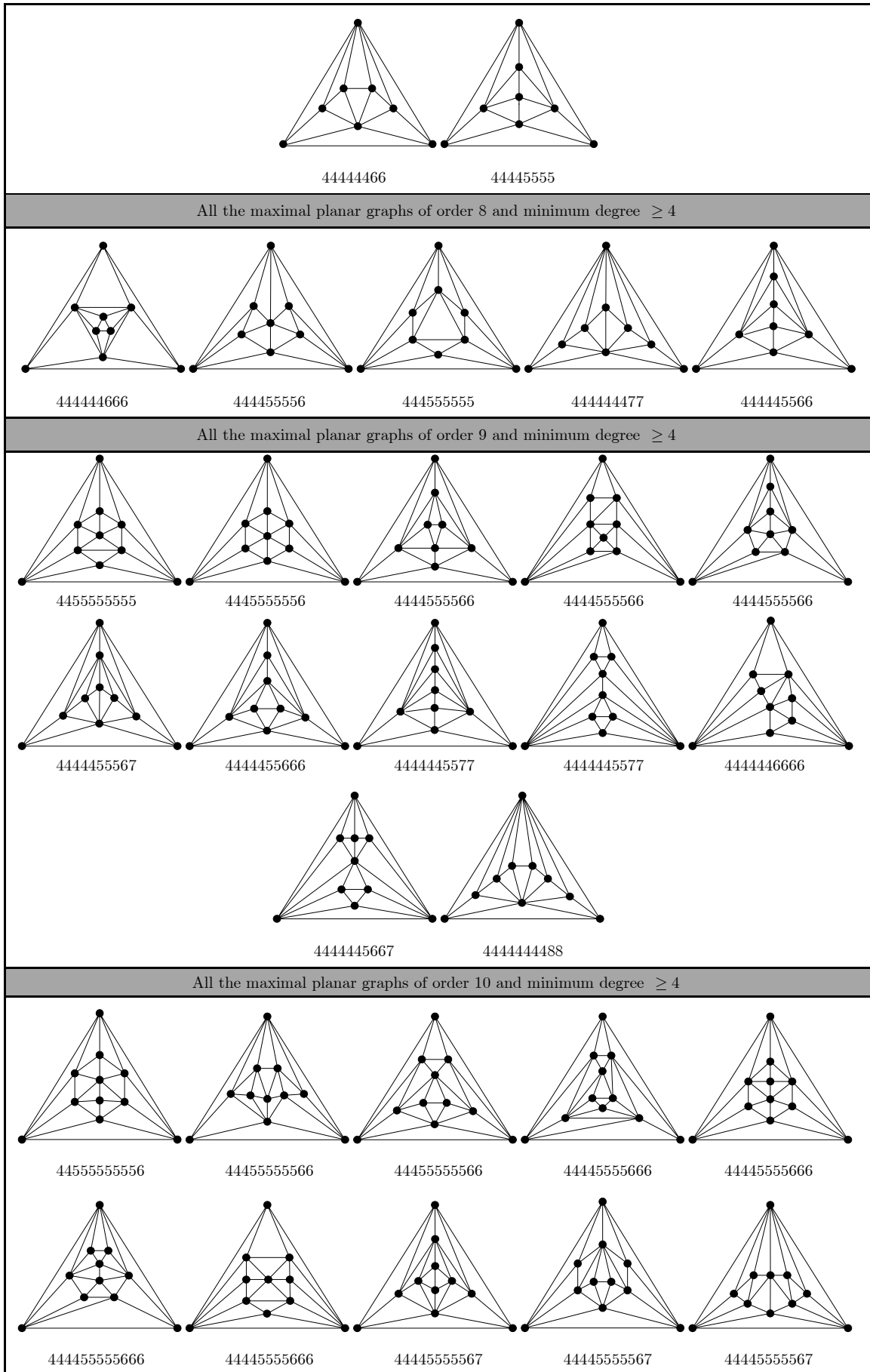
In order to verify the main results in Section 5, we need to know the total number of maximal planar graphs with order 6~12 and minimum degree ≥ 4 . Here, we count the number of all maximal planar graphs of order 6~23 and minimum degree ≥ 4 by using the algorithm proposed by BRINKMANN and MCKAY^[15] in 2007, see the Table A1.

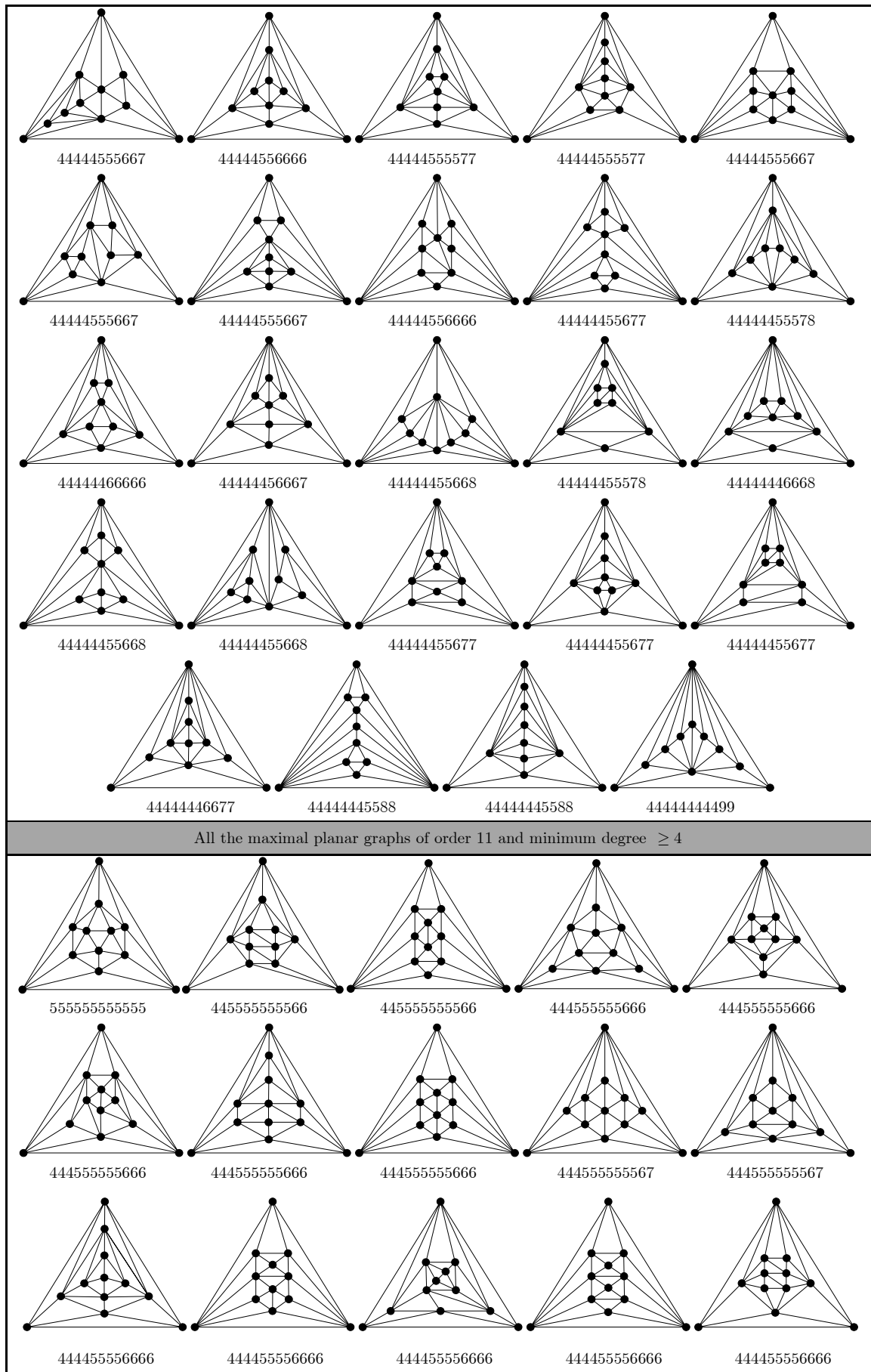
Table A1 The number of all the maximal planar graphs of order 6~23 and minimum degree ≥ 4

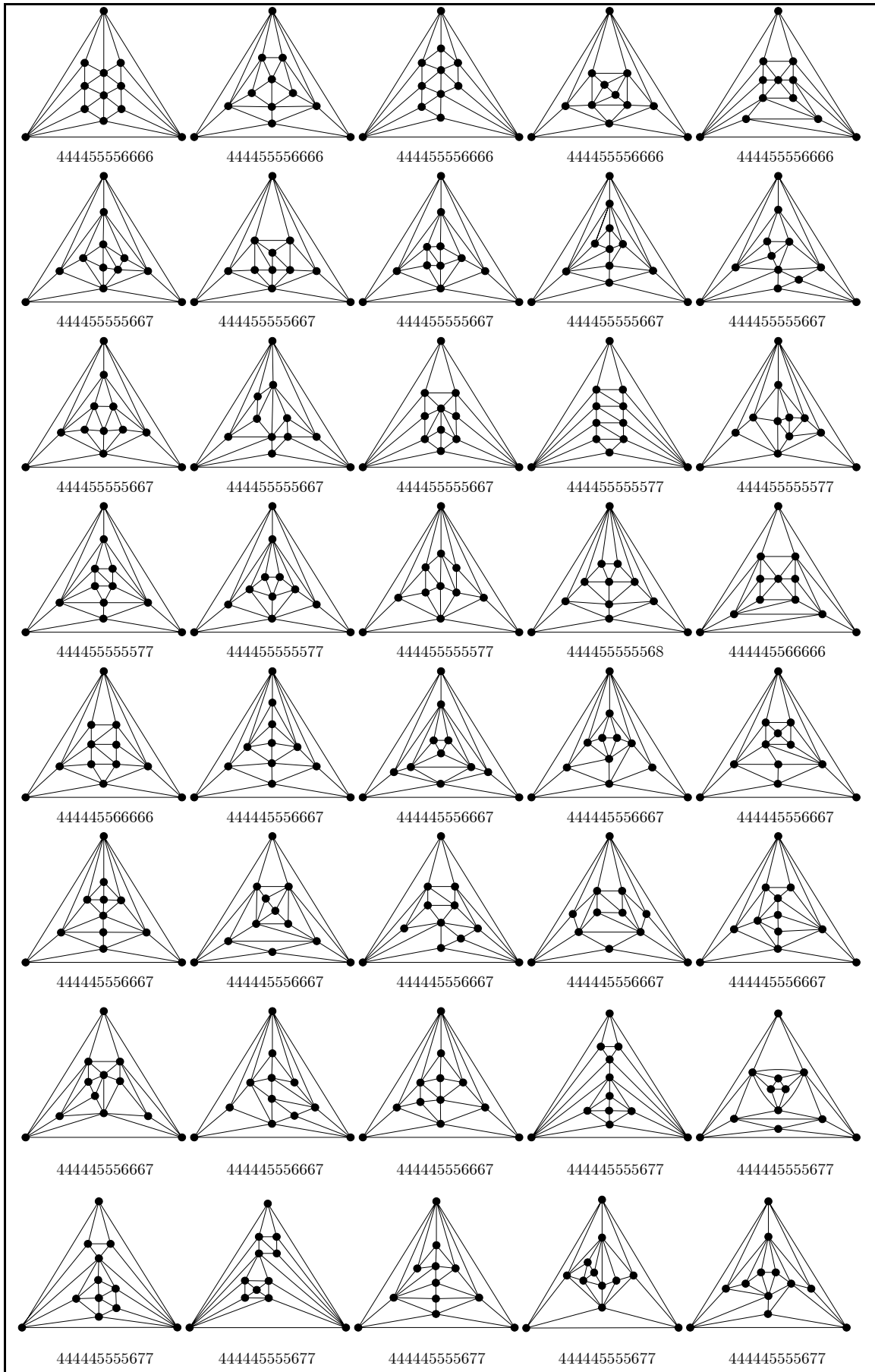
| | | | | | | | |
|--------|-----------|-----------|-----------|-----------|------------|-----------|-------------|
| Order | 6 | 7 | 8 | 9 | 10 | 11 | 12 |
| Number | 1 | 1 | 2 | 5 | 12 | 34 | 130 |
| Order | 13 | 14 | 15 | 16 | 17 | 18 | 19 |
| Number | 525 | 2472 | 12400 | 65619 | 357504 | 1992985 | 11284042 |
| Order | 20 | | 21 | | 22 | | 23 |
| Number | 64719885 | | 375126827 | | 2194439398 | | 12941995397 |

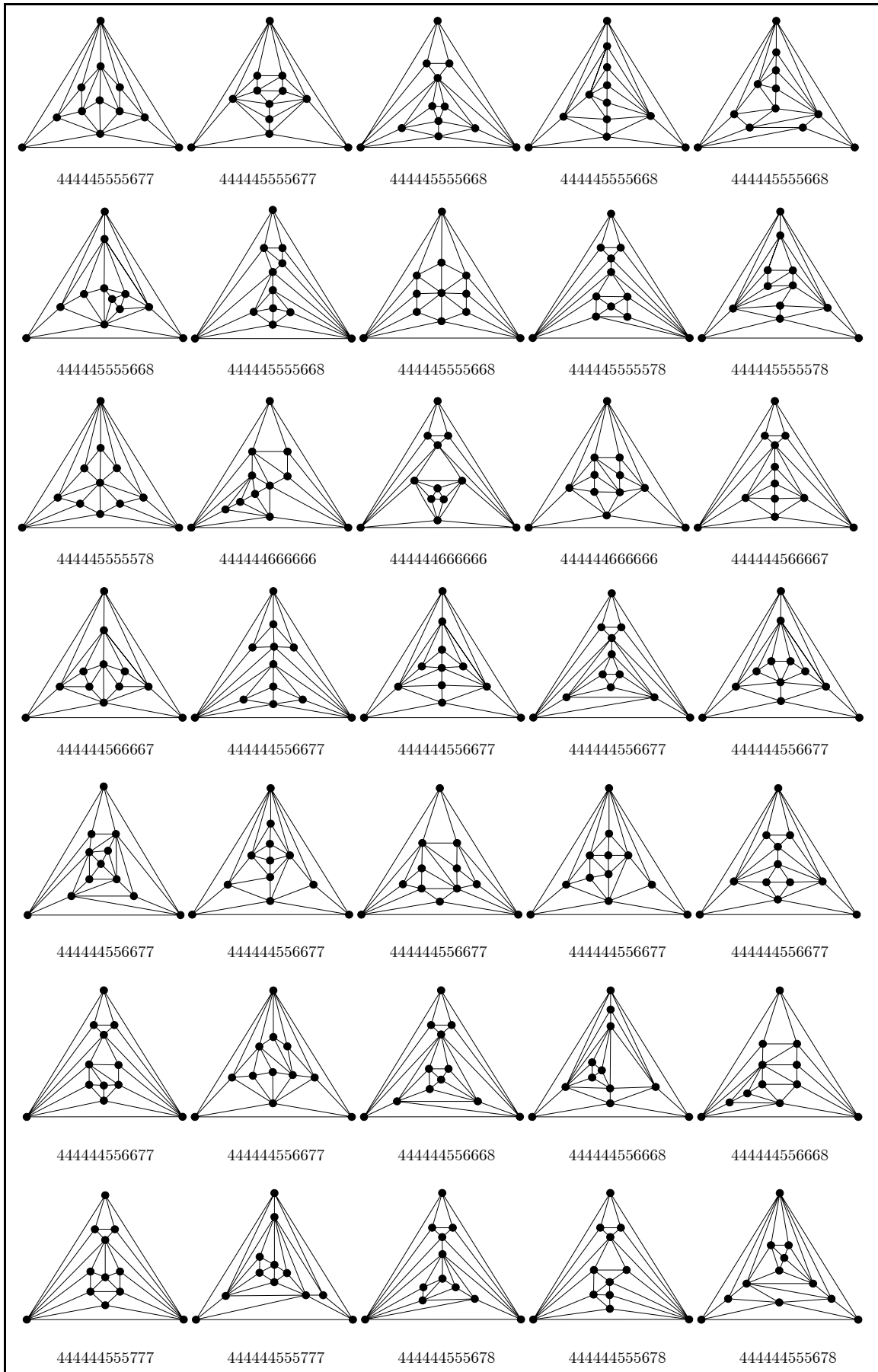
Appendix B All the maximal planar graphs of order 6~12 and minimum degree ≥ 4

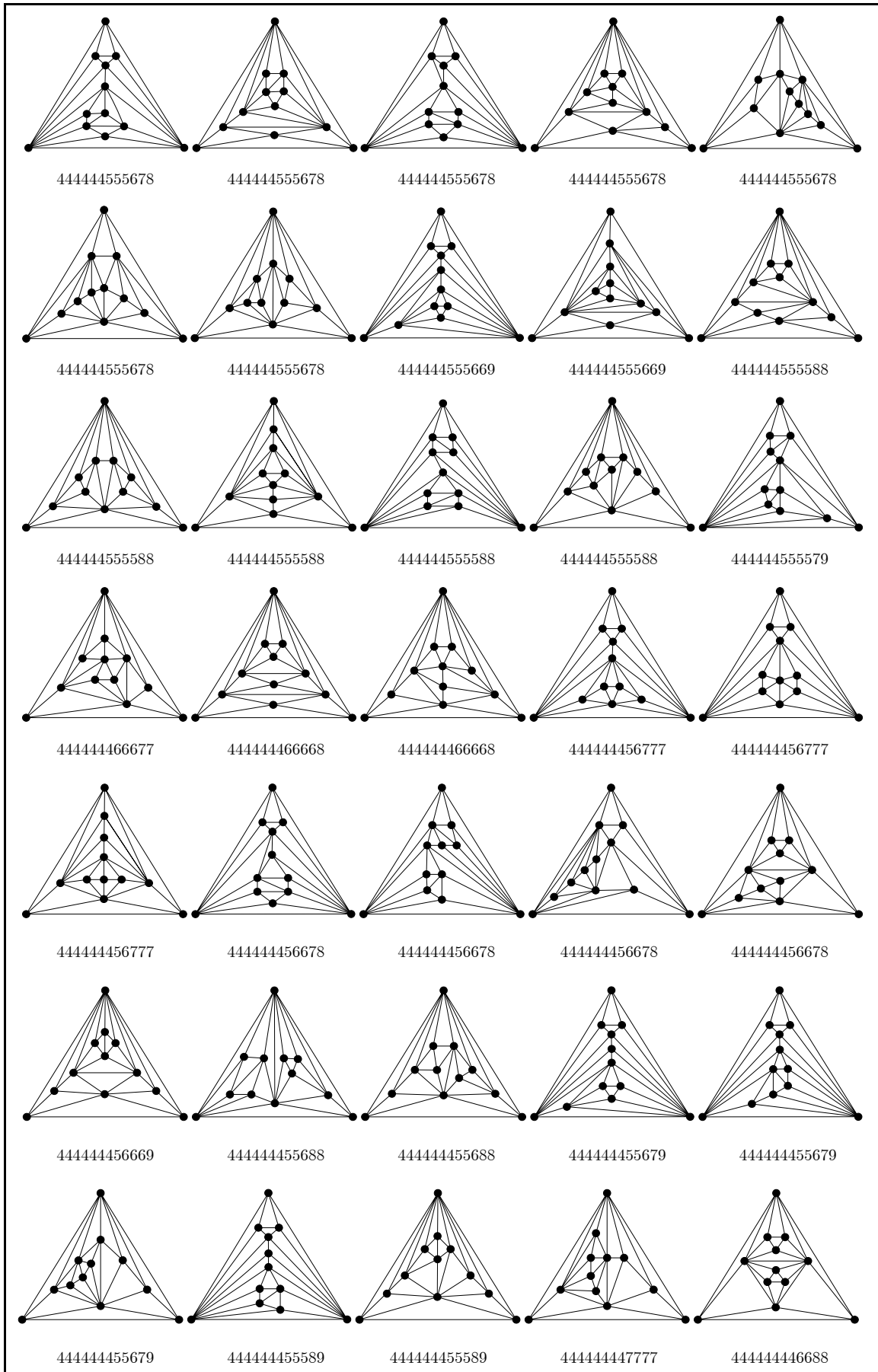












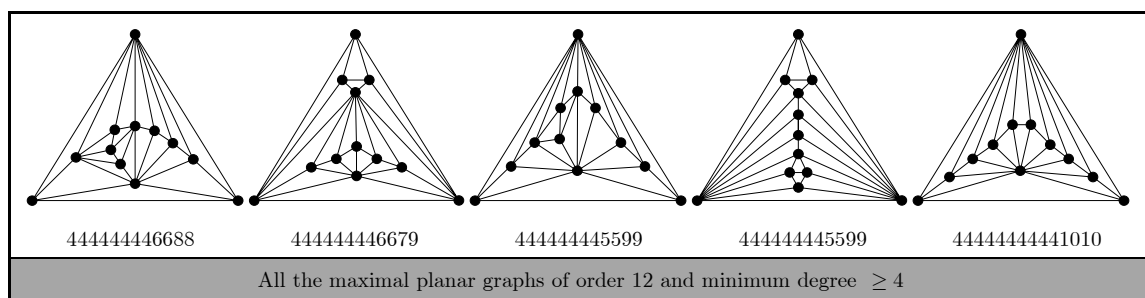


Fig. B1

References

- [1] APPEL K and HAKEN W. The solution of the four-color map problem[J]. *Science American*, 1977, 237(4): 108-121. doi: 10.1038/scientificamerican1077-108.
- [2] APPEL K and HAKEN W. Every planar map is four colorable, I: discharging[J]. *Illinois Journal of Mathematics*, 1977, 21(3): 429-490.
- [3] APPEL K, HAKEN W, and KOCH J. Every planar map is four-colorable, II: Reducibility[J]. *Illinois Journal of Mathematics*, 1977, 21(3): 491-567.
- [4] EBERHARD V. Zur Morphologie Der Polyeder, Mit Vielen Figuren Im Text[M]. Leipzig: Benedictus Gotthelf Teubner, 1891: 14-68.
- [5] 王邵文. 构造极大平面图的圈加点法[J]. 北京机械工业学院学报, 2000, 15(1): 26-29.
WANG Shaowen. Method of cycle add-point to construct a maximum plate graph[J]. *Journal of Beijing Institute of Machinery*, 2000, 15(1): 26-29.
- [6] 王邵文. 构造极大平面图的三种方法[J]. 北京机械工业学院学报, 1999, 14(1): 16-22.
WANG Shaowen. Three methods to construct maximum plain graph[J]. *Journal of Beijing Institute of Machinery*, 1999, 14(1): 16-22.
- [7] BARNETTE D. On generating planar graphs[J]. *Discrete Mathematics*, 1974, 7(3-4): 199-208. doi: 10.1016/0012-365X(74)90035-1.
- [8] BUTLER J W. A generation procedure for the simple 3-polytopes with cyclically 5-connected graphs[J]. *Journal of the Mechanical Behavior of Biomedical Materials*, 1974, 26(2): 138-146.
- [9] BATAGELJ V. An inductive definition of the class of all triangulations with no vertex of degree smaller than 5[C]. Proceedings of the Fourth Yugoslav Seminar on Graph Theory, Novi Sad, 1983: 15-24.
- [10] WAGNER K. Bemerkungen zum vierfarbenproblem[J]. *Jahresbericht der Deutschen Mathematiker-Vereinigung*, 1936, 46: 26-32.
- [11] BRINKMANN G and MCKAY B D. Construction of planar triangulations with minimum degree 5[J]. *Discrete Mathematics*, 2005, 301: 147-163. doi: 10.1016/j.disc.2005.06.019.
- [12] MCKAY B D. Isomorph-free exhaustive generation[J]. *Journal of Algorithms*, 1998, 26(2): 306-324. doi: 10.1006/jagm.1997.0898.
- [13] AVIS D. Generating rooted triangulations without repetitions[J]. *Algorithmica*, 1996, 16(6): 618-632.
- [14] NAKANO S. Efficient generation of triconnected plane triangulations[J]. *Computational Geometry*, 2004, 27(2): 109-122.
- [15] BRINKMANN G and MCKAY B. Fast generation of planar graphs[J]. *MATCH Communications in Mathematical and in Computer Chemistry*, 2007, 58(58): 323-357.
- [16] BRINKMANN G and MCKAY B D. The program plantri [OL]. <http://cs.amu.edu.au/~bdm/plantri>.
- [17] NEGAMI S and NAKAMOTO A. Diagonal transformations of graphs on closed surfaces[J]. *Science Reports of the Yokohama National University. Section I. Mathematics, Physics, Chemistry*, 1994, 40(40): 71-96.
- [18] KOMURO H. The diagonal flips of triangulations on the sphere[J]. *Yokohama Mathematical Journal*, 1997, 44(2): 115-122.
- [19] MORI R, NAKAMOTO A, and OTA K. Diagonal flips in Hamiltonian triangulations on the sphere[J]. *Graphs and Combinatorics*, 2003, 19(3): 413-418. doi: 10.1007/s00373-002-0508-6.
- [20] GAO Z C, URRUTIA J, and WANG J Y. Diagonal flips in labeled planar triangulations[J]. *Graphs and Combinatorics*, 2004, 17(4): 647-656. doi: 10.1007/s003730170006.
- [21] BOSE P, JANSSENS D, VAN RENNSSEN A, et al. Making triangulations 4-connected using flips[C]. Proceedings of the 23rd Canadian Conference on Computational Geometry, Toronto, 2014, 47(2): 187-197. doi: 10.1016/j.comgeo.2012.10.012.
- [22] 许进. 极大平面图的结构与着色理论(1): 色多项式递推公式与四色猜想[J]. 电子与信息学报, 2016, 38(4): 763-779. doi: 10.11999/JEIT160072.
XU Jin. Theory on the structure and coloring of maximal planar graphs(1): recursion formula of chromatic polynomial and four-color conjecture[J]. *Journal of Electronics & Information Technology*, 2016, 38(4): 763-779. doi: 10.11999/JEIT160072.
- [23] BONDY J A and MURTY U S R. Graph Theory[M]. Springer, 2008: 5-46.
- [24] XU Jin, LI Zepeng, and ZHU Enqiang. On purely tree-colorable planar graphs[J]. *Information Processing Letters*, 2016, 116(8): 532-536. doi: 10.1016/j.ipl.2016.03.011.

XU Jin: Born in 1959, Professor. His main research includes graph theory and combinatorial optimization, biocomputing, social networks, and information security.